5-2012

Plant Protein-Based Nanocomposite Materials: Modification of Layered Nanoclay by Surface Coating and Enhanced Interactions by Enzymatic and Chemical Cross-linking

Minfeng Jin
The University of Tennessee, Knoxville, mjin1@tennessee.edu

To the Graduate Council:

I am submitting herewith a dissertation written by Minfeng Jin entitled "Plant Protein-Based Nanocomposite Materials: Modification of Layered Nanoclay by Surface Coating and Enhanced Interactions by Enzymatic and Chemical Cross-linking." I have examined the final electronic copy of this dissertation for form and content and recommend that it be accepted in partial fulfillment of the requirements for the degree of Doctor of Philosophy, with a major in Food Science and Technology.

Qixin Zhong, Major Professor

We have read this dissertation and recommend its acceptance:

Federico Harte, Svetlana Zivanovic, Bin Zhao

Accepted for the Council:

Carolyn R. Hodges

Vice Provost and Dean of the Graduate School

(Original signatures are on file with official student records.)

To the Graduate Council:

I am submitting herewith a dissertation written by Minfeng Jin entitled "Plant Protein-Based Nanocomposite Materials: Exfoliation of Layered Nanoclay by Surface Coating and Enhanced Interactions by Enzymatic and Chemical Cross-linking." I have examined the final electronic copy of this dissertation for form and content and recommend that it be accepted in partial fulfillment of the requirements for the degree of Doctor of Philosophy, with a major in Food Science and Technology.

Qixin Zhong, Major Professor

We have read this dissertation
and recommend its acceptance:

Federico Harte

Svetlana Zivanovic

Bin Zhao

Accepted for the Council:

Carolyn R. Hodges
Vice Provost and Dean of Graduate School

Plant Protein-Based Nanocomposite Materials: Exfoliation of Layered Nanoclay by Surface Coating and Enhanced Interactions by Enzymatic and Chemical Cross-linking

A Dissertation Presented for the
Doctor of Philosophy
Degree
The University of Tennessee, Knoxville

Minfeng Jin
May 2012

Dedication

I would like to dedicate this dissertation to my mother, Jinfang Shen, and my sister Weihong Jin and her family, my relatives and my friends, and especially in loving memory of my dearest father, Mingzu Jin, for always believing in me, inspiring me, supporting me and encouraging me to pursue my goals.

Acknowledgements

I would like to thank all the support and people who helped me in my pursuit of this Doctor of Philosophy Degree in Food Science and Technology. I would like to thank Dr. Qixin Zhong for kindly funding me for three years and patiently guiding me throughout the whole project as my advisor. I would also like to thank my committee members, Drs. Federico Harte, Svetlana Zivanovic, and Bin Zhao for enthusiastically encouraging, generously supporting, and always being ready to help my project and studies; thank you so much for showing me different ways of critical thinking as scientists in my qualifying oral exams.

I appreciate the entire faculty and graduate students in our department, which is "small" enough to make it like close family. You are not only my instructors, co-workers or labmates, but also my wonderful friends here. Thank you Ray for making me stay here for another three and a half years in such a great place, thanks to Sutida and Bhavini for cheering each other up in the lab, thank you to Dr. Shinya for revising my dissertation, and thanks to my cute roommate Stella as well as so many names who have already left UTK, Zhixiong Hu, Ye Liu, Jiajie Li, Shan Xu, who kidnapped me to the Smokey Mountain from my depression, etc., and so many faces who are still here around and share your moments with me.

And a special thank to all the students, postdocs and professors, who helped me with this project. From this project, I hereby understand doctoral study is not only an intelligent work but also a physical work, which really needs great muscles to finish so many "missions impossible" for me, such as pressing the KBr pellets to be translucent, as well as other physically hard work. Thank all the guys who ever helped me and showed me your strong muscles. In other aspects, here named are Drs. Juan Luis Jurat-Fuentes and Cristopher Jon Oppert, and Dr. Carl Sams and

his student from Plant Science Department, who helped me with Two-dimensional Gel Electrophoresis and Na^+ ion concentration determination, Dr. Joseph E. Spruiell from Department of Materials Science and Engineering for the training and permission on my operation of the instrument – XRD, Dr. Jimmy Mays from Chemistry Department for generous permission for me to use the freeze-dryer in his laboratory when ours was down for an entire year, and Dr. John Dunlap for all the information and trials on TEM. Without all their help, I couldn't finish just by myself. Also I want to thank all my Chinese friends throughout the UTK, who offered me plenty of information about everything, e.g. life information and research equipments, etc. Special appreciations to Lu Wang and Xiaojun for helping me a lot on equipment hunting, and Ximin for the rebooting of my computers from time by time. And I appreciate all other colleagues and lab members who were always there and ready to help me. Your suggestions and help were invaluable in completing this task.

Finally, I would like to thank my family and relatives for always caring about me, giving me freedom to pursue my interested life and supporting me without doubt when I need them.

Abstract

Highly intercalated or exfoliated nanoclay montmorillonite (MMT) has promises to improve mechanical and barrier properties of nanocomposite materials that may be further improved by strengthening interactions between matrix polymers and nanofillers. In this work, water-soluble proteins extracted from hominy feed and soy flour were utilized to modify the structures of MMT layers by surface-coating. Following coating at 60 °C using different MMT:protein mass ratios (49:1-2:1) and pH (2.0-10.0), the nanoclay was triple-washed for zeta potential analysis and lyophilized for X-ray diffraction and Fourier transform infrared spectroscopy analyses. Results showed that protein adsorption on MMT occurred at all pH conditions by coulumbic and/or non-coulumbic forces. With a sufficient amount of protein, highly intercalated or fully exfoliated MMT structures were achieved. MMT coated by soy protein was incorporated in soy protein dispersions for enzymatic and chemical cross-linking. Dynamic rheological tests were applied as a non-destructive method to illustrate the gel network formation and the interactions between protein-coated MMT and matrix proteins. Variables in enzymatic cross-linking included concentrations of NaCl and microbial transglutaminase (mTGase), and the absence or presence of protein-coated-MMT at pH 6.5. Without MMT, the maximum storage modulus was achieved at 100 mM NaCl and stronger gels with shorter gelling times were observed at higher mTGase concentrations. Conversely, the incorporation of coated-MMT inhibited the effect of ionic strength on soy protein gelation, and further shortened the gelation time and increased synergistic development of storage modulus with the combined treatments of 100 mM NaCl and mTGase. For chemical cross-linking, glutaradehyde was used as a cross-linker and studied for the impacts of pH, temperature and cross-linker concentration on

dynamic rheological properties. Without MMT, storage moduli gradually increased with increasing glutaradehyde concentration; while the increase of storage modulus was in a higher order of magnitude in the presence of MMT. The practical approach and established parameters from this work can be used to manufacture nanocomposite materials with improved properties.

TABLE OF CONTENTS

LIST OF TABLES

LIST OF FIGURES

CHAPTER 1 . INTRODUCTION

1.1. FOOD PACKAGING AND PLASTICS

Food packaging is utilized in order to prevent the negative changes to the safety and quality of the food against chemical, physical, enzymatic, and microbiological hazards, and to maintain foods in an appropriate condition for retail or consumption. Metal, glass, paper, cardboard, and petroleum-derived plastics are the traditional packaging materials utilized in the food industry. However, although the application of food packaging enhances food safety, quality and convenience in distribution and consumption, the solid waste from food packaging negatively impacts the environment with the increased popularity of food packaging applications. It is reported that the overall municipal solid waste increased by 37% from 179.6 million tons in 1988 to 245.7 million tons in 2005. Packaging waste consists of up to 31.2% total solid wastes, of which food packaging waste accounts for approximately two-thirds by volume (Marsh & Bugusu, 2007).

Plastic packages, due to the advantages of low cost, light weight, and chemical inertness, have been greatly used in food applications (Kumar, 2009) since the first plastic bag was invented in 1957. In 2010, the global production of plastics reached 300 million tons, almost the same amount as that produced in the first decade of the 21st century and that produced during the entire 1900s. Since petroleum derived plastics are non-degradable, the consumption of large amounts of petro-plastics has resulted in a big environment issue of disposing plastics waste. Additionally, the production of petro-plastics consumes valuable and non-renewable natural fossil resources (de Azeredo, 2009).

The concerns of negative environmental impacts of persistent petro-plastic wastes, fossil fuel depletion, and increase of petroleum prices have been driving forces in using plant-based degradable polymers to produce economical, biodegradable, and renewable bio-plastic

packaging materials. The demand for biodegradable plastic packaging has been continuously increasing from both consumers and the food industry in order to alleviate the waste problem to some extent.

1.2. PROGRESSES, OPPORTUNITIES AND CHALLENGES OF FOOD PACKAGING MATERIALS BASED ON NATRUALLY-OCCURRING BIO-POLYMERS

Naturally-occurring biopolymers, including thermoplastic starch, cellulose, chitosan, gelatin and plant oils, have been studied extensively as possible bio-packaging material resources in the past two decades because of their renewable and bio-degradable properties (Cao, Fu, & He, 2007; Krochta & DeMulderJohnston, 1997; Le Corre, Bras, & Dufresne, 2010; Tang, Alavi, & Herald, 2008a). Synthesized bio-degradable packaging materials will have the potential to replace or partially replace petroleum-based plastics and foams predominantly in use today (Krochta & DeMulderJohnston, 1997), thereby potentially alleviating environmental pollution concerns.

Commercialization of some biopolymer-based food packages has already been attempted to some extent. Disposable "green" paper and bio-synthetic polylactide (PLA) are the most popular new advances. Bio-degradable dishware from sugar cane pulp fiber has been widely used in the dining system at Massachusetts Institute of Technology (MIT). Natureworks, LLC (Minnetonka, MN) manufactures biodegradable spring water bottles from biodegradable polylactide that is synthesized from lactic acid produced by fermentation of carbohydrates derived from resources such as corn stach. Frito-Lay, Inc. had replaced traditional Sunchips®

bags with bio-degradable bags for more than a year although finally moves back to the normal ones. Wal-Mart stores, Inc. is using polylactide to package fresh-cut produce (Marsh & Bugusu, 2007). As released in the "Food & Beverage Packaging" website in July 2011, the annual growth of bio-plastics has been ca. 17-20% since 2006, and the global demand for bio-plastics is estimated to quadruple by 2013 (Markets, 2011).

According to "The Global Outlook for Biodegradable Packaging" report (Markets, 2011), "PLA dominates bioplastics use, but more new materials are being developed from algae and microbacterial sources and advances in nanotechnology offer potential for interesting developments in smart packaging." Proteins, due to their good film forming properties, moderate cost, and biodegradable nature, have been extensively studied in forming biopolymer films. When comparing to whey protein, casein, collagen, corn zein, and gelatin, soy protein and gluten have the advantage of the low cost in order to develop affordable packaging materials (Krochta & DeMulderJohnston, 1997). Soy protein isolate (SPI), consisting of more than 90% protein, is a cheaper source than whey protein isolate (WPI) and corn zein (Fishman, 1997; Krochta & DeMulderJohnston, 1997). However, when compared to conventional plastic products, packaging films prepared from proteins have poor mechanical and barrier properties such as brittleness, rigidity, low elongation percentage, and relatively low moisture resistance due to its hydrophilic nature (Kim, Ko, & Park, 2002; Krochta & DeMulderJohnston, 1997; Paetau, Chen, & Jane, 1994). These challenges are to be overcome before realistic applications in the food packaging industry.

With the emerging nanotechnology, nanocomposite packaging materials have received great interests in overcoming the property shortages of these natural biopolymer-based packaging materials. Nanotechnology uses and studies materials at a scale that normally ranges

from 1 to 100 nanometers. Materials composed of building blocks with different scales, e.g. micrometer (μm) versus nanometer (nm), have significantly different properties, with much improved for an ultra-small level (nm), even when these building blocks have same chemical compositions. In comparison to the micro scale materials, the nano scale materials are endowed with much better mechanical and barrier properties due to their ultra-small size and huge reactive surface area (Kumar, 2009). A nanocomposite consists of a biopolymer matrix incorporated with nanofillers. The composition, dimension, and shape of the nanofillers, as well as their spatial distribution in the matrix, are important factors that impact the properties of nanocomposite products (Capek, 2006).

Polymer-clay-nanocomposite (PCN) is a group of nanocomposites, in which nanoclays are the nanoscale fillers dispersed in a polymer matrix. The inorganic nanoclays have at least one dimension in the nanometer range. Due to the high aspect ratio and high surface area of incorporated nanoclays and their uniform distribution in and enhance the interfacial interaction with the biopolymer matrix, PCN works effectively to enhance the mechanical (tensile strength, tensile modulus and percent elongation at break) and the barrier (resistance against gas, moisture, and volatiles) properties for bio-degradable and renewable natural raw materials. Four possible arrangements of layered clays dispersed in a polymer matrix have been established, i.e., microcomposite (phase separated or immiscible), intercalated, disordered intercalated (partially exfoliated), and exfoliated nanocomposite (Kumar, 2009; Tang, Alavi, & Herald, 2008a). The structure-property relationship illustrates that the final structure of nanocomposite materials greatly impacts the properties and performance of the final products. Therefore, achieving either intercalation or exfoliation of layered nanoclay is critical to improve the properties of nanocomposite materials. (Le Corre, Bras, & Dufresne, 2010; Tang, Alavi, & Herald, 2008a).

As a naturally-existing clay, montmorillonite (MMT) is one of the most widely studied layered silicates in developing bio-polymer nanocomposites due to its low cost, abundant supply, large surface area, large specific aspect ratio (ratio of length to thickness), and very high elastic modulus (Arora & Padua, 2010; de Azeredo, 2009; Essington, 2003; Gunister, Pestreli, Unlu, Atici, & Gungor, 2007; Zhao, Torley, & Halley, 2008). MMT behaves as rigid fillers in a nanocomposite to enhance the mechanical properties. Highly intercalated or exfoliated MMT has repeatedly been shown to improve mechanical and barrier properties of bionanocomposite materials (Chen & Zhang, 2006; Kumar, Sandeep, Alavi, Truong, & Gorga, 2010a, 2010b). Well dispersed MMT in SPI matrix resulted in significant improvements in thermal-stability and mechanical strength. Disordered intercalation or exfoliation is the desired arrangement for enhancing the properties of PCN, and the authors only obtained this at a low MMT concentration. Generally speaking, because a bigger d-spacing (distance between clay layer platelets) helps the polymer chains enter into the galleries more easily, the intercalation, even further the exfoliation of nanocomposites would be much more easily obtained by modified MMT with enlarged d-spacing than pristine MMT. Thus, modification of MMT structures with enlarged basal spacing and intercalated and/or exfoliated structures prior to incorporation into the polymer matrix is a viable approach in improving the structure and properties of final nanocomposite materials.

1.3. SCOPE OF THE WORK

The overall goals of this work were to investigate the potential modification of MMT structures by surface-coating with water soluble plant proteins and the strengthening of interactions between the matrix biopolymer and protein-coated MMT by enzymatic and chemical crosslinking.

Hominy protein and soy protein, widely available plant-sourced proteins, were utilized to modify the ordered structure of MMT parallel layers by surface coating with a goal to obtain intercalated and/or exfoliated platelets prior to nanocomposite production. Different pH (2.0-10.0) and MMT:protein mass ratios (from 49:1 to 2:1) were investigated for the impact on MMT structures studied by using X-ray diffraction (XRD), Fourier transform infrared spectroscopy (FTIR), and ζ (zeta)-potential analysis.

The modified MMT was then incorporated in soy protein dispersions for enzymatic and chemical crosslinking by utilizing transglutaminase (TGase) and glutaraldehyde, respectively. Dynamic rheological measurements were performed to illustrate the gel network formation and strength. Variables in enzymatic crosslinking included concentrations of sodium chloride and TGase in the absence or presence of modified MMT. Chemical crosslinking was studied for the impacts of pH, temperature and glutaraldehyde concentration, with or without modified MMT.

LIST OF REFERENCES

Arora, A., & Padua, G. W. (2010). Review: nanocomposites in food packaging. *Journal of Food Science, 75*(1), R43-R49.

Cao, N., Fu, Y. H., & He, J. H. (2007). Preparation and physical properties of soy protein isolate and gelatin composite films. *Food Hydrocolloids, 21*(7), 1153-1162.

Capek, I. (2006). Nanocomposite structures and dispersions : science and nanotechnology--fundamental principles and colloidal particles

Chen, P., & Zhang, L. (2006). Interaction and properties of highly exfoliated soy protein/montmorillonite nanocomposites. *Biomacromolecules, 7*(6), 1700-1706.

de Azeredo, H. M. C. (2009). Nanocomposites for food packaging applications. *Food Research International, 42*(9), 1240-1253.

Essington, M. E. (2003). Soil and water chemistry: an intergrative approach *CRC Press*, p58, 65, 68.

Fishman, M. L. (1997). Edible and biodegradable polymer films: challenges and opportunities. *Food Technology, 51*(2), 16-16.

Gunister, E., Pestreli, D., Unlu, C. H., Atici, O., & Gungor, N. (2007). Synthesis and characterization of chitosan-MMT biocomposite systems. *Carbohydrate Polymers, 67*(3), 358-365.

Kim, K. W., Ko, C. J., & Park, H. J. (2002). Mechanical properties, water vapor permeabilities and solubilities of highly carboxymethylated starch-based edible films. *Journal of Food Science, 67*(1), 218-222.

Krochta, J. M., & DeMulderJohnston, C. (1997). Edible and biodegradable polymer films: challenges and opportunities. *Food Technology, 51*(2), 61-74.

Kumar, P. (2009). Development of bio-nanocomposite films with enhanced mechanical and barrier properties using extrusion processing. *North Carolina State University. Ph.D dissertation*.

Kumar, P., Sandeep, K. P., Alavi, S., Truong, V. D., & Gorga, R. E. (2010a). Effect of type and content of modified montmorillonite on the structure and properties of bio-nanocomposite films based on soy protein isolate and montmorillonite. *Journal of Food Science, 75*(5), N46-N56.

Kumar, P., Sandeep, K. P., Alavi, S., Truong, V. D., & Gorga, R. E. (2010b). Preparation and characterization of bio-nanocomposite films based on soy protein isolate and montmorillonite using melt extrusion. *Journal of Food Engineering, 100*(3), 480-489.

Le Corre, D., Bras, J., & Dufresne, A. (2010). Starch nanoparticles: a review. *Biomacromolecules, 11*(5), 1139-1153.

Markets, R. a. (2011). The global outlook for biodegradable packaging. Accessed by website: http://www.researchandmarkets.com/research/5e27e0/the_global_outlook. *Business Insights, June*, 110.

Marsh, K., & Bugusu, B. (2007). Food packaging - Roles, materials, and environmental issues. *Journal of Food Science, 72*(3), R39-R55.

Paetau, I., Chen, C. Z., & Jane, J. L. (1994). Biodegradable plastics made from soybean products.1. effect of preparation and processings on mechanical-properties and water-absorption. *Industrial & Engineering Chemistry Research, 33*(7), 1821-1827.

Tang, X. Z., Alavi, S., & Herald, T. J. (2008). Barrier and mechanical properties of starch-clay nanocomposite films. *Cereal Chemistry, 85*(3), 433-439.

Zhao, R. X., Torley, P., & Halley, P. J. (2008). Emerging biodegradable materials: starch- and protein-based bio-nanocomposites. *Journal of Materials Science, 43*(9), 3058-3071.

CHAPTER 2 . LITERATURE REVIEW

2.1. RECENT RESEARCH OF BIODEGRADABLE SILLICATE NANOCOMPOSITE IN PROTEIN-BASED FOOD PACKAGING

Concerns of fossil fuel depletion, increase of petroleum prices, and negative environmental impacts of persistent petro-plastic wastes have been the driving forces behind the investigation of bio-plastic packaging based on renewable, low-cost, and degradable biopolymers (Jahangir, & Leber, 2007; Sorrentino, Gorrasi, & Vittoria, 2007; Zhao, Torley, & Halley, 2008). Since 2006, the annual growth of bio-plastics has been reported as ca. 17-20%, and the global demand for bio-plastics is estimated to quadruple by 2013 (Markets, 2011). Companies like Coca-Cola, Frito-Lay, and Walmart have already adopted bio-plastic bottles, pouches and wraps (Marsh & Bugusu, 2007).

Natural biopolymers, like thermoplastic starch, cellulose, chitosan, gelatin, gluten, soy protein and whey protein, as listed in Table 2.1, have been studied extensively as bio-packaging material resources in the past two decades due to their renewable and bio-degradable nature (Cao, Fu, & He, 2007; Krochta & DeMulderJohnston, 1997; Le Corre, Bras, & Dufresne, 2010; Tang, Alavi, & Herald, 2008a). Poly-lactic-acid (PLA), synthesized from monomers derived from corn starch, has been a dominating polymer in manufacturing bioplastics (Ahmed & Varshney, 2011). As seen in Table 2.1, the films made from PLA showed good mechanical properties, moderate water barrier property, but poor oxygen barrier property. Materials from other sources and advanced technologies such as nanotechnology are emerging in the bioplastic industry (Markets, 2011) to improve the material properties. Therefore, the emerging renewable and bio-degradable packaging materials have the potential to replace or partially replace the dominant petroleum-based plastics and foams (Krochta & DeMulderJohnston, 1997), thereby potentially alleviating environmental pollution derived from non-degradable petroleum-based plastic products.

2.1.1. Soy Protein-based Packaging Materials

Due to good film forming properties, low cost, renewable and biodegradable nature, proteins have been intensively studied as renewable film-forming biopolymers (Cuq, Gontard, & Guilbert, 1998; Kumar, Sandeep, Alavi, Truong, & Gorga, 2010a, 2010b; Paetau, Chen, & Jane, 1994; Xiang, Tang, Cao, Wang, Wang, Zhang, et al., 2009). Among plant and animal-derived proteins, soy protein and gluten have the advantage of low cost to develop affordable packaging materials. As illustrated in Table 2.1, the unit price (dollars per pound) of soy protein isolate (SPI) and gluten was 1.30-1.70 and 0.80-0.90, respectively, which was much lower than 6.00-12.00 and 10.25-15.50 for whey protein isolate (WPI) and corn zein, respectively, in 1997 (Fishman, 1997; Krochta & DeMulderJohnston, 1997). In the middle of 2011, from the Food Expo of Institute of Food Technologist Annual Meeting, the unit price for SPI was ca. $2/lb. in comparison to ca. $14/lb. for WPI. Therefore, soy protein still has the advantage to develop competitive bio-packaging materials.

Soy protein ingredients used in the food industry are classified as three groups based on the protein content, i.e. soy flours and grits, soy protein concentrate (SPC), and SPI. Soy flour contains 50-59% protein and is obtained by grinding defatted soy flakes, SPC has 65-72% protein and is produced by aqueous extraction or acid leaching process, SPI is manufactured by aqueous or mild alkali extraction followed by isoelectric precipitation and contains more than 90% protein (Council, 1987). Soy proteins are widely applied in the food industry because of their excellent functional properties. Functional properties of soy proteins important to food systems include solubility, viscosity, gelation, cohesion/adhesion, water absorption and binding, emulsification, forming, fat adsorption, flavor-binding, etc., as shown in Table 2.2 (Kinsella,

1979). The mode of action for each function is also listed in Table 2.2, as well as the potential applicable food systems and the form of soy proteins. (Kinsella, 1979)

Soy proteins are composed of a complex mixture of proteins with the minimum solubility near pH 4.5 (isoelectric point, pI) and have molecular weights ranging from 8000 to 600,000 Da (Wolf, 1970). Soy proteins are classified into four fractions (2S, 7S, 11S, and 15S) based on their sedimentation values, as shown in Table 2.3. The β-conglycinin (7S, about 35%) and glycinin (11S, about 52%) are the two major components in SPC and SPI; while 2S is the fraction of a small molecular weight that is degraded to some extent during heat treatment, which causes its limited presence in SPC and SPI (Wolf, 1970). β-conglycinin is a trimeric glycoprotein with a molecular weight of 180 kDa, consisting of three types of subunits, i.e., α', α and β subunits, corresponding to 60, 67 and 71 kDa (Maruyama, Katsube, Wada, Oh, Barba De La Rosa, Okuda, et al., 1998), while glycinin, having a molecular weight of ca. 360 kDa, is composed of an acidic and a basic polypeptide, linked by a disulfide bond (Koshiyam.I, 1968; Renkema, Knabben, & van Vliet, 2001; Thanh & Shibasaki, 1976a, 1976b). Badley *et al.* (Badley, Atkinson, Hauser, Oldani, Green, & Stubb, 1975) also reported that glycinin has 6 acidic subunits of ca. 35 kDa and 6 basic units of ~20 kDa. β-conglycinin and glycinin have a peak denaturation temperature of 76.7 and 94.1 °C, respectively (Tang, Choi, & Ma, 2007). The onset and peak denaturation temperatures are highly dependent on pH, with higher onset and peak denaturation temperatures at higher pH conditions. Since glycinin has 3-4 times more –SH than β-conglycinin, glycinin has a higher tendency to form disulfide bonds than β-conglycinin. Therefore, the films formed from 11S had a higher tensile strength than those from 7S (Okamoto, 1978).

The association and dissociation of soy protein subunits are dependent on temperature and pH (Badley, Atkinson, Hauser, Oldani, Green, & Stubb, 1975; Maruyama, et al., 1998),

which in turn affect most of their physicochemical properties (Kinsella, 1979). Concentrated dispersions of SPI increase in viscosity and form gels when heated. Soy protein dispersions form pro-gels during heating, while forming gels after cooling. The concentration of the SPI in dispersions, normally, should be at least 8%w/v to form a pro-gel. Excess heating strengthens gel elasticity, further solution again when the temperature is above 120 °C. As for the effect of pH, concentrated SPI dispersions form firm and turbid gels at low pH, called "coagulum gel", but form translucent and weak gels at high pH. Under alkaline conditions, β-conglycinin trimers dissociate into individual subunits and glycinin is denatured, dissociating into acidic and basic polypeptide components (Petruccelli & Anon, 1995). The denaturation of β-conglycinin results in the decrease in viscosity. When a mixture of glycinin and β-conglycinin are treated at alkaline conditions at elevated temperatures, the dissociated basic polypeptides from glycicin react with β-conglycinin subunits to form soluble aggregates, more actively than acid polypeptides do. Upon cooling the soluble aggregates become highly organized complexes. (Utsumi & Kinsella, 1985)

Various chemical treatments have shown significant impacts on soy protein films (Kumar, 2009). The addition of plasticizers improves the water resistance and decreases the brittleness of soy protein polymers. Water and glycerol, behaving as typical plasticizers, greatly enhance the flexibility of soy protein polymers (Mo, Sun, & Wang, 1999). Cross-linked protein films have lower solubility and less soluble mass than the controls. Other factors, such as pH, heating, and blending, also played important roles in the formation and properties of soy protein films (Song, Tang, Wang, & Wang, 2011). Besides to the chemical treatments, the molecular weight of the SPI fraction also have an effect on the moisture barrier and physical properties of soy protein films (Cho & Rhee, 2004).

In comparison to starch films, protein films have moderate mechanical properties, lower water vapor permeability and better oxygen barrier properties (Cao, Fu, & He, 2007; de Azeredo, 2009; Zhao, Torley, & Halley, 2008). However, when comparing to petro-plastics, protein films have poorer mechanical properties such as brittleness, rigidness, and lower elongation percentage and relatively lower moisture and gas resistance due to their hydrophilic nature. This, in turn, limits the realistic applications of protein films in the food packaging industry. These drawbacks can be potentially lessened by the application of nanotechnology (Arora & Padua, 2010; Krochta & DeMulderJohnston, 1997; Song, Tang, Wang, & Wang, 2011).

2.1.2. Nanotechnology and Soy Protein-Based Nanocomposites

Nanotechnology uses and studies materials with at least one dimension between 1 and 100 nanometers. At different scales, i.e. micro versus nano, materials possess significantly different properties, even for identical compositions. Nanoscale materials have frequently demonstrated much better mechanical and barrier properties than those at the micro scale. Composites consist of fillers dispersed in the matrix polymers. As for the nanocomposite materials, at least one dimension of the incorporated fillers is in the nanometer range. Nanocomposites have much improved mechanical and barrier properties than conventional composite materials containing fillers dispersed as micrometer-sized structures (Le Corre, Bras, & Dufresne, 2010; Tang, Alavi, & Herald, 2008a).

Bio-nanocomposite consists of inorganic nanoparticles dispersed in a biopolymer matrix, and has the promise to improve mechanical, barrier, and thermo-resistance properties of natural biopolymer-based packaging films (Arora & Padua, 2010; Dang, Lu, Yu, Sun, & Yuan, 2010; de Azeredo, 2009). These properties are currently technological challenges of developing bio-packaging to replace conventional petro-plastics dominantly in use now. Clay-based

nanocomposite effectively enhances the tensile strength and the barrier resistance against gas, moisture, and volatiles for products derived from bio-degradable and renewable natural raw materials (Arora & Padua, 2010; Chang, Yang, Huang, Xia, Feng, & Wu, 2009; Weiss, Takhistov, & McClements, 2006). Thus, biopolymer-based nanocomposites as novel packaging materials have the potential to be substitutes for petroleum-derived plastics due to their renewability and bio-degradability.

2.1.3. Nanocomposites Based on MMT

Researchers proposed different nano-particles based on their physical shapes, including spheres, rods, palates, particles, etc. The composition, dimension, and shape of nanofillers, as well as their spatial distribution in the matrix, are important factors impacting the properties of nanocomposite products (Capek, 2006).

MMT, as a naturally-existing clay, has been one of the intensively studied nanofillers in developing bio-polymer nanocomposites (Arora & Padua, 2010; Capek, 2006). As depicted in Figure 2.1, the structure of MMT is composed of a layer of octahedral sheet sandwiched with two silica tetrahedral parallel layers (Figure 2.1). The surfaces of MMT are highly negatively charged and the different layers are attracted with a weak electrostatic force (Essington, 2003; Kumar, 2009; Tang, Alavi, & Herald, 2008a). The extensive usage of MMT for developing nanocomposites is due to its abundance in supply, easy availability at a low cost, and physical characteristics, including high elastic modulus (178 GPa), high surface area (750 m^2/g), and high specific aspect ratio (50-1000). These physical characteristics contribute to both enhanced mechanical and barrier properties of nanocomposite materials (de Azeredo, 2009; Essington, 2003; Gunister, Pestreli, Unlu, Atici, & Gungor, 2007; Le Corre, Bras, & Dufresne, 2010).

There are four proposed structures of silicate layers dispersing in a composite polymer matrix (Tang, Alavi, & Herald, 2008b). Basically, three identical arrangements, i.e., microcomposite (phase separated or immiscible), intercalated, and exfoliated nanocomposite, have been well accepted (Alexandre & Dubois, 2000), and the fourth one is an intermediate status between intercalated and exfoliated structures, called "disordered intercalation". As shown in Figure 2.2, phase separated structures exist in conventional composites, referred as microcomposites, in which clay platelets are stacked and exist as tactoids, encapsulated by the polymer matrix. Intercalation of silicate platelets occurs once a monolayer of extended polymer chains penetrates into the galleries between clay layers. The intercalation leads to finite expansion of clay layers to ca. 2-3 nm. In this category of intercalation, clay platelets remain parallel to each other. Exfoliation or delamination of silicate platelets occurs when polymer chains extensively penetrate into the galleries, causing the separation of layers by ca. 10 nm or more. Exfoliation of nanocomposite reveals the homogeneous distribution of nanoclays throughout the polymer matrix. The disordered intercalation is the structure with regards to non-parallel intercalation. (Alexandre & Dubois, 2000; Kumar, 2009; Tang, Alavi, & Herald, 2008a; Zeng, Yu, Lu, & Paul, 2005)

Several studies illustrated that the structures of nanocomposite materials greatly impact properties and performances (Chen & Zhang, 2006; Kumar, Sandeep, Alavi, Truong, & Gorga, 2010a). Studies correlating structures and properties have repeated demonstrated that achieving either intercalation or exfoliation of layered nanoclay is critical to improve the properties of nanocomposite materials (Le Corre, Bras, & Dufresne, 2010; Tang, Alavi, & Herald, 2008a). Toward this direction, modification of nanoclays by increasing basal spacing (distance between clay layer platelets, d-spacing) with intercalated and/or exfoliated structures, prior to

incorporation into the polymer matrix, is a viable approach in improving the structure and properties of the final nanocomposite materials (Feng, Zhao, Gong, & Yang, 2004; Lin, Wei, Juang, & Tsai, 2007; Mallakpour & Dinari, 2011). Physically, the enlarged d-spacing makes it easier for polymer chains to enter the galleries between clay layers.

To enlarge d-spacing, strategies have been developed by chemically modifying surface properties of MMT or physically coating MMT with molecules (Feng, Zhao, Gong, & Yang, 2004; Lin, Wei, Juang, & Tsai, 2007; Mallakpour & Dinari, 2011; Yang, Zhu, Yin, Wang, & Qi, 1999). Yang *et al.* (Yang, Zhu, Yin, Wang, & Qi, 1999) surface-modified MMT by using three types of intercalation agents – amino acids, primary aliphatic amines, and quaternary ammonium salt, and found that the dispersion behavior of MMT in organic solvents depended on the type of the functional group and the bulky group of the intercalation agent. Also, d-spacing was found to increase with the length of the alkyl group of an intercalation agent, which makes it possible for modification by molecules with large molecular weight. Ion exchange was applied to modify the Na^+-MMT by hydrochloric acid to enlarge the d-spacing from 1.2 nm to 1.5 nm, followed by intercalation of MMT with bovine serum albumin (BSA), resulting in a further enlarged d-spacing of 3.2 nm (Lin, Wei, Juang, & Tsai, 2007). The above studies show that chemical and physical modification could increase the d-spacing.

2.1.4. Soy Protein-Based Nanocomposite

Soy proteins have been extensively studied for bio-derived packaging materials, with several recent studies investigating the improvement of mechanical and barrier properties of nanocomposite films after incorporating nanoclays such as montmorillonite (MMT) (Arora & Padua, 2010; Chang, Yang, Huang, Xia, Feng, & Wu, 2009; Chen & Zhang, 2006; Guilherme, Mattoso, Gontard, Guilbert, & Gastaldi, 2010; Kumar, Sandeep, Alavi, Truong, & Gorga, 2010a,

2010b; Lee & Kim, 2010; Martucci & Ruseckaite, 2010). SPI/MMT nanocomposite films have been reported for decreased water vapor and oxygen permeabilites and increased elastic modulus and tensile strength (Lee & Kim, 2010). Chen & Zhang (Chen & Zhang, 2006) developed SPI-based nanocomposite bioplastics with highly exfoliated MMT that demonstrated significantly improved mechanical strengths and thermal-stabilities when compared to the control without MMT. Kumar *et al*. (2010a, 2010b) applied melt extrusion to achieve intercalation/exfoliation of MMT, and the resultant SPI/MMT cast films were greatly improved for tensile strength, storage modulus, glass transition temperature, water barrier property, and thermal stability. Exfoliation of nanocomposite was achieved with modified MMT at MMT content lower than 5%, while intercalated to disorderly intercalated structures were developed at higher MMT content (15%). The studies above indicate that both mechanical and barrier properties of soy protein films could be improved when nanoclays are incorporated to form soy protein-based nanocomposite materials and films.

2.2. CROSSLINKING AS A POTENTIAL METHOD TO ENHANCE THE PROPERTIES OF PROTEIN-BASED NANOCOMPOSITES

The highly intercalated or exfoliated MMT nanoclay has repeatedly been shown to improve the mechanical and barrier properties of bio-nanocomposite materials, which may be further improved by strengthening the interactions between matrix polymers and MMT. Crosslinking is a potential method for improving the interaction among the protein-based nanocomposite system since crosslinking could form the strong covalent bondings between protein molecules, and enhance the interactions of the nanocomposite system. In addition, crosslinking decreases the solubility of protein and enhances the hydrophobic effect (Mohamed,

Hojilla-Evangelista, Peterson, & Biresaw, 2007). Enzymatic and chemical cross-linking approaches have been studied for soy proteins to enhance the gel or polymer properties (Caillard, Remondetto, & Subirade, 2009, 2010; de Carvalho & Grosso, 2004; Gan, Latiff, Cheng, & Easa, 2009; Jiang, Tang, Wen, Li, & Yang, 2007; Yildirim & Hettiarachchy, 1998).

2.2.1. Chemical Crosslinking

Chemical crosslinking of soy protein includes crosslinking induced by chemicals containing aldehyde groups (Song, Tang, Wang, & Wang, 2011). Chemical crosslinkers containing aldehyde groups include glutaraldehyde, formaldehyde, glyxoal, dialdehyde starch, hexanedial, biacetyl, and cyclopentane-dione (Figure 2.3) and have been widely utilized for crosslinking proteins (Gerrard, Meade, Millera, Brown, Yasir, Sutton, et al., 2005). Glutaraldehyde was observed to be more reactive than formaldehyde and glyceraldehyde in crosslinking wheat protein (Gerrard, Brown, & Fayle, 2003).

Crosslinking of proteins via aldehyde groups formed covalent bonds, i.e., amide (CO-NH) bonds, between protein chains by crosslinking the amino residues of lysine on protein molecules and aldehyde groups on cross-linkers, resulting in the loss of lysine residues on proteins (Gerrard, et al., 2005; Gonzalez, Strumia, & Igarzabal, 2011; Song, Tang, Wang, & Wang, 2011). This type of crosslinking reaction is called “Maillard-type” crosslinking because of the covalent amide bonds formed (Caillard, Remondetto, & Subirade, 2009, 2010).

In the presence of NaCl, cross-linking soy protein led to the formation of a less porous network, consisting of smaller flocs and/or smaller particles, and formed stronger gels (Caillard, Remondetto, & Subirade, 2009). Soy protein crosslinkd by glutaraldehyde had a lower solubility, lower emulsifying properties and higher foaming stabilities than original SPI. Conversely, glutaraldehyde treatment enhanced tensile strength and elongation at break of SPI films, more

significantly at increased glutaraldehyde concentrations (Park, Bae, & Rhee, 2000). Increased tensile properties and improved processability as a resin of SPC were obtained by crosslinking with glutaraldehyde to manufacture flax fabric-reinforced composites (Chabba & Netravali, 2005).

2.2.2. Enzymatic Crosslinking

Enzymes showing the capability of cross-linking proteins include transglutaminase (EC 2.3.2.13, protein-glutamine γ-glutamyltransferase, TGase), lipoxygenase, lysyl oxidase, polyphenol oxidase and peroxidase. TGase is the most used enzyme, with the capability of catalyzing crosslinking reactions between protein molecules, peptides, and primary amines through acyl transfer reactions to form inter- or intramolecular ε-(γ-glutamyl)lysine isopeptidic bonds (Seguro, Nio, & Motoki, 1996; Zhu, Bol, Rinzema, Tramper, & Wijngaards, 1999). The enzymatic crosslinking reaction is presented in Figure 2.4 for the formation of an isopeptide bond between two protein molecules. TGase is ubiquitous, and modern biotechnology has made it possible to produce microbial TGase (mTGase) for commercial applications. The mTGase has been studied extensively to improve functional properties of food proteins and protein-containing products such as meat (Motoki & Seguro, 1998; Seguro, Nio, & Motoki, 1996). The studied functionalities include hydration ability, emulsifying activities, thermal properties, and gel or film-forming ability (Jiang, Tang, Wen, Li, & Yang, 2007a).

Enzyme activity of TGase is effectively affected by pH and temperature. In one study, the catalyzing activity of TGase from *Streptoverticillium ladakanum* was observed to be optimum at pH 6.0 and 50 °C and stable at pH 5.0-7.0 (Tsai, Lin, & Jiang, 1996). Another group claimed the best enzyme activity at pH 5.5 and 40 °C (Ho, Leu, Hsieh, & Jiang, 2000). Both groups agreed that TGase activity was high and stable at the pH range of 5.0-7.0. The deactivation of TGase

was observed after treatment at 55°C for ca. 30 min and was more noticeable at increased temperatures, e.g., at 65 °C for 2-3 min (Nury, Meunier, & Mouranche, 1989). However, soy proteins treated by mTGase at pH 6.0 did not form films by casting. At pH 7.0, TGase with high enzyme activity might catalyze the initial protein aggregates in film-forming dispersions to achieve more gigantic aggregates, leading to a remarkable decrease in tensile strength and the percentage of elongation at break for formed films (Jiang, Tang, Wen, Li, & Yang, 2007). The slower cross-linking reaction forms a more compact network for SPI film with higher mechanical properties.

Besides pH and temperature, enzyme concentration is critical for generating TGase-treated protein films with enhanced properties. Treatment with a relatively low concentration of mTGase (4 U/g), compared up to 60 U/g SPI, significantly increased the tensile strength and surface hydrophobicity of enzyme-treated SPI films, indicating that approximate 4U/g SPP is an optimum concentration for obtaining improved mechanical and barrier properties from TGase-crosslinked soy protein films (Jiang, Tang, Wen, Li, & Yang, 2007; Tang & Jiang, 2007). Slow cross-linking reactions by mTGase, corresponding to relatively low TGase addition, favored the formation of a more compact network for SPI films (Jiang, Tang, Wen, Li, & Yang, 2007). At higher concentration of mTGase, mTGase-treated protein films had decreased mechanical properties. In addition, Gan *et al.* (Gan, Latiff, Cheng, & Easa, 2009) reported that reduced solubility and increased surface hydrophobicity of soy protein was observed after treatment by mTGase, and the films prepared from mTGase-treated soy protein had decreased solubility and improved mechanical properties such as tensile strength and elongation at break .

2.3. CONCLUSIONS AND OUTLOOK

Bio-nanocomposites, consisting of inorganic nanoclays dispersed in a biopolymer matrix, have the potential to improve the mechanical, barrier, and thermo-resistance properties of naturally renewable and degradable biopolymer-based packaging films. The properties of nanocomposite materials are highly impacted by their structure, and the present review suggests that modification of nanoclays by increasing basal spacing with intercalated and/or exfoliated structures prior to its incorporation into the polymer matrix is a viable approach. Further, for protein-based nanocomposites, crosslinking has the potential to improve the structures and thus mechanical and barrier properties. This dissertation research was thus conducted based on these two directions, with Chapters 3 and 4 probing modification of MMT structures by surface-coating with plant proteins and Chapters 5 and 6 investigating enzymatic and chemical approaches in improving interactions in soy protein-based nanocomposite systems. The study may provide a feasible approach to develop new nanocomposites with enhanced mechanical and barrier properties.

LIST OF REFERENCES

Ahmed, J., & Varshney, S. K. (2011). Polylactides-chemistry, properties and green packaging technology: a review. *International Journal of Food Properties, 14*(1), 37-58.

Alexandre, M., & Dubois, P. (2000). Polymer-layered silicate nanocomposites: preparation, properties and uses of a new class of materials. *Materials Science & Engineering R-Reports, 28*(1-2), 1-63.

Arora, A., & Padua, G. W. (2010). Review: nanocomposites in food packaging. *Journal of Food Science, 75*(1), R43-R49.

Badley, R. A., Atkinson, D., Hauser, H., Oldani, D., Green, J. P., & Stubb, J. M. (1975). The structure, physical and chemical properties of the soy bean protein glycinin. *Biochim Biophys Acta, 412*, 214-428.

Caillard, R., Remondetto, G. E., & Subirade, M. (2009). Physicochemical properties and microstructure of soy protein hydrogels co-induced by Maillard type cross-linking and salts. *Food Research International, 42*(1), 98-106.

Caillard, R., Remondetto, G. E., & Subirade, M. (2010). Rheological investigation of soy protein hydrogels induced by Maillard-type reaction. *Food Hydrocolloids, 24*(1), 81-87.

Cao, N., Fu, Y. H., & He, J. H. (2007). Preparation and physical properties of soy protein isolate and gelatin composite films. *Food Hydrocolloids, 21*(7), 1153-1162.

Capek, I. (2006). Nanocomposite structures and dispersions : science and nanotechnology--fundamental principles and colloidal particles

Chabba, S., & Netravali, A. N. (2005). 'Green' composites Part 1: Characterization of flax fabric and glutaraldehyde modified soy protein concentrate composites. *Journal of Materials Science, 40*(23), 6263-6273.

Chang, P. R., Yang, Y., Huang, J., Xia, W. B., Feng, L. D., & Wu, J. Y. (2009). Effects of layered silicate structure on the mechanical properties and structures of protein-based bionanocomposites. *Journal of Applied Polymer Science, 113*(2), 1247-1256.

Chen, P., & Zhang, L. (2006). Interaction and properties of highly exfoliated soy protein/montmorillonite nanocomposites. *Biomacromolecules, 7*(6), 1700-1706.

Cho, S. Y., & Rhee, C. (2004). Mechanical properties and water vapor permeability of edible films made from fractionated soy proteins with ultrafiltration. *Lebensmittel-Wissenschaft Und-Technologie-Food Science and Technology, 37*(8), 833-839.

Council, S. P. (1987). Soy protein products: characteristics, nutritional aspects, and utilization. Washington, DC.

Cuq, B., Gontard, N., & Guilbert, S. (1998). Proteins as agricultural polymers for packaging production. *Cereal Chemistry, 75*(1), 1-9.

Dang, Q. Q., Lu, S. D., Yu, S., Sun, P. C., & Yuan, Z. (2010). Silk fibroin/montmorillonite nanocomposites: effect of pH on the conformational transition and clay dispersion. *Biomacromolecules, 11*(7), 1796-1801.

de Azeredo, H. M. C. (2009). Nanocomposites for food packaging applications. *Food Research International, 42*(9), 1240-1253.

de Carvalho, R. A., & Grosso, C. R. F. (2004). Characterization of gelatin based films modified with transglutaminase, glyoxal and formaldehyde. *Food Hydrocolloids, 18*(5), 717-726.

Essington, M. E. (2003). Soil and water chemistry: an intergrative approach *CRC Press*, p58, 65, 68.

Feng, M., Zhao, C. G., Gong, F. L., & Yang, M. S. (2004). Study on the modification of sodium montmorillonite with amino silanes. *Acta Chimica Sinica, 62*(1), 83-87.

Fishman, M. L. (1997). Edible and biodegradable polymer films: challenges and opportunities. *Food Technology, 51*(2), 16-16.

Gan, C.Y., Latiff, A. A., Cheng, L.H., & Easa, A. M. (2009). Gelling of microbial transglutaminase cross-linked soy protein in the presence of ribose and sucrose. *Food Research International, 42*(10), 1373-1380.

Gerrard, J. A., Brown, P. K., & Fayle, S. E. (2003). Maillard crosslinking of food proteins II: the reactions of glutaraldehyde, formaldehyde and glyceraldehyde with wheat proteins in vitro and in situ. *Food Chemistry, 80*(1), 35-43.

Gerrard, J. A., Meade, S. J., Millera, A. G., Brown, P. K., Yasir, S. B. M., Sutton, K. H., & Newberry, M. P. (2005). Protein cross-linking in food. In J. W. Baynes, V. M. Monnier, J. M. Ames & S. R. Thorpe (Eds.), *Maillard Reaction: Chemistry at the Interface of Nutrition, Aging, and Disease*, vol. 1043 (pp. 97-103).

Gonzalez, A., Strumia, M. C., & Igarzabal, C. I. A. (2011). Cross-linked soy protein as material for biodegradable films: Synthesis, characterization and biodegradation. *Journal of Food Engineering, 106*(4), 331-338.

Guilherme, M. R., Mattoso, L. H. C., Gontard, N., Guilbert, S., & Gastaldi, E. (2010). Synthesis of nanocomposite films from wheat gluten matrix and MMT intercalated with different quaternary ammonium salts by way of hydroalcoholic solvent casting. *Composites Part a-Applied Science and Manufacturing, 41*(3), 375-382.

Gunister, E., Pestreli, D., Unlu, C. H., Atici, O., & Gungor, N. (2007). Synthesis and characterization of chitosan-MMT biocomposite systems. *Carbohydrate Polymers, 67*(3), 358-365.

Ho, M. L., Leu, S. Z., Hsieh, J. F., & Jiang, S. T. (2000). Technical approach to simplify the purification method and characterization of microbial transglutaminase produced from Streptoverticillium ladakanum. *Journal of Food Science, 65*(1), 76-80.

Jahangir, S., & Leber, M. J. . (2007). Biodegradable good packaging: an environmental imperative. *Industry Report*, 1-20.

Jiang, Y., Tang, C.H., Wen, Q.B., Li, L., & Yang, X.Q. (2007). Effect of processing parameters on the properties of transglutaminase-treated soy protein isolate films. *Innovative Food Science & Emerging Technologies, 8*(2), 218-225.

Kinsella, J. E. (1979). Functional properties of soy proteins. *J. Am. Oil Chem. Soc., 56*(3), 242-258.

Koshiyam.I. (1968). Factors influencing conformation changes in a 7S protein of soybean globulins by ultracentrifugal investigations. *Agricultural and Biological Chemistry, 32*(7), 879-&.

Krochta, J. M., & DeMulderJohnston, C. (1997). Edible and biodegradable polymer films: challenges and opportunities. *Food Technology, 51*(2), 61-74.

Kumar, P. (2009). Development of bio-nanocomposite films with enhanced mechanical and barrier properties using extrusion processing. *North Carolina State University. Ph.D dissertation*.

Kumar, P., Sandeep, K. P., Alavi, S., Truong, V. D., & Gorga, R. E. (2010a). Effect of type and content of modified montmorillonite on the structure and properties of bio-

nanocomposite films based on soy protein isolate and montmorillonite. *Journal of Food Science, 75*(5), N46-N56.

Kumar, P., Sandeep, K. P., Alavi, S., Truong, V. D., & Gorga, R. E. (2010b). Preparation and characterization of bio-nanocomposite films based on soy protein isolate and montmorillonite using melt extrusion. *Journal of Food Engineering, 100*(3), 480-489.

Le Corre, D., Bras, J., & Dufresne, A. (2010). Starch nanoparticles: a review. *Biomacromolecules, 11*(5), 1139-1153.

Lee, J. E., & Kim, K. M. (2010). Characteristics of Soy Protein Isolate-Montmorillonite Composite Films. *Journal of Applied Polymer Science, 118*(4), 2257-2263.

Lin, J. J., Wei, J. C., Juang, T. Y., & Tsai, W. C. (2007). Preparation of protein-silicate hybrids from polyamine intercalation of layered montmorillonite. *Langmuir, 23*(4), 1995-1999.

Mallakpour, S., & Dinari, M. (2011). Preparation and characterization of new organoclays using natural amino acids and Cloisite Na(+). *Applied Clay Science, 51*(3), 353-359.

Markets, R. a. (2011). The global outlook for biodegradable packaging. Accessed by website: http://www.researchandmarkets.com/research/5e27e0/the_global_outlook. *Business Insights, June*, 110.

Marsh, K., & Bugusu, B. (2007). Food packaging - Roles, materials, and environmental issues. *Journal of Food Science, 72*(3), R39-R55.

Martucci, J. F., & Ruseckaite, R. A. (2010). Biodegradable three-layer film derived from bovine gelatin. *Journal of Food Engineering, 99*(3), 377-383.

Maruyama, N., Katsube, T., Wada, Y., Oh, M. H., Barba De La Rosa, A. P., Okuda, E., Nakagawa, S., & Utsumi, S. (1998). The roles of the N-linked glycans and extension

regions of soybean beta-conglycinin in folding, assembly and structural features. *Eur J Biochem, 258*, 854-862.

Mo, X. Q., Sun, X. S., & Wang, Y. Q. (1999). Effects of molding temperature and pressure on properties of soy protein polymers. *Journal of Applied Polymer Science, 73*(13), 2595-2602.

Mohamed, A., Hojilla-Evangelista, M. P., Peterson, S. C., & Biresaw, G. (2007). Barley protein isolate: Thermal, functional, rheological, and surface properties. *Journal of the American Oil Chemists Society, 84*(3), 281-288.

Motoki, M., & Seguro, K. (1998). Transglutaminase and its use for food processing. *Trends in Food Science & Technology, 9*(5), 204-210.

Nury, S., Meunier, J. C., & Mouranche, A. (1989). The kinetics of the thermal deactivation of transglutaminase from guinea-pig liver. *European Journal of Biochemistry, 180*(1), 161-166.

Okamoto, S. (1978). Factors affecting protein film formation. *Cereal Foods World, 23*(5), 256-262.

Paetau, I., Chen, C. Z., & Jane, J. L. (1994). Biodegradable plastics made from soybean products.1. effect of preparation and processings on mechanical-properties and water-absorption. *Industrial & Engineering Chemistry Research, 33*(7), 1821-1827.

Park, S. K., Bae, D. H., & Rhee, K. C. (2000). Soy protein biopolymers cross-linked with glutaraldehyde. *Journal of the American Oil Chemists Society, 77*(8), 879-883.

Petruccelli, S., & Anon, M. C. (1995). Soy protein isolate components and their interactions. *Journal of Agricultural and Food Chemistry, 43*(7), 1762-1767.

Renkema, J. M. S., Knabben, J. H. M., & van Vliet, T. (2001). Gel formation by beta-conglycinin and glycinin and their mixtures. *Food Hydrocolloids, 15*(4-6), 407-414.

Seguro, K., Nio, N., & Motoki, M. (1996). Some characteristics of a microbial protein cross-linking enzyme: Transglutaminase. In N. K. A. C. L. K. P. J. Parris (Ed.), *Macromolecular Interactions in Food Technology*, vol. 650 (pp. 271-280).

Song, F., Tang, D. L., Wang, X. L., & Wang, Y. Z. (2011). Biodegradable soy protein isolate-based materials: a review. *Biomacromolecules, 12*(10), 3369-3380.

Song, F., & Zhang, L. M. (2008). Enzyme-catalyzed formation and structure characteristics of a protein-based hydrogel. *Journal of Physical Chemistry B, 112*(44), 13749-13755.

Sorrentino, A., Gorrasi, G., & Vittoria, V. (2007). Potential perspectives of bio-nanocomposites for food packaging applications. *Trends in Food Science & Technology, 18*(2), 84-95.

Tang, C.H., & Jiang, Y. (2007). Modulation of mechanical and surface hydrophobic properties of food protein films by transglutaminase treatment. *Food Research International, 40*(4), 504-509.

Tang, C. H., Choi, S. M., & Ma, C. Y. (2007). Study of thermal properties and heat-induced denaturation and aggregation of soy proteins by modulated differential scanning calorimetry. *International Journal of Biological Macromolecules, 40*(2), 96-104.

Tang, X. Z., Alavi, S., & Herald, T. J. (2008a). Barrier and mechanical properties of starch-clay nanocomposite films. *Cereal Chemistry, 85*(3), 433-439.

Tang, X. Z., Alavi, S., & Herald, T. J. (2008b). Effects of plasticizers on the structure and properties of starch-clay nanocomposite films. *Carbohydrate Polymers, 74*(3), 552-558.

Thanh, V. H., & Shibasaki, K. (1976a). Heterogeneity of beta-conglycinin. *Biochimica Et Biophysica Acta, 439*(2), 326-338.

Thanh, V. H., & Shibasaki, K. (1976b). Major proteins of soybean seeds - straightforward fractionation and their characterization. *Journal of Agricultural and Food Chemistry, 24*(6), 1117-1121.

Tsai, G. J., Lin, S. M., & Jiang, S. T. (1996). Transglutaminase from Streptoverticillium ladakanum and application to minced fish product. *Journal of Food Science, 61*(6), 1234-1238.

Utsumi, S., & Kinsella, J. E. (1985). Function relationships in food proteins: subunit interactions in heat-induced gelation of 7S, 11S, and soy isolate proteins. *Journal of Agricultural and Food Chemistry, 33*(2), 297-303.

Weiss, J., Takhistov, P., & McClements, D. J. (2006). Functional materials in food nanotechnology. *Journal of Food Science, 71*(9), R107-R116.

Wolf, W. J. (1970). Soybean protiens - their functional, chemical, and physical properties. *Journal of Agricultural and Food Chemistry, 18*(6), 969-&.

Xiang, L. X., Tang, C. Y., Cao, J., Wang, C. Y., Wang, K., Zhang, Q., Fu, Q., & Zhao, S. G. (2009). Preparation and characterization of soy protein isolate (SPI)/montmorillonite (MMT) bionanocomposites. *Chinese Journal of Polymer Science, 27*(6), 843-849.

Yang, Y., Zhu, Z. K., Yin, J., Wang, X. Y., & Qi, Z. E. (1999). Preparation and properties of hybrids of organo-soluble polyimide and montmorillonite with various chemical surface modification methods. *Polymer, 40*(15), 4407-4414.

Yildirim, M., & Hettiarachchy, N. S. (1998). Properties of films produced by cross-linking whey proteins and 11S globulin using transglutaminase. *Journal of Food Science, 63*(2), 248-252.

Zeng, Q. H., Yu, A. B., Lu, G. Q., & Paul, D. R. (2005). Clay-based polymer nanocomposites: Research and commercial development. *Journal of Nanoscience and Nanotechnology, 5*(10), 1574-1592.

Zhao, R. X., Torley, P., & Halley, P. J. (2008). Emerging biodegradable materials: starch- and protein-based bio-nanocomposites. *Journal of Materials Science, 43*(9), 3058-3071.

Zhu, Y., Bol, J., Rinzema, A., Tramper, J., & Wijngaards, G. (1999). Transglutaminase as a potential tool in developing novel protein foods. *Agro Food Industry Hi-Tech, 10*(1), 8-10.

APPENDIX

Table 2. 1 Examples of biopolymer films and their barrier and mechanical properties. Adapted from Krochta and De Mulder-Johnston (1997).

Material	Preparation	H_2O barrier[a]	O_2 barrier[b]	Mech. properties[c]	Cost, $/lb
Cellophane	Aqueous	Moderate	Good	Good	2.20
Cellulose Acetate	Extrusion	Moderate	Poor	Moderate	1.60-2.10
Starch/PVOH	Extrusion	Poor	Good	Good	1.50-3.00
PHB/V	Extrusion	Good	Good	Moderate	3.00-6.00
PLA	Extrusion	Moderate	Poor	Good	1.00-5.00
High Amylose Starch	Aqueous	Poor	Moderate	Moderate	0.60-0.70
Zein	95%EtOH	Moderate	Moderate	Moderate	10.25-15.50
Gluten	Aqueous-EtOH	Moderate	Good	Moderate	0.80-0.90
SPI	Aqueous	Poor	Good	Moderate	1.30-1.70
WPI	Aqueous	Poor	Good	Moderate	6.00-12.00

Table 2. 2 Functional properties performed by soy protein preparations in actual food systems.

Adapted from Kinsella (1979).

Functional property	Mode of action	Food system	Preparation used
Solubility	Protein solvation, pH dependent	Beverages	F,C,1, H
Water absorption and binding	Hydrogen-bonding of HOH, entrapment of HOH, no drip	Meats, sausages, breads, cakes	F,C
Viscosity	Thickening, HOH binding	Soups, gravies	F,C,1
Gelation	Protein matrix formation and setting	Meats, curds, cheese	C,1
Cohesion-adhesion	Protein acts as adhesive material	Meats, sausages, baked goods, pasta products	F,C,1
Elasticity	Disulfide links in gels deformable	Meats, bakery	1
Emulsification	Formation and stabilization of fat emulsions	Sausages, bologna, soup, cakes	F,C,1
Fat adsorption	Binding of free fat	Meats, sausages, donuts	F,C,1
Flavor-binding	Adsorption, entrapment, release	Simulated meats, bakery	C,1,H
Foaming	Forms stable films to entrap gas	Whipped toppings, chiffon desserts, angel cakes	1,W,H
Color control	Bleaching of lipoxygenase	Breads	F

[a]F, C, I, H, W denote soy flour, concentrate, isolate, hydrolyzate and soy whey, respectively.

Table 2. 3 Approximate amounts and molecular weights of components of soybean protein fractions.

Adapted from Wolf (1970).

Fraction	Percent of Total[a]	Components	Molecular Weight
2S	22	Trypsin inhibitors	8000, 21,500
		Cytochrome c	12,000
7S	37	Hemagglutinin	110,000
		Lipoxygenase	102,000
		β-Amylase	61,700
		7S Globulin	180,000–210,000
11S	31	11S Globulin	350,000
15S	11	...	~600,000

[a] Taken from Wolf *et al.* (1962).

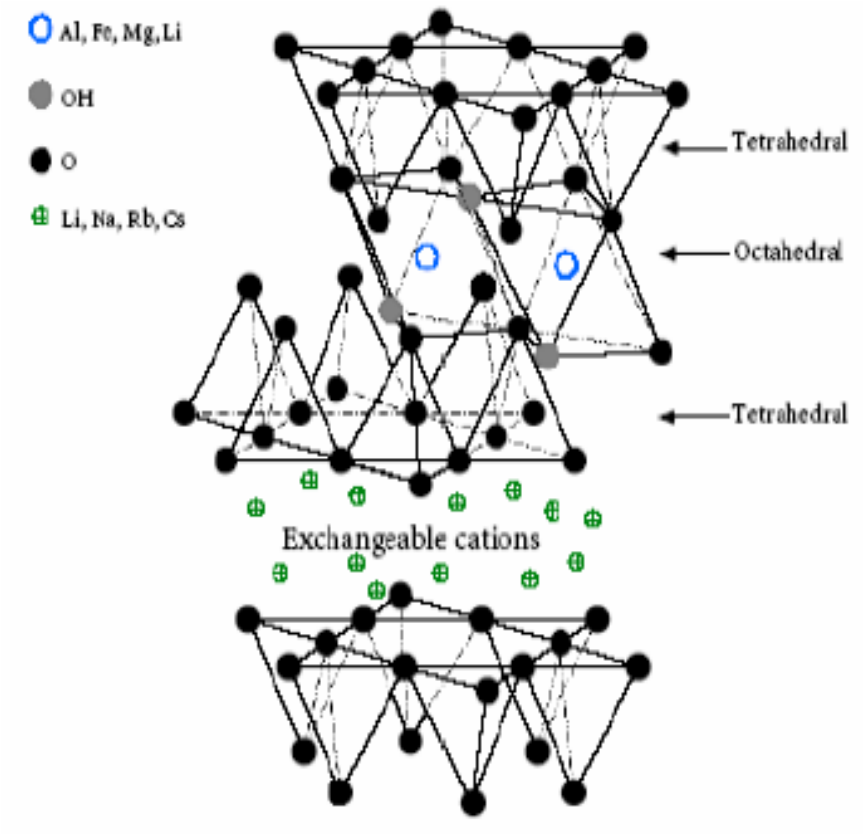

Figure 2. 1. Structure of montmorillonite clay.

Adapted from Kumar (2009).

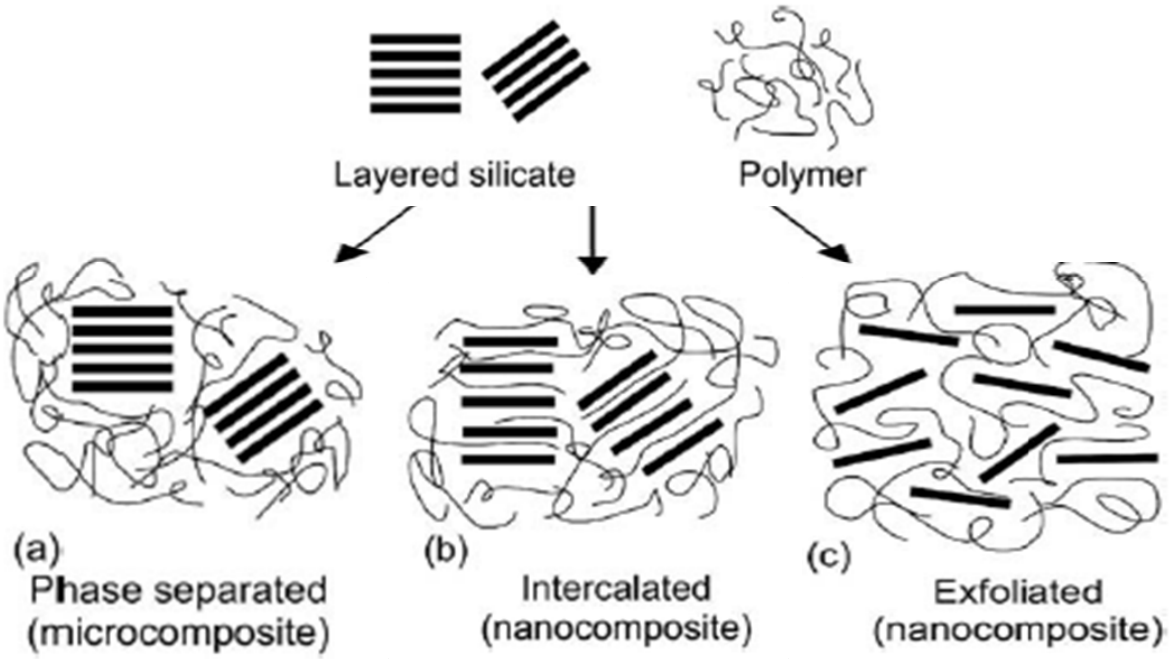

Figure 2. 2. Types of composites derived from interaction between clays and polymers: (a) phase-separated microcomposite; (b) intercalated nanocomposite and (c) exfoliated nanocomposite.

Adapted from Alexandre & Dubois (2000).

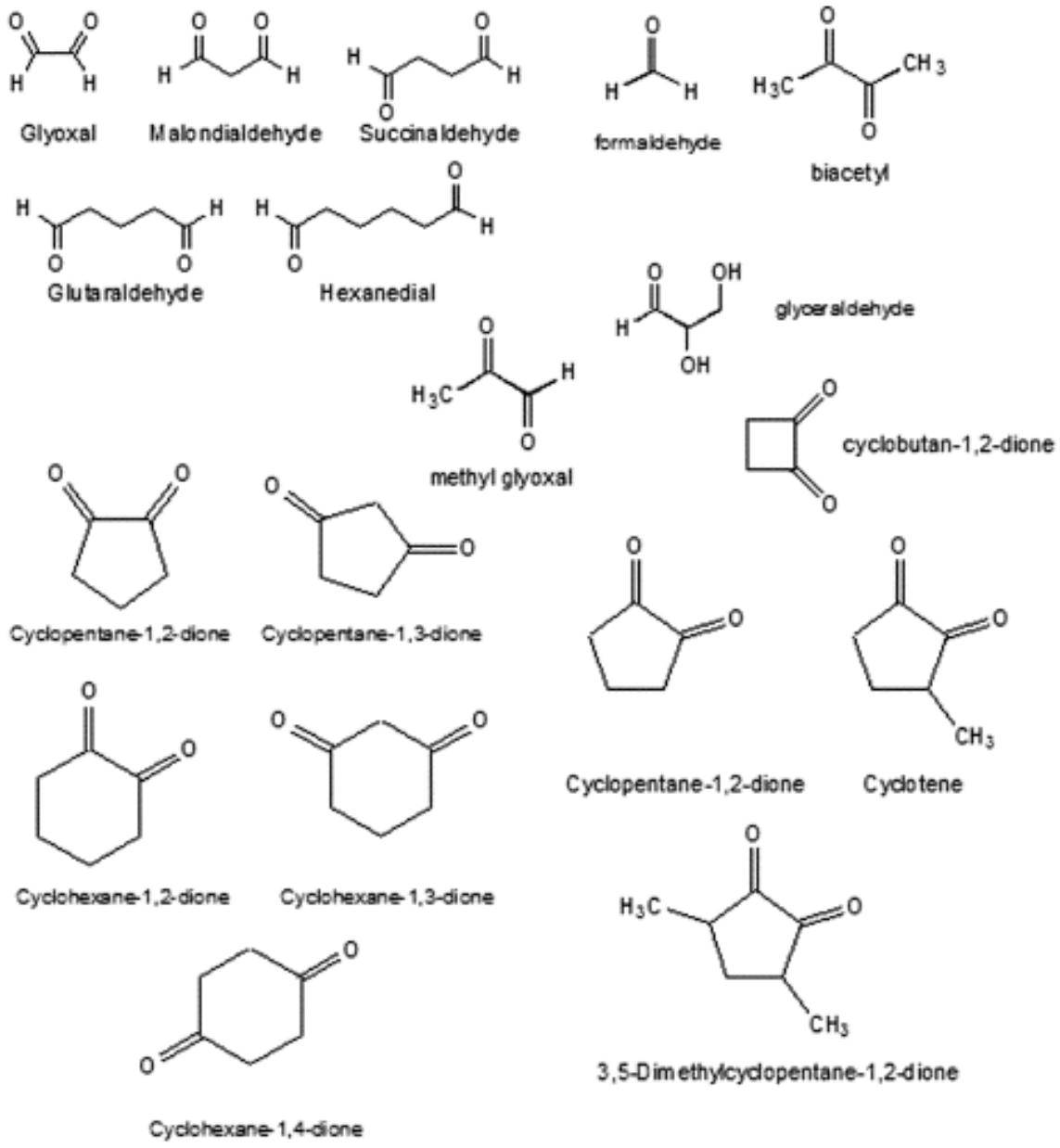

Figure 2. 3. List of chemicals containing aldehyde group.

Adapted from (Gerrard, et al., 2005).

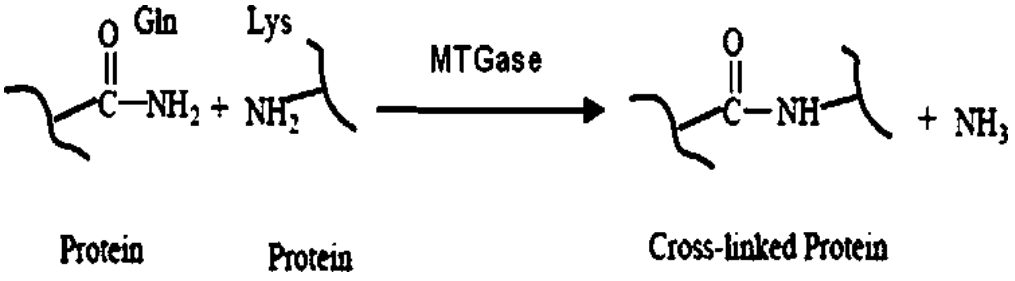

Figure 2. 4. A schematic of cross-linking reaction between proteins in enzyme crosslinking induced by TGase.

Adapted from (Song & Zhang, 2008).

CHAPTER 3 . SURFACE-COATING OF MONTMORILLONITE NANOCLAYS BY WATER SOLUBLE PROTEINS EXTRACTED FROM HOMINY FEED

3.1. ABSTRACT

Montmorillonite (MMT) nanoclay was surface-coated by water-soluble proteins, precipitated from hominy feed extract at pH 6.0, 5.5, and 4.3, to modify its native structure. Surface-coating was performed at 60 °C, pH 2.0-10.0, and MMT:protein mass ratios from 49:1 to 2:1, followed by lyophilizing the triple-washed precipitate for characterization. Proteins precipitated at pH 5.5 were most effective in developing intercalated and/or exfoliated MMT structures that were also impacted by the protein level and pH during coating. At pH 2.0, X-ray diffraction peaks of pristine MMT were no longer observed at an MMT:protein mass ratio of 4:1 or lower, while different degrees of intercalation were achieved at other pH conditions. The adsorptions of proteins on MMT at all studied pH conditions were confirmed by FTIR, analysis of adsorbed proteins, and zeta-potential. These results suggest that interactions involved in coating MMT include coulombic and non-coulombic forces.

Keywords: layered montmorillonite nanoclay, surface-coating, hominy protein, pH, intercalation, X-ray diffraction

3.2. INTRODUCTION

Natural biopolymers, including starches and proteins, have been studied extensively as packaging materials in the past two decades because they are renewable and bio-degradable (Cao, Fu, & He, 2007; Krochta & DeMulderJohnston, 1997; Le Corre, Bras, & Dufresne, 2010; Tang, Alavi, & Herald, 2008a), thereby potentially alleviating environmental pollution derived from non-degradable petroleum-based plastic products (Jahangir & Leber, 2007; Rimdusit, Jingjid, Damrongsakkul, Tiptipakorn, & Takeichi, 2008). However, when compared to the petro-plastic products, packaging films prepared from natural biopolymers have poor mechanical and barrier properties such as rigidness, brittleness and high water vapor and gas permeabilities (Kim, Ko, & Park, 2002; Krochta & DeMulderJohnston, 1997; Paetau, Chen, & Jane, 1994).

Nanocomposite materials recently have shown promises to improve mechanical and barrier properties because nanometer-sized fillers with high surface area facilitate the uniform distribution in and enhance the interfacial interaction with the biopolymer matrix (Adame & Beall, 2009; Le Corre, Bras, & Dufresne, 2010; Zhao, Torley, & Halley, 2008). The composition, dimension, and shape of nanofillers, as well as their spatial distribution in the matrix, are important factors impacting the properties of nanocomposite products (Capek, 2006).

Layered nanoclays have been extensively investigated to improve mechanical and barrier properties of biopolymer materials because of their availability, abundance and eco-friendliness (Dang, Lu, Yu, Sun, & Yuan, 2010; Tunc, Angellier, Cahyana, Chalier, Gontard, & Gastaldi, 2007; Zhao, Torley, & Halley, 2008). As a naturally existing clay, montmorillonite (MMT) has been one of the most studied nanofillers not only due to its low cost and abundance (Essington, 2003; Gunister, Pestreli, Unlu, Atici, & Gungor, 2007) but also because of the high surface area and large aspect ratios (ratio of length to thickness) from 50 to 1000 (de Azeredo, 2009; Le Corre,

Bras, & Dufresne, 2010). The large aspect ratio of MMT is a very important factor enhancing the properties of nanocomposites because, according to the theory of torturous path developed by Nielsen (Nielsen, 1967), MMT layers dispersed in biopolymer film matrix increase the tortuosity of the diffusion path for permeate molecules. The increased mass transfer resistance thereby reduces the diffusion coefficient of permeate molecules and improves the barrier properties of the nanocomposite films (Adame & Beall, 2009; Capek, 2006). Improving the dispersibility of nanoclay layers and their compatibility with matrix biopolymer plays an important role in developing the structures of final nanocomposite products, which in turn determines their mechanical and barrier properties. It is well accepted that nanocomposites with intercalated and/or exfoliated MMT nanolayers have much improved mechanical and barrier properties than conventional composite materials prepared with fillers dispersed as micrometer-sized structures (Le Corre, Bras, & Dufresne, 2010; Tang, Alavi, & Herald, 2008a).

Native MMT has platelet clusters with little specific surface area exposed to polymers (Arora & Padua, 2010), but the proper pretreatment or modification of MMT enhances its dispersion in the continuous phase and increases the surface area available for interaction with bulk polymer, that in turn improves nanocomposite performance. Arora & Padus (Arora & Padua, 2010) reported that chemical modification of hydrophilic nanoclays to be possessing hydrophobic surfaces improved the compatibility with hydrophobic polymers. Rimdusit *et al*. (Rimdusit, Jingjid, Damrongsakkul, Tiptipakorn, & Takeichi, 2008) observed that proper pre-swelling conditions promoted the dispersion of MMT and resulted in a highly exfoliated nanocomposite with methylcellulose being the matrix polymer. Adsorption of amines and amino acids was greater on marine sediments with a higher organic content, which changed surface chemistry of clay matter to improve compatibility with organic compounds (Wang & Lee, 1993).

Thus, surface-coating of MMT with protein may modify the structure of MMT for the enhanced affinity with bulk biopolymer and performance of the nanocomposite.

In this work, MMT was surface coated by water-soluble proteins extracted from hominy feed, a low-cost byproduct after separating starch from corn kernels in the dry-milling industry, in order to modify native structure of MMT nanoclay layers. In general, protein has a net zero charge at the isoelectric point (pI), a net positive charge at a pH below pI and a net negative charge at a pH above pI. MMT surface has highly negative charges (Chen & Zhang, 2006) that allow the adsorption of positively-charged hominy proteins based on the electrostatic interactions. The objective of this work was to study the effects of coating conditions such as pH and the mass ratio of MMT:protein on properties of modified MMT, including surface properties, basal spacing (d-spacing) and degrees of intercalation and/or exfoliation of MMT nanoclay. The prior-intercalated or exfoliated MMT can be used in production of nanocomposite materials.

3.3. MATERIALS AND METHODS

3.3.1. Materials

Na^+-montmorillonite, with a brand name of Cloisite® Na^+ Nanoclay, was purchased from Southern Clay Products, Inc. (Gonzales, TX) and had a cation exchange capacity of 92.6 mequiv/100g, according to the manufacturer. Hominy feed was a free sample from Bunge Milling (Danville, IL). Other chemicals were from Fisher Scientific (Fair Lawn, NJ), Sigma-Aldrich Co. (St. Louis, MO), or GE Healthcare (Amersham Biosciences Corp., Piscataway, NJ).

3.3.2. Extraction of Water Soluble Hominy Protein

The literature procedures and parameters for extracting proteins from soybean and corn kernels were adopted (L'Hocine, Boye, & Arcand, 2006; Paulis, Bietz, & Wall, 1975). The

preliminary experiments showed a higher protein content for extracts prepared at a higher pH value between 6.0 and 10.0. Thus, protein extraction in this study was conducted at pH 10.0. Specifically, hominy feed was ground with a coffee grinder (Hamilton Beach Proctor-Silex, Inc., Southern Pines, NC) to decrease the particle size and enhance the extraction efficiency. To remove lipids, the powder was suspended in hexane at a solid:liquid volume ratio of 1:4 for 30 min using a stirring plate followed by gravitational sedimentation, decanting the serum, and re-suspending the slurry in hexane, which was repeated for at least 7 times. The defatted powder was left in a fume hood overnight to evaporate hexane. The final powder was suspended in deionized water at a solid:liquid mass ratio of 1:10, adjusted to pH 10.0 using 4 N NaOH, and heated to 48 °C under constant agitation for 3 h (model Isotemp®, Fisher Scientific, Fair Lawn, NJ). The extract was separated by centrifugation (Sorvall RC 5B Plus, Newtown, CT) at 3,778*g* for 15 min at ambient temperature, followed by filtration twice with #2 filter paper (Whatman®, Lawrence, KS). To improve the protein extraction yield, the extraction was repeated three times on the same batch of defatted hominy feed powder. Since little information is available about the acid-precipitation of water soluble hominy protein, the filtrate was adjusted to pH 6.0, 5.5 and 4.3, in sequence, using 6 N HCl to precipitate water soluble proteins. Protein precipitated at each pH was separated by centrifugation at 3,778*g* for 30 min, and the supernatant was collected for acidification to a lower pH. To wash off impurities, the precipitate from centrifugation was re-suspended in deionized water, adjusted to pH 10.0, re-precipitated at the corresponding pH, and centrifuged at 3,778*g* for 15 min. The washing procedures were repeated three times at ambient temperature. The final precipitate was neutralized and freeze-dried (model Freezone 4.5, Labconco Corp., Kansas City, MO). The lyophilized samples were collected and stored in a -20 °C freezer till further experiments.

To estimate the protein content, 0.1 g of lyophilized powder was dissolved in 2 mL of deionized water, and the total protein content was determined according to the Bradford method. A Coomassie® Plus Protein Assay kit (product 23236, Pierce Biotechnology, Rockford, IL) was used, and the absorbance was measured at 595 nm by using a UV/Vis spectrophotometer (model Biomate 5, Thermo Electron Corporation, Woburn, MA). Bovine serum albumin (BSA) was used as a reference. Triplicate tests were performed for each sample.

3.3.3. Characterization of Hominy Protein by Two-dimensional Gel Electrophoresis (2D-GE)

The 2D-GE was conducted according to the method of GE Healthcare. To remove non-protein impurities, the lyophilized powder was dissolved in a solubilization solution, consisting of 2% sodium dodecyl sulfate (SDS), 40 mM Tris™ base and 60 mM dithiothreitol (DTT), and concentrated using a 2-D Clean-up Kit (Amersham Biosciences Corp., Piscataway, NJ). The protein content after clean-up was quantified with a Quant Kit (Amersham Biosciences Corp., Piscataway, NJ). The absorbance at 480 nm (BioTek Synergy HT, Winooski, VT) was applied to determine protein content from the standard curve established from BSA standard solutions. The concentrated protein sample was diluted with a re-hydration buffer to a final total volume of 200 μL and protein content estimated as 120 μg, which was used to rehydrate one 11-cm gel strip of either pH 3-10 or pH 4-7 (Immobiline™ DryStrip gels, GE Healthcare, Piscataway, NJ). The first dimension (isoelectric focusing, IEF) separation was conducted at steps of 500 V for 1 h, a linear gradient increase in voltage to 1000 V in 1 h, another linear gradient increase of voltage to 6000 V in 2 h, and holding at 6000 V for approximately 30 min. The second dimension step was performed using a linear polyacrylamide gel laboratory-prepared. Proteins on the gel strip were reduced by 5 mL of 2% SDS buffer with 1% DTT for 15 min, and the separation was conducted

using the DALTsix gel electrophoresis instrument (GE Healthcare, Amersham Biosciences Corp., Piscataway, NJ) at a beginning voltage of 80 V for 1 h and then a running voltage of 500 V for around 5 h till the bromophenol blue in EZ-Run™ Rec Protein Ladder marker (Fisher Scientific, Fair Lawn, NJ) reached the gel bottom. The gels were stained in a mixture of methanol, acetic acid and coomassie Blue and de-stained by methanol and acetic acid till satisfactory visibility of protein spots, followed by scanned to obtain images.

3.3.4. Determination of Protein Solubility

To test the solubility of protein at coating conditions, 10 mg of the lyophilized extract powder was dissolved in 10 mL of 10 mM NaH_2PO_4 buffer with 4 mM sodium chloride, which corresponded to sodium ion concentration of 1% w/v MMT dispersion determined by atomic absorption spectroscopy at Department of Plant Science, the University of Tennessee (Knoxville, TN). After adjusting pH to 2.0-10.0 and centrifugation at 14,500*g* for 30 min, the supernatant was determined for protein concentration using the bicinchoninic acid (BCA) method. Commercial BCA™ Protein Assay Reagent A (product 23228, Pierce Biotechnology, Thermo Scientific, Rockford, IL) was utilized, and reagent B (4%w/v cupric sulfate) was freshly laboratory-prepared. The incubation was performed at 37 °C for 30 min, and the absorbance was recorded at 562 nm by using a UV/Vis spectrophotometer (model Biomate 5, Thermo Electron Corporation, Woburn, MA). BSA was used as a reference and tests were performed in triplicate for each sample.

3.3.5. Surface Coating of MMT

Coating experiments were performed using a solution intercalation method at 60 °C (P. Chen & Zhang, 2006). The lyophilized protein powder was dispersed in 10 mM NaH_2PO_4 buffer and adjusted to a desired pH. The dispersion was heated to 60 °C and stirred at 300 rpm for 30

min using a stirring hot plate. A dispersion of MMT was similarly prepared in a separate beaker. The MMT dispersion was slowly added to the protein solution to a predetermined MMT: protein mass ratio (49:1, 9:1, 4:1, 3:1 or 2:1), while being vigorously agitated at 1000 rpm and maintained at 60 °C. After stirring for 3 h at 60 °C, the resultant slurry was centrifuged at 3,778*g* for 15 min at ambient temperature. The supernatant was decanted, while the precipitate was re-suspended with the same amount of fresh buffer to wash off unbound and loosely bound proteins. The washing procedure was repeated three times, and the supernatants from the three repetitions were combined. Both the final precipitate and combined supernatant were freeze-dried (mode l Freezone 4.5, Labconco Corp., Kansas City, MO). The lyophilized samples were collected and stored in a -20 °C freezer for further characterization.

3.3.6. Determination of Amount of Protein Coated on MMT

The above lyophilized supernatant samples were dissolved in 10 mM NaH_2PO_4 buffer at pH 9, followed by centrifugation at 14,500*g* for 30 min to remove fine MMT. The protein remaining in the supernatant was measured using the BCA method and treated as the portion that did not coat MMT. The amount of bound protein was then determined by mass balance – the difference between the total protein used in coating and that unbound.

3.3.7. Zeta Potential of MMT

Zeta potential was determined for the final re-suspended precipitate in the above coating experiments and bare MMT samples suspended in phosphate buffer at pH 2.0-10.0 using a Delsa™ Nano C Zeta-Potential/Particle Size Analyzer (Beckman Coulter, Fullerton, CA). The bare MMT suspensions adjusted to a target pH were also stirred at 60 °C for 3 h prior to analysis. Three measurements were performed for each sample. Each measurement included 5 runs, each run for 10 cycles.

3.3.8. Wide-angle X-Ray Diffraction (WXRD)

WXRD experiments were performed at ambient temperature using an X-ray diffractometer (model X'Pert, PANalytical Inc., Westborough, MA) with a generator voltage of 45 kV and a current of 40 mA. The diffraction data was collected in the 2θ range from 2° to 12° in a fixed time mode with an increment of 0.02°. The XRD patterns were obtained from the X'Pert Data Viewer software (PANalytical Inc., Westborough, MA) as a function of 2θ angle. The identification of peaks and determination of d-spacing according to Bragg's equation (Prabhat. Kumar, 2009) were assisted by using the X'Pert HighScore Plus software (PANalytical Inc., Westborough, MA). The present experimental limit of detectable d-spacing also was calculated using eq. 1 (Dang, Lu, Yu, Sun, & Yuan, 2010; Tang, Alavi, & Herald, 2008a) at a 2θ angle of 2°.

$$d = \frac{\lambda}{2\sin(\theta)} \quad (1)$$

where θ is the angle of incidence, and λ is the wavelength of X-ray beam, which is 1.54 Å.

3.3.9. Fourier Transform Infrared Spectroscopy (FTIR)

FTIR analyses were conducted using a spectrometer (model Nicolet 670, Thermo Nicolet, Madison, WI) in the wavenumber range of 4000-400 cm^{-1} using a powdered potassium bromide (KBr) pellet method (Chen & Zhang, 2006; Gunister, Pestreli, Unlu, Atici, & Gungor, 2007). One mg of a sample and 100 mg of KBr were mixed and ground to fine powder that was then pressed into a clear or translucent pellet for measurement. A pristine KBr pellet was used as a background. The outputs were recorded in %Transmittance as a function of wavenumber.

3.3.10. Statistical Data Analysis

Data analyses were carried out by using SAS software (v. 9.3, SAS Institute Inc., Cary, NC). Significant differences were analyzed with a least-significant-difference ($P < 0.05$) mean separation method (LSD).

3.4. RESULTS AND DISCUSSION

3.4.1. Protein Extracted from Hominy Feed

The lyophilized powder mass corresponding to precipitation at pH 5.5 was about 2 and 5 times of that precipitated at pH 4.3 and 6.0, respectively. The protein content of freeze-dried protein extracts precipitated at pH 4.3, 5.5, and 6.0 was 58.75, 54.00, and 51.03%, respectively. The 2D-GE patterns of proteins precipitated at pH 4.3, 5.5 and 6.0 are presented in Figure 3.1. The IEF was conducted at pH ranges of 3.0-10.0 and 4.0-7.0. Extracts precipitated at pH 4.3 (Figure 3.1C) and pH 5.5 (Figure 3.1B) both showed proteins corresponding to pI of 4.8-5.1 and molecular weights of 13, 20 and 28 kDa and those with pI of 5.0-5.6 and molecular weights of 50 and 60-68 kDa, with the extract precipitated at pH 5.5 showing more proteins in the latter group. In addition, the sample precipitated at pH 4.3 had some spots corresponding to molecular weights of 80-90 kDa and pI of 4.8-5.0. As for the sample precipitated at pH 6.0 (Figure 3.1A), although the same amount of purified protein was loaded onto the gel strip, it showed very few spots on the gel, and most spots were located at molecular weights of 20-23 kDa and pI of 5.5-6.2. Molecular weights of most protein spots were consistent with the reported range of 10-66 kDa for proteins extracted from the dry-milled corn germ (Parris, Moreau, Johnston, Singh, & Dickey, 2006).

3.4.2. Coating of MMT at pH 2.0 Using Proteins Precipitated at Different pH Conditions

Theoretically, the highly negatively-charged MMT attracts the positively-charged proteins by coulombic forces (Dang, Lu, Yu, Sun, & Yuan, 2010; Ding & Henrichs, 2002; Essington, 2003; Wang & Lee, 1993). The first group of study was conducted at pH 2.0 where most proteins in the lyophilized extract powder are expected to be positively charged based on 2D-GE (Figure 3.1). To simplify description, PP4.3, PP5.5, and PP6.0 refer to proteins precipitated at pH 4.3, 5.5, and 6.0, respectively, while MP-4.3, -5.5, and -6.0 represent MMT coated by PP4.3, PP5.5, and PP6.0, respectively, hereafter. Further, coating experiments were performed by using a mass ratio of MMT:lyophilized extract powder for convenience of sample preparation, and the lyophilized extract powder is substituted by "protein" hereafter, although the powder has a significant portion of non-protein matter. This group of experiments was conducted at an MMT:protein mass ratio of 2:1 and pH 2.0. After coating, MMT was collected by centrifugation, triple-washed, and lyophilized. The lyophilized precipitates were characterized for crystalline structures and d-spacing by XRD and interactions by FTIR.

3.4.2.1. XRD patterns

As indicated in Figure 3.2, the XRD patterns of lyophilized extract powders did not show characteristic peaks in the 2θ range from 2° to 12°, indicating that all extract powders did not have ordered structures detectable within this 2θ range. Figure 3.3 shows that bare MMT had a sharp peak at 2θ of 7.1°, corresponding to d-spacing of 1.24 nm, characteristic for pristine MMT (Tang, Alavi, & Herald, 2008a). The sharp peak of MMT was no longer observed for MP-4.3 and MP-5.5. The disappearance of characteristic peaks in XRD patterns is due to changes from highly ordered structures to fully exfoliated or highly intercalated structures that are beyond the detectable 2θ range, i.e., <2° in our study, corresponding to a d-spacing value bigger than 4.41

nm (Chen & Zhang, 2006; Dang, Lu, Yu, Sun, & Yuan, 2010; Tang, Alavi, & Herald, 2008a). As for MP-6.0, a very broad and weak peak appeared at 2θ angle of ~ 6.5°, corresponding to a d-spacing value of 1.35 nm. Although the increase of d-spacing from 1.24 to 1.35 nm was not big, the onset 2θ angle shifted to left from 7.1° for pristine MMT to less than 5.0° for MP-6.0. According to Bragg's law, the shift of the diffraction peak towards a lower angle indicates the formation of a bigger basal spacing of intercalated clay layers (Tang, Alavi, & Herald, 2008a).

Because dilution of MMT by other compounds may lead to the misinterpretation of XRD patterns (Prabhat. Kumar, 2009), simple mixtures of MMT and protein powders at MMT:protein mass ratios of 2:1-49:1 were also characterized by XRD. Results in Figure 3.4 showed that the mixtures all demonstrated peaks corresponding to a 2θ angle of 7.0-7.1° and d-spacing values of 1.24-1.28 nm, very similar to that of the bare MMT (Figure 3.3). Therefore, coating of MMT by hominy protein resulted in exfoliated and/or intercalated structures.

3.4.2.2. FTIR

FTIR spectra of proteins precipitated at different pH conditions (Figure 3.5) showed characteristic peaks of proteins at wavenumbers of 3300 and 3110, 2925 and 2855, 1618-1681, 1530-1550 and 1244 cm^{-1}, which are due to the absorbance by functional groups of C–H, amide I (C=O stretching vibration), amide II (N-H bending and C-N stretching modes) and amide III bands (C-N stretching and N-H bending), in possible structures of $–CO-NH_2$, –CO-NH–, and/or –CO-N– (P. Chen & Zhang, 2006; Nakasato, Ono, Ishiguro, Takamatsu, Tsukamoto, & Mikami, 2004; Servagent-Noinville, Revault, Quiquampoix, & Baron, 2000). Among these peaks, the greatest difference between protein samples was observed at a wavenumber around 2855 cm^{-1}, which is attributed to C–H stretching vibration bands. PP4.3 had a smaller peak than PP5.5 and PP6.0 at this wavenumber, indicating a smaller amount of –CH structure. In addition, relative

intensities of the double-peaks at 1450-1400 cm^{-1} are different, implying different ratios of carboxyl (stronger peak at approximately 1450 cm^{-1}) to carboxylate (stronger peak at approximately 1410 cm^{-1}) groups. Since all extracts were neutralized before freeze-drying, the difference between double-peak intensities is then likely due to difference in compositions, including proteins as revealed in 2D-GE (Figure 3.1).

The FTIR spectra of MP-4.3, MP-5.5 and MP-6.0 (Figure 3.5) showed major peaks at wavenumbers of 2925, 2855, 1618-1681 and 1530-1550 cm^{-1}, indicating the presence of proteins in coated-MMT samples. The disappearance of peaks at 1244 cm^{-1} demonstrated the decreases in α-helix structure and β-sheet of proteins (Cai & Singh, 2004; Wang, Ke, Wang, Xi, & Cui, 2010), implying that secondary conformational changes in proteins occurred by adsorption on clay surfaces (Quiquampoix & Burns, 2007; Servagent-Noinville, Revault, Quiquampoix, & Baron, 2000). Compared to the spectra of protein samples, the double-peak at 1450-1400 cm^{-1} on the spectra of protein-coated MMT disappeared or was highly reduced, more significant for the treatment coated with protein precipitated at a lower pH. This observation implies the reduction of carboxyl or carboxylate groups, likely due to unpairing of some carboxylate side chains and binding of cationic side group with negatively charged MMT surface (Quiquampoix & Burns, 2007; Servagent-Noinville, Revault, Quiquampoix, & Baron, 2000). Meanwhile, the peak intensity of protein in coated MMT varied at wavenumbers of 1681-1618 cm^{-1}, with a less intensive peak at 1618 cm^{-1}, implying a reduced amount of amide I band than that for the protein sample (Servagent-Noinville, Revault, Quiquampoix, & Baron, 2000), agreeing with the structure transition of protein induced by self-association after coating. Additionally, hydrogen bonds can form between proteins and MMT platelets (Chen & Zhang, 2006), likely between either the amide or ketone groups of proteins and Si-O-Si or –OH groups of MMT. Hydrogen

bonding between protein and MMT surface was observed by slightly enhanced peaks at approximate 1100-1000 cm^{-1}, when comparing with either bare MMT or bare protein samples (Figure 3.5).

This group of experiments showed that PP4.3 and PP5.5 were more effective in surface-coating MMT than PP6.0. PP4.3 and PP5.5 were used in the next group of experiments to further study the impacts of coating pH and the MMT:protein mass ratio.

3.4.3. Effect of MMT:protein Mass Ratio on Surface-coating at pH 2.0

Our preliminary experiments at an MMT:protein mass ratio of 49:1 revealed that the addition of an insufficient amount of protein did not alter the XRD pattern of MMT. For this group of treatments, MMT was coated by PP4.3 and PP5.5 at pH 2.0 and additional MMT:protein mass ratios of 9:1 and 4:1. Figure 3.6A illustrates XRD patterns for MMT coated by PP4.3. Compared to the absence of the characteristic peak of MMT when coated at an MMT:protein mass ratio of 2:1, samples prepared with the two higher MMT:protein mass ratios demonstrated peaks appearing at 2θ angles smaller than that of the pristine MMT - the left shift, which is more noticeable at a smaller MMT:protein mass ratio, i.e., a higher protein mass level. Correspondingly, the d-spacing increased with an increase in protein mass, from ca. 1.32 nm at an MMT:protein mass ratio of 9:1 to 1.38 nm at an MMT:protein mass ratio of 4:1 (Table 3.1). At the MMT:protein mass ratio of 4:1, although the increase of d-spacing was modest (from 1.24 to 1.38 nm), the onset 2θ angle was less than 4.5°, showing a significant left shift when comparing to that of the pristine MMT (Figure 3.3), and the peak was overall much broader. The left-shift of the diffraction peak indicates the formation of some intercalated clay layers with a bigger basal spacing, according to the Bragg function (Tang, Alavi, & Herald, 2008a). Furthermore, a broader peak implies more disordered intercalated structures (Kumar, 2009). The

results in Figure 3.6A indicated that a higher amount of protein facilitates the formation of a higher extent of intercalated and/or exfoliated nanoclay platelet structures.

XRD patterns for MMT coated by PP5.5 are shown in Figure 3.6B. No peaks were detected via the software at MMT:protein mass ratios of 2:1 and 4:1. As for the sample coated at an MMT:protein mass ratio of 9:1, the diffraction peak also shifted to a lower 2θ angle and the d-spacing was enlarged to 1.50 nm with a lower onset of 4.0° as shown in Table 3.1, significantly different from those of pristine MMT. The FTIR spectra verified the coating of MMT by both PP4.3 and PP5.5 (data not shown).

3.4.4. Effect of pH on Surface Coating

3.4.4.1. Effect of pH on the structure of bare MMT

To verify the pH effect on MMT structure, bare MMT powder was dispersed in phosphate buffer and adjusted to pH 3.0, 5.0, 7.0, and 9.0, mixed at 60 °C for 3 h and freeze-dried to prepare powder for XRD. The lyophilized samples all showed a peak at the same 2θ angle of 7.1° (Figure 3.7) and had a d-spacing of 1.24 nm, identical to those of pristine MMT (Figure 3.3). Therefore, adjusting dispersion pH alone either does not change the structure of MMT platelets or changes the structures, if any, that are completely reversible after hydration and drying.

3.4.4.2. Structure of protein-coated MMT at different pH conditions

This group of experiments was conducted to study the impact of coating pH on MMT properties. The PP5.5 was used because it was more effective than PP4.3 in changing MMT structures (Figure 3.6). Further, because no XRD peaks were detected at MMT:protein mass ratios of 2:1 and 4:1, an intermediate ratio of 3:1 was adopted.

The XRD patterns show a strong impact by the coating pH (Figure 3.8). No distinct peaks were detected at pH 2.0 and 7.0, suggesting a higher extent of exfoliated and highly-disordered intercalated MMT structures than those at other coating pH conditions. Disordered intercalation was observed at pH 3.0, showing a very broad peak. At pH 4.0-6.0, peaks were easily detected at a 2θ angle of 6.9-7.0° with a low onset at a 2θ angle of 3°, corresponding to d-spacing values around 1.25-1.29 nm (Table 3.2) and thus some disordered or intercalated structures. Higher degrees of intercalation occurred at pH 8.0-10.0, with a low onset of 3° and d-spacing of 1.93-1.95 nm. As indicated in Figure 3.9, FTIR results showed peaks at wavenumbers of 2925, 2855, 1618-1681 and 1530-1550 cm^{-1}, verifying the adsorption of protein on MMT surface at all coating conditions. The disappearance of double-peaks at 1450-1400 cm^{-1} indicates the breakup or unpairing of carboxylate and carboxyl groups.

The amount of unbound protein in the supernatant at different pH was also quantified, as listed in Table 3.3. At pH 4.0 and 5.0 and alkali conditions (pH 8.0-10.0), a greater amount of protein remained in the supernatant after coating. The least percentage of protein adsorbing onto MMT was observed at pH 2.0, followed by treatments at pH 3.0, 7.0, and 6.0. The solubility of PP5.5 was also quantified at coating conditions, as shown in Table 3.3. The lowest solubility was observed at pH 4.0 and 5.0, followed by that at pH 6.0. Further, the solubility of PP5.5 was not statistically different at pH 7.0 and above and greater than those at lower pH conditions. The solubility data agrees with the 2D-GE results showing that the pI range of most proteins is 4.5-6.2 (Figure 3.1). Thus, the absolute amount of protein adsorbed on the MMT platelets was lower when proteins have poorer solubility (at pH 4.0 and 5.0) or extensively negative charges (at pH 8.0-10.0).

To understand the significance of electrostatic attraction on coating, the precipitates, after triple washing, were re-suspended in the phosphate buffer at the corresponding pH for zeta potential analysis. Zeta potential of both bare MMT and protein-coated MMT after coating was less negative at a lower pH with significant difference ($P < 0.05$) when pH was below 4.0 (Figure 3.10). In this case, the zeta potential data agrees with the expectations that proteins have more positive charges at a lower pH below pI and thus the negative charges of coated MMT were partially neutralized by adsorbed proteins. Above pH 4.0, zeta potential values of bare MMT were statistically different between two pH groups, i.e. pH 5.0-8.0 and pH 9.0-10.0, while no statistical difference for protein-coated MMT samples. Zeta potential values of protein-coated MMT were similar at pH above 4.0, especially at alkaline conditions. These results may be explained with the complicated composition of the hominy protein extract. Hominy protein extracted from hominy feed is a complex mixture of proteins with a wide range of molecular weight of 10-98 kDa and narrow pI range of 4.5-6.2 (Figure 3.1). It has been observed that proteins can still bind with polyelectrolytes although both polymers carry same types of net charge, likely due to specific charged patches (opposite to polyelectrolytes) on protein surface (Dickinson, 2003). This localized binding, along with hydrogen bonding between MMT and protein (P. Chen & Zhang, 2006), resulted in coating of MMT by proteins at all studied conditions in our study.

3.5. CONCLUSION

Water soluble proteins extracted from hominy feed are complex mixtures of proteins, most of which have pI of 4.5-6.2 and molecular weight of 10-68 kDa. The PP5.5 had the best surface coating effect among the three precipitates, as indicated by the greater extent of

disorderly intercalated and/or exfoliated strutures. The degree of intercalation or exfoliation of MMT structures was affected by the amount of protein applied during coating, while pH did not affect the d-spacing of bare MMT but affected the amount of protein adsorbing onto MMT and the degree of exfoliated/intercalated platelets after coating. The presence of protein after coating MMT at all pH conditions suggests that coating involved not only electrostatic attraction but non-coulombic forces such as hydrogen bonding. This study demonstrated a simple coating method to modify highly-ordered structures of pristine MMT to intercalated and/or exfoliated structures. The protein-coated MMT may be utilized to manufacture bio-nanocomposite materials with improved physical properties for applications such as bio-degradable packaging films.

LIST OF REFERENCES

Adame, D., & Beall, G. W. (2009). Direct measurement of the constrained polymer region in polyamide/clay nanocomposites and the implications for gas diffusion. *Applied Clay Science, 42*(3-4), 545-552.

Arora, A., & Padua, G. W. (2010). Review: nanocomposites in food packaging. *Journal of Food Science, 75*(1), R43-R49.

Cao, N., Fu, Y. H., & He, J. H. (2007). Preparation and physical properties of soy protein isolate and gelatin composite films. *Food Hydrocolloids, 21*(7), 1153-1162.

Capek, I. (2006). Nanocomposite structures and dispersions : science and nanotechnology--fundamental principles and colloidal particles

Chen, P., & Zhang, L. (2006). Interaction and properties of highly exfoliated soy protein/montmorillonite nanocomposites. *Biomacromolecules, 7*(6), 1700-1706.

Dang, Q. Q., Lu, S. D., Yu, S., Sun, P. C., & Yuan, Z. (2010). Silk fibroin/montmorillonite nanocomposites: effect of pH on the conformational transition and clay dispersion. *Biomacromolecules, 11*(7), 1796-1801.

de Azeredo, H. M. C. (2009). Nanocomposites for food packaging applications. *Food Research International, 42*(9), 1240-1253.

Dickinson, E. (2003). Hydrocolloids at interfaces and the influence on the properties of dipsersed systems. *Food Hydrocolloids, 17*, 25-39.

Ding, X. L., & Henrichs, S. M. (2002). Adsorption and desorption of proteins and polyamino acids by clay minerals and marine sediments. *Marine Chemistry, 77*(4), 225-237.

Essington, M. E. (2003). *Soil and water chemistry: an intergrative approach* CRC Press, LLC. Boca Raton, FL.

Gunister, E., Pestreli, D., Unlu, C. H., Atici, O., & Gungor, N. (2007). Synthesis and characterization of chitosan-MMT biocomposite systems. *Carbohydrate Polymers, 67*(3), 358-365.

Jahangir, S., & Leber, M. J. (2007). Biodegradable good packaging: an environmental imperative. *Industry Report*, 1-20.

Kim, K. W., Ko, C. J., & Park, H. J. (2002). Mechanical properties, water vapor permeabilities and solubilities of highly carboxymethylated starch-based edible films. *Journal of Food Science, 67*(1), 218-222.

Krochta, J. M., & DeMulderJohnston, C. (1997). Edible and biodegradable polymer films: challenges and opportunities. *Food Technology, 51*(2), 61-74.

Kumar, P. (2009). Development of bio-nanocomposite films with enhanced mechanical and barrier properties using extrusion processing. *North Carolina State University. Ph.D dissertation*.

L'Hocine, L., Boye, J. I., & Arcand, Y. (2006). Composition and functional properties of soy protein isolates prepared using alternative defatting and extraction procedures. *Journal of Food Science, 71*(3), C137-C145.

Le Corre, D., Bras, J., & Dufresne, A. (2010). Starch nanoparticles: a review. *Biomacromolecules, 11*(5), 1139-1153.

Nakasato, K., Ono, T., Ishiguro, T., Takamatsu, M., Tsukamoto, C., & Mikami, M. (2004). Rapid quantitative analysis of the major components in soymilk using fourier transform infrared spectroscopy (FT-IR). *Food Science and Technology Research, 10*(2), 137-142.

Nielsen, L. E. (1967). Models for the permeability of filled polymer systems. *Journal of Macromolecular Science: Part A - Chemistry, 1*(5), 14.

Paetau, I., Chen, C. Z., & Jane, J. L. (1994). Biodegradable plastics made from soybean products.1. effect of preparation and processings on mechanical-properties and water-absorption. *Industrial & Engineering Chemistry Research, 33*(7), 1821-1827.

Parris, N., Moreau, R. A., Johnston, D. B., Singh, V., & Dickey, L. C. (2006). Protein distribution in commercial wet- and dry-milled corn germ. *Journal of Agricultural and Food Chemistry, 54*(13), 4868-4872.

Paulis, J. W., Bietz, J. A., & Wall, J. S. (1975). Corn protein subunits: molecular weights determined by sodium dodecyl sulfate-polyacrylamide gel-electrophoresis. *Journal of Agricultural and Food Chemistry, 23*(2), 197-201.

Quiquampoix, H., & Burns, R. G. (2007). Interactions between proteins and soil mineral surfaces: Environmental and health consequences. *Elements, 3*(6), 401-406.

Rimdusit, S., Jingjid, S., Damrongsakkul, S., Tiptipakorn, S., & Takeichi, T. (2008). Biodegradability and property characterizations of Methyl Cellulose: Effect of nanocompositing and chemical crosslinking. *Carbohydrate Polymers, 72*(3), 444-455.

Servagent-Noinville, S., Revault, M., Quiquampoix, H., & Baron, M. H. (2000). Conformational changes of bovine serum albumin induced by adsorption on different clay surfaces: FTIR analysis. *Journal of Colloid and Interface Science, 221*(2), 273-283.

Tang, X. Z., Alavi, S., & Herald, T. J. (2008). Barrier and mechanical properties of starch-clay nanocomposite films. *Cereal Chemistry, 85*(3), 433-439.

Tunc, S., Angellier, H., Cahyana, Y., Chalier, P., Gontard, N., & Gastaldi, E. (2007). Functional properties of wheat gluten/montmorillonite nanocomposite films processed by casting. *Journal of Membrane Science, 289*(1-2), 159-168.

Wang, X. C., & Lee, C. (1993). Adsorption and desorption of aliphatic-amines, amino-acids and acetate by clay-minerals and marine-sediments. *Marine Chemistry, 44*(1), 1-23.

Zhao, R. X., Torley, P., & Halley, P. J. (2008). Emerging biodegradable materials: starch- and protein-based bio-nanocomposites. *Journal of Materials Science, 43*(9), 3058-3071.

APPENDIX

Table 3. 1 Basal spacing of MMT coated with protein at MMT:protein mass ratios of 9:1, 4:1 and 2:1 at pH 2.0.

Protein	MMT:protein Mass Ratio	2θ (°)	*d*-spacing (nm)
PP4.3[a]	9:1	6.67	1.32
	4:1	6.39	1.38
	2:1	N/A	N/A
PP5.5[b]	9:1	5.87	1.50
	4:1	N/A	N/A
	2:1	N/A	N/A

[a] Proteins precipitated at pH 4.3; [b] proteins precipitated at pH 5.5.

Table 3. 2 Basal spacing of MMT coated with hominy protein precipitated at pH 5.5 at an MMT:protein mass ratio of 3:1 and pH 2.0-10.0.

Coating pH	2θ (°)	*d*-spacing (nm)
2.0	N/A	N/A
3.0	6.854	1.2886
4.0	6.990	1.2636
5.0	7.009	1.2602
6.0	7.044	1.2540
7.0	N/A	N/A
8.0	4.586	1.927
	6.865	1.287
9.0	4.576	1.929
	6.892	1.285
10.0	4.532	1.948
	6.796	1.303

Table 3. 3 Impact of pH on hominy protein solubility and coating on MMT[1].

pH	Protein Solubility(%)	Unbound Protein%[2]
2.0	91.38 ± 1.71^{b}	0.93 ± 0.02^{G}
3.0	65.97 ± 3.04^{c}	1.26 ± 0.01^{F}
4.0	17.21 ± 1.34^{e}	3.36 ± 0.04^{BC}
5.0	17.19 ± 1.36^{e}	3.48 ± 0.07^{B}
6.0	35.42 ± 1.56^{d}	1.80 ± 0.03^{E}
7.0	101.16 ± 2.04^{a}	1.37 ± 0.02^{F}
8.0	103.01 ± 0.96^{a}	3.34 ± 0.07^{C}
9.0	100.51 ± 1.53^{a}	2.64 ± 0.05^{D}
10.0	103.22 ± 0.55^{a}	4.95 ± 0.06^{A}

[1] The lyophilized extract powder from precipitation at pH 5.5 (PP5.5) was used. The total protein content measured by the Bradford method was used as the basis of calculation. Different superscripts in each row indicate significant difference ($P<0.001$). Numbers are averages ± standard deviations from three measurements using the BCA method.

[2] Coating was performed at an MMT:protein mass ratio of 3:1.

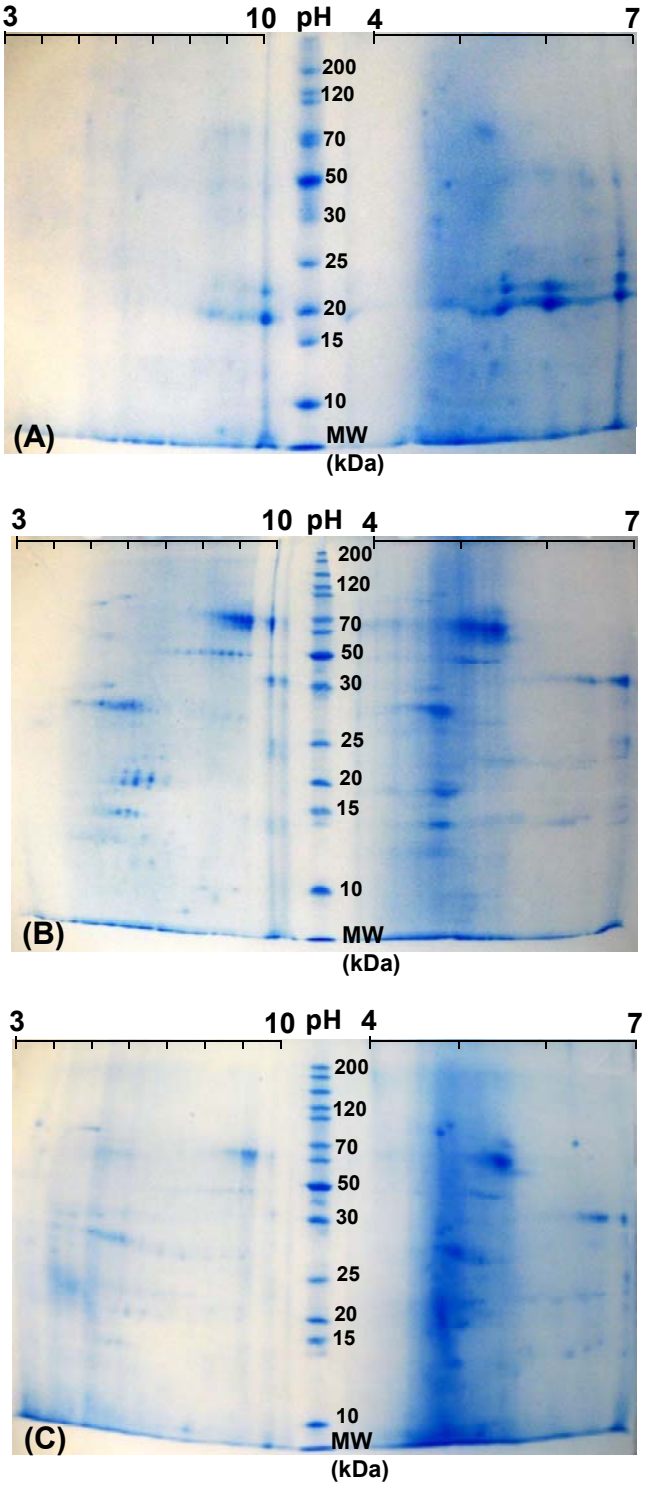

Figure 3. 1. Two-dimension gel electrophoresis analysis of hominy protein precipitated at (A) pH 6.0, (B) pH 5.5, and (C) pH 4.3.

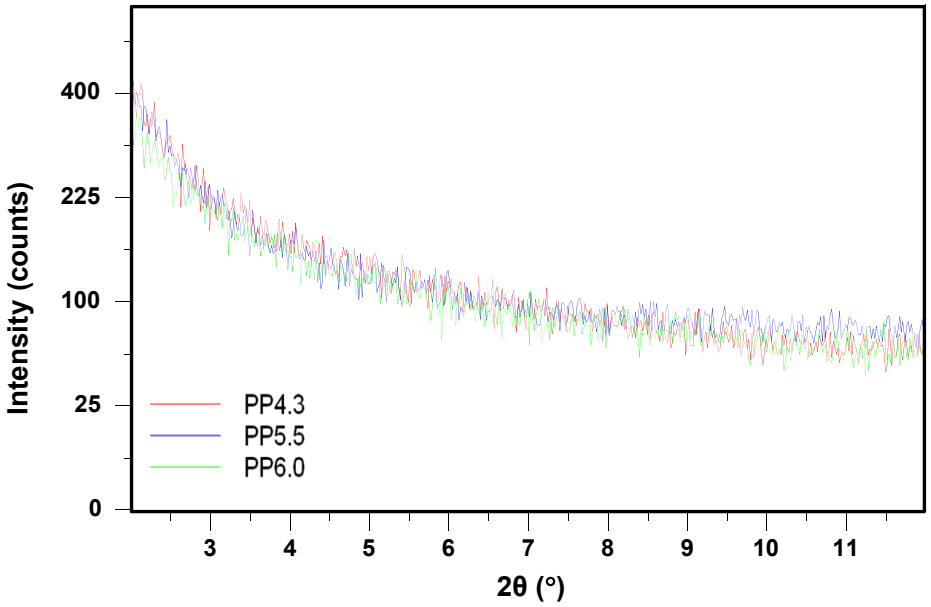

Figure 3. 2. XRD patterns of protein extracts precipitated at pH 4.3 (PP4.3), 5.5 (PP5.5) and 6.0 (PP6.0).

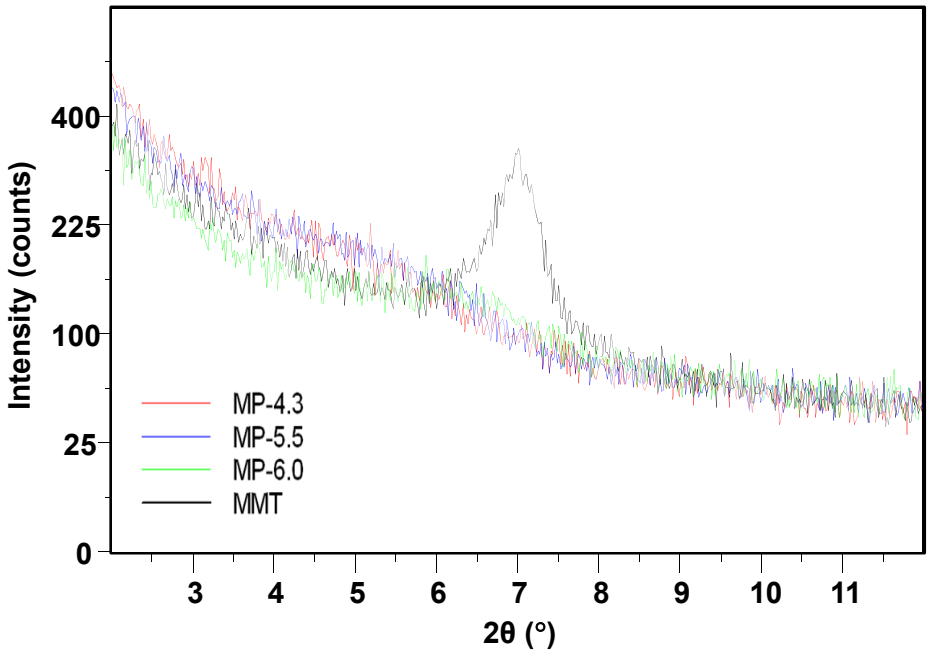

Figure 3. 3. XRD patterns of pristine MMT (black) after coating by hominy protein precipitated at pH 4.3 (MP-4.3, red), 5.5 (MP-5.5, blue) and 6.0 (MP-6.0, green). Coating was conducted at pH 2.0 and an MMT:protein powder mass ratio of 2:1.

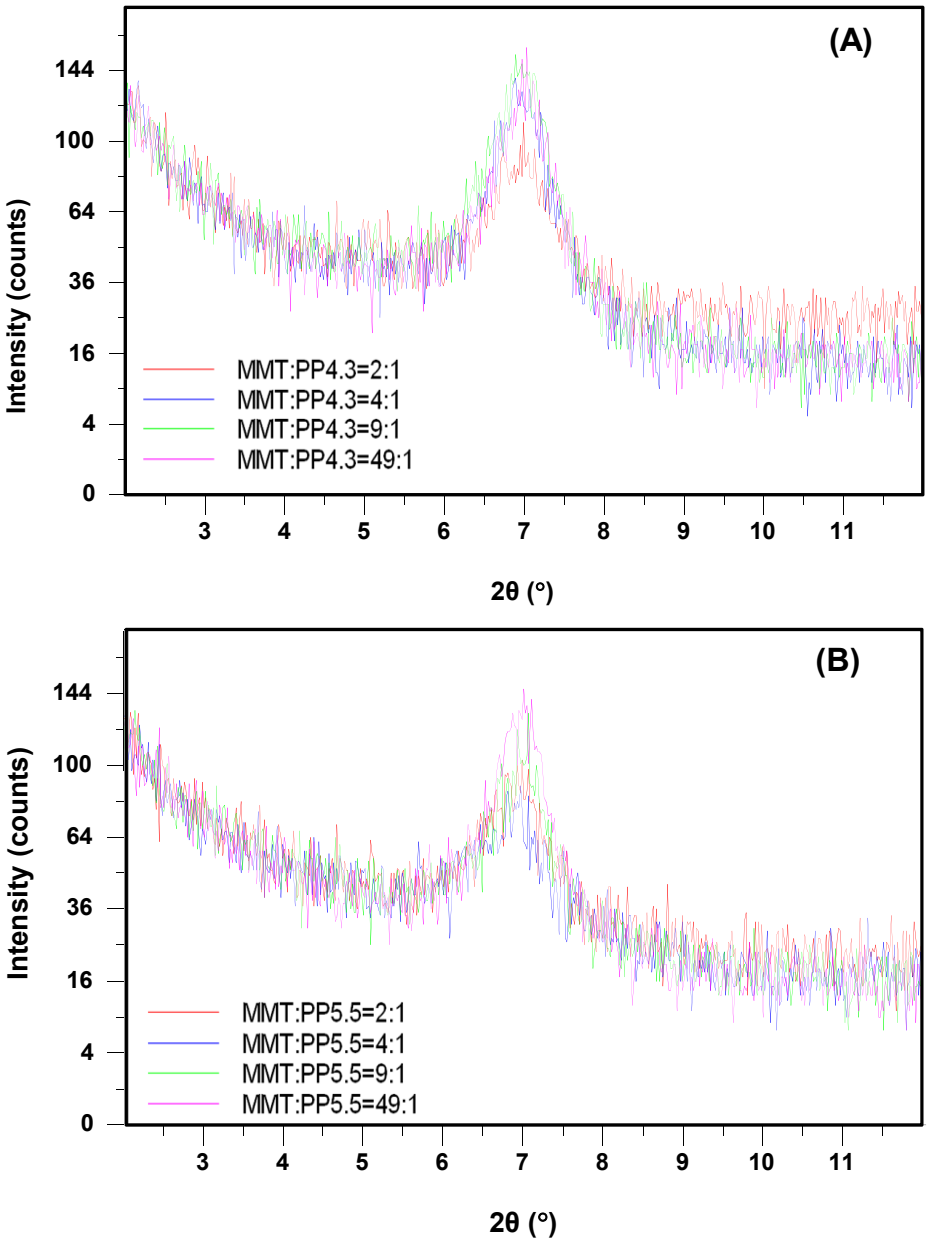

Figure 3. 4. XRD patterns of simple mixtures with different mass ratios of pristine MMT and lyophilized powder of hominy protein precipitated at (A) pH 4.3 and (B) pH 5.5.

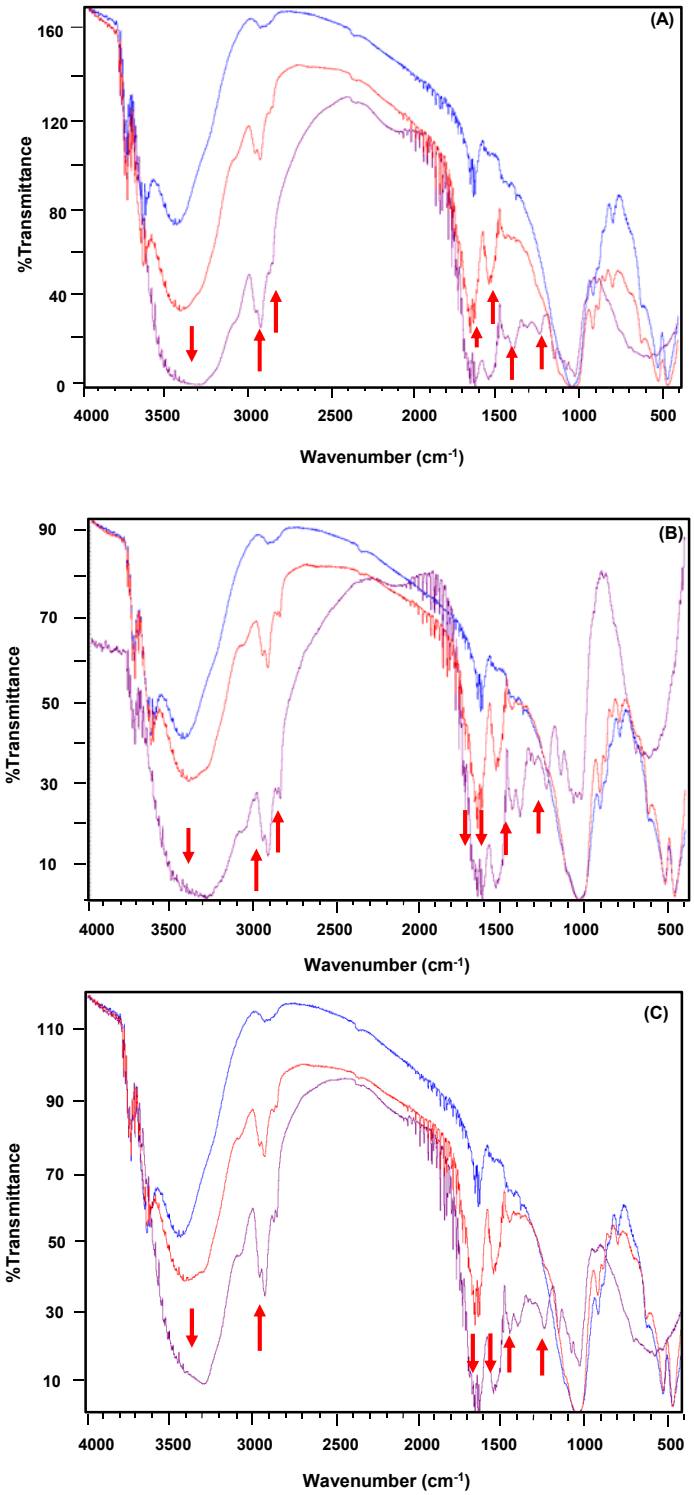

Figure 3. 5. Comparison of FTIR spectra of pristine MMT (blue), protein (purple), and protein-coated MMT (red). Coating was perormed at pH 2.0 and an MMT:protein powder mass ratio of 2:1 using proteins precipitated at pH (A) 4.3, (B) 5.5 and (C) 6.0. Arrows are used to highlight the peaks discussed in the text.

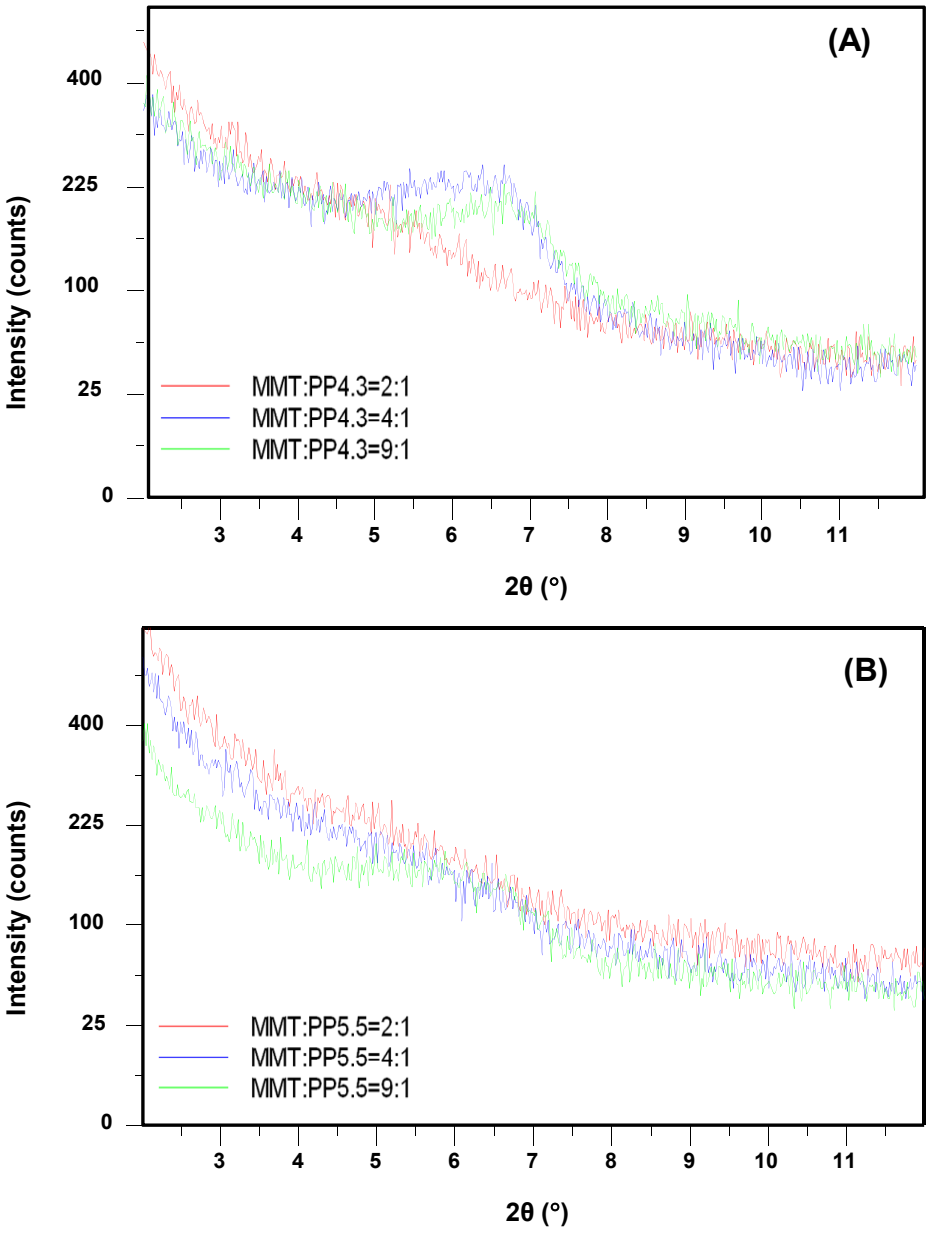

Figure 3. 6. XRD patterns of MMT coated by hominy protein precipitated at pH (A) 4.3 (PP4.3) and (B) 5.5 (PP5.5). Coating was perfomed at pH 2.0 and MMT:protein mass ratios of 9:1 (green), 4:1 (blue) and 2:1 (red). Data in Figure 3 (at a ratio of 2:1) are repeated here for convenience of comparison

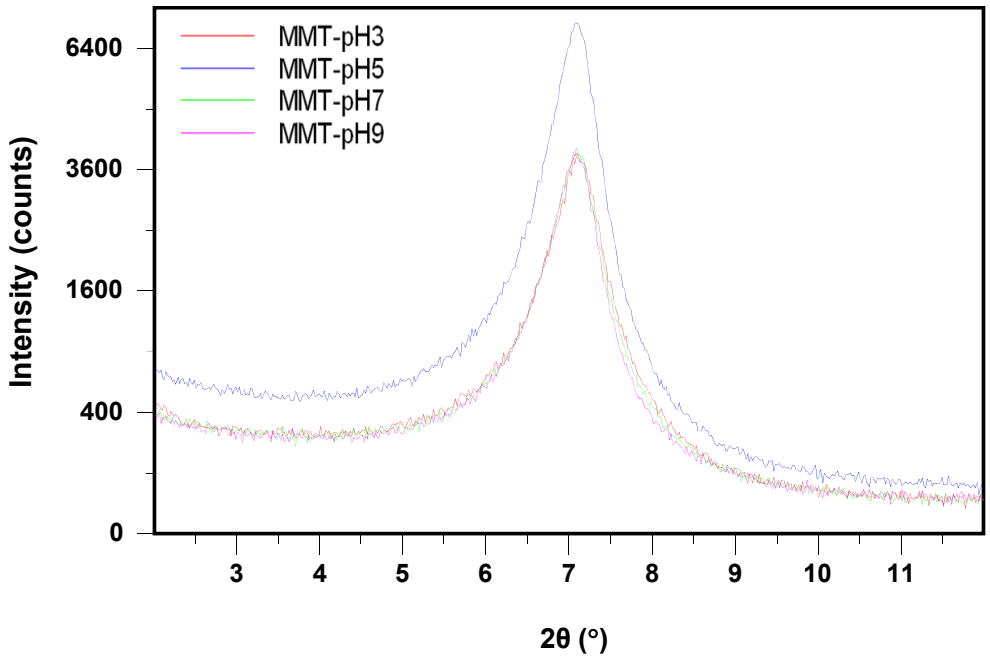

Figure 3. 7. XRD patterns of MMT powder freeze-dried from MMT suspensions in 10 mM NaH_2PO_4 buffer adjusted to pH 3.0, 5.0, 7.0, and 9.0 and mixed at 60°C for 3 h. 2θ =7.11. D-spacing = 1.24 nm.

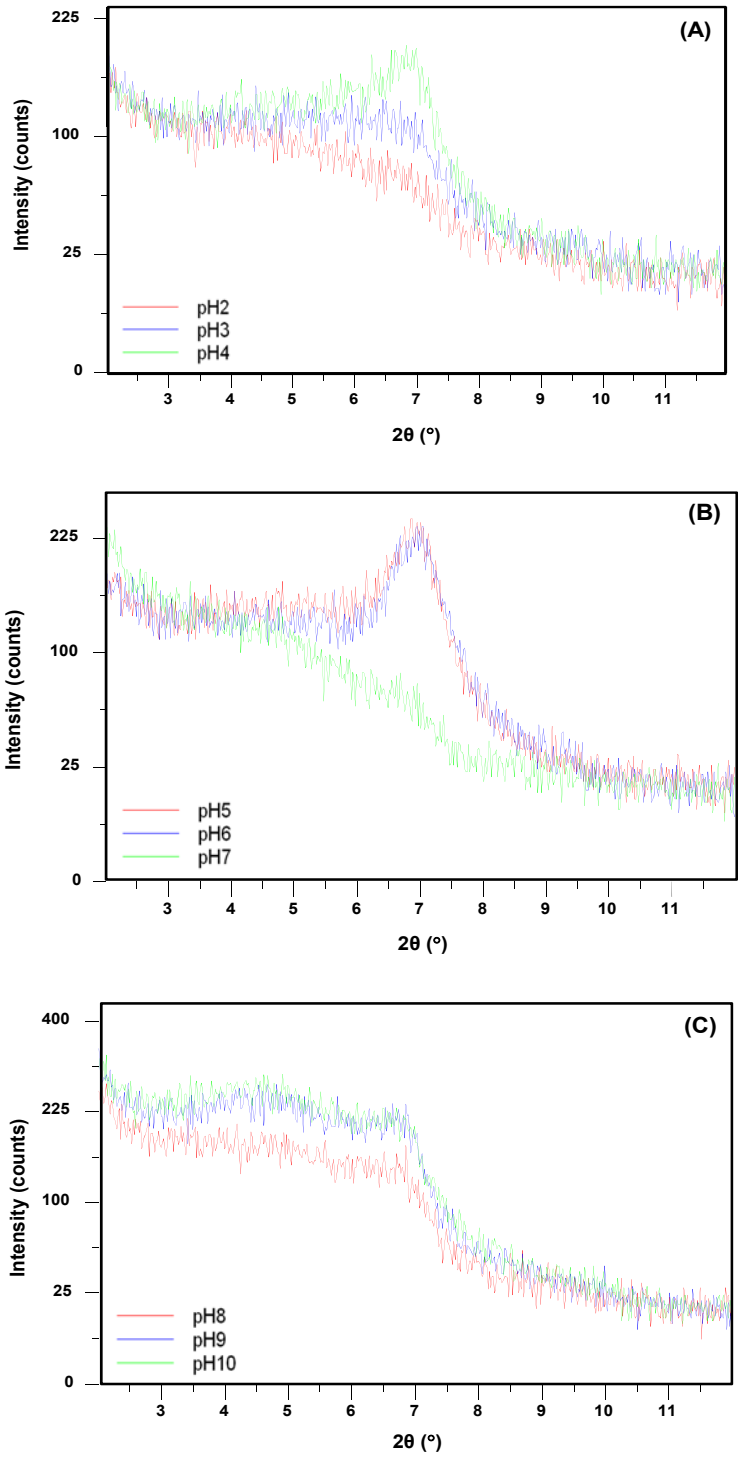

Figure 3. 8. XRD patterns of MMT coated with hominy protein at varied pH conditions: (A) pH 2.0-4.0, (B) pH 5.0-7.0, and (C) pH 8.0-10.0 with an MMT:protein mass ratio of 3:1 using hominy protein precipitated at pH 5.5.

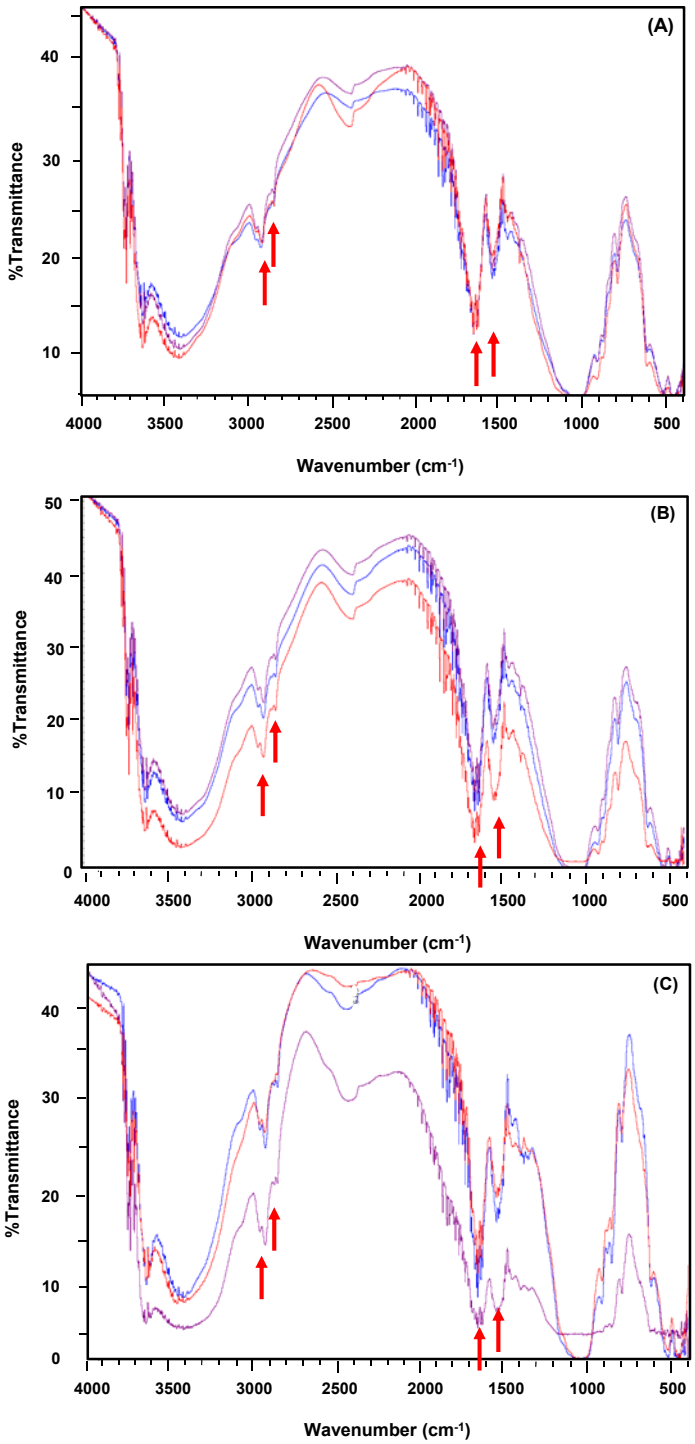

Figure 3. 9. FTIR spectra of MMT coated by hominy protein precipitated at pH 5.5. Coating was perfomed at an MMT:protein mass ratio of 3:1 and (A) pH 2.0 (blue), 3.0 (purple), and 4.0 (red), (B) pH 5.0 (blue), 6.0 (purple), and 7.0 (red) and (C) pH 8.0 (blue), 9.0 (purple), and 10.0 (red). Arrows are used to highlight the peaks discussed in the text.

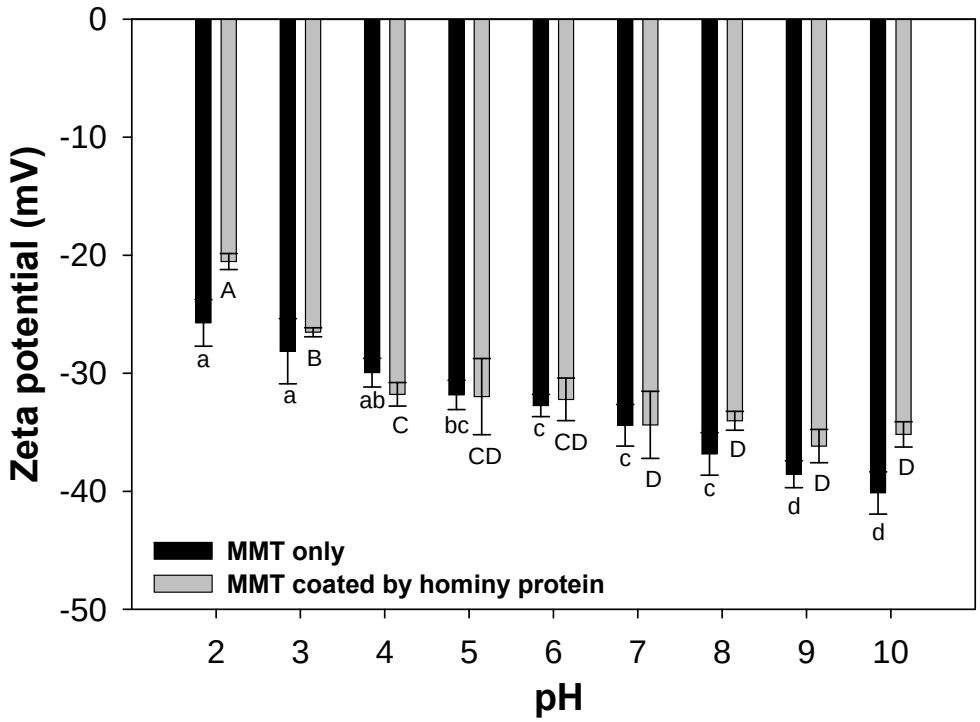

Figure 3. 10. Comparison of zeta potential of bare MMT and protein-coated MMT at pH 2.0-10.0. Coating was conducted at an MMT:protein powder mass ratio of 3:1 using protein precipitated at pH 5.5.

Error bars are standard deviations for duplicate coating experiments, each measured for three times. Different letters in each group indicate significant difference ($P < 0.001$).

CHAPTER 4 . STRUCTURE MODIFICATION OF MONTMORILLONITE NANOCLAYS BY SURFACE-COATING WITH SOY PROTEIN

4.1. ABSTRACT

To achieve exfoliated and/or intercalated structures, montmorillonite (MMT) was surface-coated by soy protein at 60 °C, MMT:soy protein powder mass ratios of 49:1, 9:1, 4:1 or 2:1, and pH 2.0-10.0. The protein-coated MMT was triple-washed and lyophilized for characterization. MMT structural modification was observed using protein coating at all pH conditions, based on X-ray diffraction, Fourier transform infrared spectroscopy, and zeta potential analyses, as well as the quantification of proteins remaining in the continuous phase and present in triple-washed MMT. At a mass ratio of 4:1, more than 90% protein bound with MMT, with the largest d-spacing at pH 9.0. When the mass ratio was reduced to 2:1, protein-coated MMT at pH 9.0 demonstrated the highest degree of intercalation/exfoliation, corresponding to the disappearance of the diffraction peak characteristic of pristine MMT. This study thus demonstrated that intercalation/exfoliation of MMT can be easily achieved by coating with low cost soy protein for manufacturing nanocomposite materials.

Keywords: layered montmorillonite nanoclay, surface-coating, soy protein, intercalation, X-ray diffraction

4.2. INTRODUCTION

Concerns of fossil fuel depletion, increase of petroleum price, and negative environmental impact of persistent petro-plastic wastes have been the driving forces in investigating bio-plastic packaging based on renewable, low-cost, and degradable biopolymers (Jahangir & Leber, 2007; Sorrentino, Gorrasi, & Vittoria, 2007; Zhao, Torley, & Halley, 2008). The annual growth of bio-plastics has been ca. 17-20% since 2006, and the global demand for bio-plastics is estimated to quadruple by 2013 (Markets, 2011). Some major retailers, including Coca-Cola, Frito-Lay and Walmart, have already adopted bio-plastic bottles, pouches and wraps (Marsh & Bugusu, 2007).

According to a report, poly-lactic-acid synthesized from monomers derived from corn starch has been a dominating polymer in manufacturing bioplastics, but materials from sources such as microorganisms and algae and advanced technologies such as nanotechnology are emerging in bioplastic industry (Markets, 2011). Nanocomposites, composed of nano-scale fillers uniformly dispersed in a polymer matrix, have the promise to improve mechanical, barrier and thermo-resistance properties of natural biopolymer-based packaging films (Arora & Padua, 2010; Dang, Lu, Yu, Sun, & Yuan, 2010; de Azeredo, 2009). These properties are currently technological challenges of developing bio-packaging to replace conventional petro-plastics. Montmorillonite (MMT) is one of the most popular layered silicates in developing biopolymer-based nanocomposites because of its low cost, abundance (Essington, 2003; Gunister, Pestreli, Unlu, Atici, & Gungor, 2007), large surface area, and large specific aspect ratios estimated to be around 50-1000 (Arora & Padua, 2010; de Azeredo, 2009; Zhao, Torley, & Halley, 2008).

Proteins have been extensively studied as film-forming biopolymers in the past two decades (Cuq, Gontard, & Guilbert, 1998; Kumar, Sandeep, Alavi, Truong, & Gorga, 2010a,

2010b; Paetau, Chen, & Jane, 1994; Xiang, et al., 2009). Protein films have lower water vapor permeabilities and better oxygen barrier properties than starch films (Cao, Fu, & He, 2007; de Azeredo, 2009; Zhao, Torley, & Halley, 2008). However, when comparing to petro-plastics, protein films have poor mechanical properties such as brittleness, rigidness and low elongation percentage and relatively low moisture and gas resistance, but these properties can be improved by incorporation of nanoclays (Arora & Padua, 2010; Krochta & DeMulderJohnston, 1997; Song, Tang, Wang, & Wang, 2011). Studies on structure-property relationship have repeatedly illustrated that nanocomposite materials with either intercalated or exfoliated MMT nanolayers have much improved mechanical and barrier properties than conventional composite materials containing the fillers dispersed as micrometer-sized structures (Chen & Zhang, 2006; Kumar, Sandeep, Alavi, Truong, & Gorga, 2010a; Le Corre, Bras, & Dufresne, 2010; Tang, Alavi, & Herald, 2008a).

Dispersion behavior of MMT particles plays an important role on MMT structural formation in nanocomposites (Yang, Zhu, Yin, Wang, & Qi, 1999). Generally speaking, because an enlarged d-spacing (distance between clay layer platelets) favors the penetration of polymer chains, MMT with the bigger d-spacing is much easier to be transformed to intercalated or exfoliated structures in final nanocomposites. To enlarge d-spacing, strategies have been developed by chemically modifying surface properties of MMT or physically coating MMT with molecules (Feng, Zhao, Gong, & Yang, 2004; Mallakpour & Dinari, 2011; Yang, Zhu, Yin, Wang, & Qi, 1999). Intercalation agents have been studied for amino acids, primary aliphatic amines and quaternary ammonium (Yang, Zhu, Yin, Wang, & Qi, 1999) and sequential steps of hydrochloric acid and bovine serum albumin (Lin, Wei, Juang, & Tsai, 2007). The prior-exfoliated or -intercalated MMT structures can then be used to produce nanocomposite materials,

with the possibility to maximize the extent of exfloliation/intercalation of MMT to further improve mechanical and barrier properties.

The affinity of proteins and amino acids on soil minerals is well established (Ding & Henrichs, 2002; Quiquampoix & Burns, 2007), implying the possibility of surface coating MMT with naturally occurring low-cost proteins for direct exfoliation/intercalation. The objective of this work was thus to study the feasibility to directly surface-coat MMT by soy protein to increase the d-spacing and obtain intercalation and/or exfoliation of MMT layers. In addition to the mass ratio of MMT:soy protein, experiments were conducted at different pH conditions that are expected to directly impact surface properties of MMT and soy protein based on electrostatic interactions.

4.3. MATERIALS AND METHODS

4.3.1. Materials

Na^+-MMT (Cloisite® Na^+ Nanoclay) with a cation exchange capacity of 92.6 mequiv/100g was purchased from Southern Clay Products, Inc. (Gonzales, TX). Defatted soy flour was a product from MP Biomedicals, LLC (Solon, OH). Bovine serum albumin (BSA) and BCA™ Coomassie® Plus Reagent A were ordered from Pierce Biotechnology (Rockford, IL). Other chemicals were from Thermo-Fisher Scientific Inc. (Fair Lawn, NJ) or Sigma-Aldrich Corp. (St. Louis, MO). Chemicals were used as received.

4.3.2. Extraction of Soy Protein

Soy protein was extracted from soy flour using the protocol of preparing soy protein isolate (L'Hocine, Boye, & Arcand, 2006). Soy flour after further size-reduction with a coffee grinder (Hamilton Beach Proctor-Silex, Inc., Southern Pines, NC) was suspended in deionized water at a

solid:liquid mass ratio of 1:10, adjusted to pH 9.0 using 4 N NaOH, and heated to 48 °C for 3-h extraction using a magnetic stirring hot plate (model Isotemp®, Fisher Scientific, Fair Lawn, NJ). The extract was separated by centrifugation (Sorvall RC 5B Plus, Newtown, CT) at 3,778*g* for 15 min at ambient temperature, followed by sequentially filtering with #1 and #2 filter papers (Whatman®, Lawrence, KS), twice for each. The same batch of soy flour powder was extracted three times to improve the protein extraction yield. The three filtrates were combined and acidified to pH 4.5 by using 6 N HCl, and the precipitate was separated by centrifugation at 3,778*g* for 30 min at ambient temperature. The precipitate was re-dispersed in deionized water, adjusted to pH 9.0, and re-precipitated at pH 4.5. The re-precipitation was repeated for two additional times to remove impurities. The final precipitate was re-dispersed, neutralized, and spray-dried using a B-290 Mini Spray Dryer (BÜCHI Labortechnik AG, Postfach, Switzerland) at inlet and outlet temperatures of 150 and 55-65 °C, respectively, and a feed rate of 6.67 mL/min. The spray dried soy protein powder (SPP) was collected and stored in a -20 °C freezer.

4.3.3. Surface Coating of MMT

MMT was surface-coated by SPP using a solution intercalation method (Chen & Zhang, 2006). Two groups of experiments were performed to investigate the effects of MMT:SPP mass ratio and coating pH. The first group was conducted at pH 2.0-10.0 at an MMT:SPP mass ratio of 4:1. In the second group, the MMT:SPP mass ratios of 49:1, 9:1, 4:1 and 2:1 were studied at pH 9.0 – the extraction pH where all proteins are soluble. Briefly, SPP and MMT dispersions were separately prepared in 10 mM NaH_2PO_4 buffer according to the mass ratio, adjusted to a desired pH, and preheated to 60°C. The MMT dispersion was slowly added into the SPP dispersion while being stirred at 1000 rpm using a magnetic stirring hot plate. The slurry was vigorously agitated at the same speed for 3 h with the temperature maintained at 60 °C. After

centrifugation at 3,778*g* for 15 min at ambient temperature, the supernatant was collected, and the precipitate was re-suspended in the same volume of fresh buffer to remove the unbound and loosely bound proteins. The washing step was repeated three times, and the supernatants were combined and centrifuged at 10,000*g* for 30 min to remove the fine MMT. Both the final precipitate and combined supernatant were freeze-dried (VirTis AdVantage Plus EL-85 Benchtop Freeze Dryer, SP Scientific Inc., Gardiner, NY). The lyophilized samples were collected and stored in a -20 °C freezer till further characterization.

4.3.4. Determination of Amount of Protein Coated on MMT

The above lyophilized supernatant samples were dissolved in 10 mM NaH_2PO_4 buffer at pH 9.0 for determining unbound protein using the bicinchoninic acid (BCA) method. The percentage of unbound protein was then calculated by normalizing to the total protein used in coating, also measured using the BCA method. Commercial BCA™ Protein Assay Reagent A was utilized, and reagent B (4%w/v cupric sulfate) was freshly prepared. The incubation was conducted at 37 °C for 30 min, and the absorbance was measured at 562 nm by using a UV/Vis spectrophotometer (model Biomate 5, Thermo Electron Corporation, Woburn, MA). BSA was applied as a reference to establish a standard curve. Triplicate tests were performed for each sample.

The amount of bound protein, in the lyophilized clay precipitate (coated MMT) samples from coating experiments, was determined for the total nitrogen content using the Dumas method by Atlantic MicroLab, Inc. (Norcross, GA). The nitrogen content was converted to protein content by multiplying with the Jones' factor, 6.25 for soy protein (Mariotti, Tome, & Mirand, 2008). The percentage of bound protein was then calculated after dividing by the total protein

used in coating. For consistency, the protein content of SPP in this calculation was also determined by the Dumas method.

4.3.5. Determination of Protein Solubility

SPP was hydrated in 10 mM NaH_2PO_4 buffer with 4 mM NaCl to a final concentration of 1 mg/mL and adjusted to pH 2.0-10.0 using 1 N HCl or NaOH. The 4 mM NaCl was equivalent to the free sodium ion concentration in 1%w/v MMT dispersion measured by using atomic absorption spectroscopy at Department of Plant Sciences, the University of Tennessee (Knoxville, TN). After centrifugation at 10,000*g* for 30 min, the supernatant was determined for protein concentration using the above BCA method. The protein solubility was then calculated as the percentage of the protein remaining in the supernatant with respect to the total protein content in SPP determined by the Dumas method.

4.3.6. Zeta Potential

The final precipitates in the above coating experiments were suspended in the phosphate buffer, adjusted to pH 2.0-10.0 using 1 N HCl or NaOH, and measured for zeta potential using a Delsa™ Nano C Zeta Potential and Particle Size Analyzer (Beckman Coulter, Fullerton, CA). To characterize zeta potential of the bare MMT under coating conditions, 1%w/v MMT was suspended in phosphate buffer, adjusted to a corresponding pH, heated and stirred for 3 h at 60 °C, and cooled to room temperature before testing. Triplicate measurements were conducted for each sample. Each measurement included 5 runs, each run for 10 cycles.

4.3.7. Wide-angle X-ray Diffraction (WXRD)

An X-ray diffractometer (model X'Pert, PANalytical Inc., Westborough, MA) with a generator voltage of 45 kV, a current of 40 mA, and a wavelength of 1.54 Å was used to conduct WXRD analyses at ambient temperature. The XRD patterns were obtained in the 2θ angle range

of 2-12° in a fixed time mode with an increment of 0.02°, and plots were processed using the X'Pert Data Viewer software (PANalytical Inc., Westborough, MA). Peak positions and d-spacing, calculated according to the Bragg's equation – eq. 1 (Kumar, 2009), were determined directly by using the X'Pert HighScore Plus software (PANalytical Inc., Westborough, MA). The experimental limit of detectable d-spacing in this study was also calculated using eq. 1 for a 2θ angle of 2° (Dang, Lu, Yu, Sun, & Yuan, 2010; Tang, Alavi, & Herald, 2008a).

$$d = \frac{\lambda}{2\sin(\theta)} \quad (1)$$

where λ is the wavelength of X-ray beam, and θ is the angle of incident X-ray beam.

4.3.8. Fourier Transform Infrared Spectroscopy (FTIR)

A powder potassium bromide (KBr) pellet method (Chen, Tian, Zhang, Chen, Wang, & Do, 2008; Gunister, Pestreli, Unlu, Atici, & Gungor, 2007) was applied in FTIR experiments. A mixture of 1 mg of the sample and 100 mg of KBr was ground to fine powder that was then pressed to a clear or translucent pellet loaded onto the instrument. The %Transmittance was collected at a wavenumber range of 4000-400 cm^{-1} using a model Nicolet 670 spectrometer (Thermo Nicolet, Madison, WI). A pristine KBr pellet was used as a background.

4.3.9. Statistical Analyses

Significant difference analyses were carried out with a least-significant-difference ($P < 0.05$) mean separation method (LSD). Analyses were performed using SAS software (v. 9.3, SAS Institute Inc., Cary, NC).

4.4. RESULTS AND DISCUSSION

4.4.1. Structures of MMT Coated by SPP at Different pH Conditions

4.4.1.1. XRD

XRD patterns of pristine MMT and SPP are presented in Figure 4.1. Pristine MMT had a sharp characteristic peak at a 2θ angle of 7.11° with a d-spacing value of 1.24 nm, consistent with the literatures (Essington, 2003; Tang, Alavi, & Herald, 2008a), while SPP did not have any diffraction peaks in the studied 2θ range.

Figure 4.2 shows the XRD patterns of MMT samples coated at pH 2.0-10.0 with an MMT:SPP mass ratio of 4:1. Table 4.1 lists the d-spacing values of corresponding samples. A very weak peak was observed at pH 2.0, corresponding to a d-spacing value of 1.33 nm. At pH 3.0-5.0, sharp peaks appeared at 2θ angles of 6.63-7.08°, close to the characteristic peak for pristine MMT (Figure 4.1), and the d-spacing values were around 1.25-1.27 nm, slightly smaller than that at pH 2.0. At pH 6.0 or 7.0, two peaks were detected at 2θ of ca. 4.3 and 6.9°, corresponding to d-spacing values of 2.09 and 1.27 nm at pH 6.0, and 2.01 and 1.27 nm at pH 7.0. Humps with low onset of ca. 3° and 2θ angle of ca. 4.2-4.4° were observed for MMT coated by SPP at pH 8.0-10.0, corresponding to d-spacing values of 1.99-2.12 nm (Table 4.1), without the sharp peak of pristine MMT. When bare MMT was similarly treated at coating conditions without SPP, XRD patterns did not demonstrate any changes (data not shown).

The shifting of diffraction peak to a small 2θ angle, the left-shift, and incresed d-spacing are characteristics of intercalated layer structures (Tang, Alavi, & Herald, 2008a). A greater extent of the left shift corresponds to a bigger d-spacing value. Thus, the treatment of pH 2.0 resulted in more intercalated MMT structures than other pH treatments. When analyzed using 2-dimensional sodium-dodecyl sulfate polyacrylamide gel electrophoresis (results not shown),

most proteins corresponded to pI of 4.4-5.1 and molecular weight of 15-100 kDa, consistent with the literature (Liu, Zhou, Tian, & Gai, 2007; Wu, Zhang, Kong, & Hua, 2009). Therefore, at pH 2.0, SPP carries more positive charges than other pH conditions, which facilitates the adsorption onto negatively charged MMT surface upon mixing. As for samples at pH 6.0 and 7.0, the existence of two peaks implied the occurrence of partially intercalated MMT. At pH 8.0-10.0, broad peaks at low onset of ca. 3° imply a high extent of intercalated MMT structures (Kumar, 2009). Therefore, XRD patterns in Figure 4.2 indicate that intercalation of MMT occurred after coating by SPP at all pH conditions but the extent was pH-dependent.

4.4.1.2. FTIR

FTIR spectra of pristine MMT and SPP are demonstrated in Figure 4.3. Characteristic peaks of proteins appeared at wavenumbers of 2925, 2855, 1618-1681, 1530-1550, 1244, and 1450-1400 cm^{-1}. The former five peaks are due to absorbances by functional groups of $–CH_2$, –CH (C-H stretching), amide I band (C=O stretching vibration), amide II band (N-H bending and C-N stretching modes), and amide III band (C-N stretching and N-H bending), involving possible structures of$–CO-NH_2$, –CO-NH–, and/or –CO-N– (P. Chen & Zhang, 2006; Nakasato, Ono, Ishiguro, Takamatsu, Tsukamoto, & Mikami, 2004; Servagent-Noinville, Revault, Quiquampoix, & Baron, 2000). The double peaks at 1450-1400 cm^{-1} are related with carboxyl (at ca. 1450 cm^{-1}) and carboxylate groups (at ca. 1410 cm^{-1}).

Figure 4.4 shows the FTIR spectra of MMT after coating by SPP at different pH conditions. The presence of peaks corresponding to wavenumbers of 2925, 2855, 1618-1681 and 1530-1550 cm^{-1} confirms the absorbed proteins on MMT after surface coating. The peak of SPP at 1244 cm^{-1} (Figure 4.3) disappeared after coating MMT (Figure 4.4), demonstrating the changes of protein secondary conformational structures such as α-helix and β-sheet after

adsorption on MMT (Cai & Singh, 2004; Quiquampoix & Burns, 2007; Servagent-Noinville, Revault, Quiquampoix, & Baron, 2000; Wang, Ke, Wang, Xi, & Cui, 2010). Peaks at wavenumbers of 1450-1400 cm^{-1} varied for samples coated at different pH conditions, while peaks at 1410 cm^{-1} disappeared for the ones at acidic pHs, but strengthened at alkaline pHs, illustrating more carboxylate groups formed at more basic conditions. Changes in relative intensities of the double peaks, i.e. the ratio of carboxyl to carboxylate groups, additionally indicate changes of protein structures after adsorption on MMT (Quiquampoix & Burns, 2007; Servagent-Noinville, Revault, Quiquampoix, & Baron, 2000).

In addition, more hydrogen bonds formed at lower pH, demonstrated by broader peaks at wavenumbers of 3550-3230 cm^{-1} that are characteristic of hydroxyl group (Chen & Zhang, 2006). Hydrogen bonds can be formed between Si-O-Si and –OH groups of MMT and polar groups of proteins such as amide. The Si-O absorbance band occurs at wavenumbers of ~1120-1014 cm^{-1} and the disordering of clay platelets results in the intensity increase (Chen & Zhang, 2006). The broad peaks at wavenumbers of both 3550-3230 and ~1120-1014 cm^{-1} in Figure 4.4A illustrate the significance of hydrogen bonding between MMT platelets and soy proteins at highly acidic conditions.

4.4.1.3. Total protein coated on MMT

The amount of protein coating MMT was estimated by both the percentages remaining in the supernatant and those in the precipitate (Table 4.2). Despite discrepancy, two sets of results, calculated by different protein assay methods, showed more than 90% protein bound with MMT and there was no apparent trend of pH impact. Further, although Table 4.2 showes the lowest solubility at pH 4.0, the amount of protein binding MMT was not the smallest. The two major soy protein fractions, glycinin and β-conglycinin, are composed of different subunits. Glycinin

has 6 acidic subunits of ca. 35 kDa and 6 basic units of ~20 kDa (Badley, Atkinson, Hauser, Oldani, Green, & Stubb, 1975), while β-conglycinin is a trimer corresponding to 60, 67 and 71 kDa (Maruyama, et al., 1998). The association and dissociation of these subunits are dependent on pH, temperature, and reducing agents, etc. (Badley, Atkinson, Hauser, Oldani, Green, & Stubb, 1975; Maruyama, et al., 1998) and likely impact the coating results. It however should be noted that charged patches on protein surface may allow the binding with polyelectrolytes that have a same type of net charge as proteins (Dickinson, 2003). Even at high pH of above 10.0 – far away from the pI of soy protein, the existence of positively charged amino acids such as lysine, histidine and arginine, accounting for ca. 14.77-15.39 g/100 g of soy protein despite the varieties of soybeans (Wang, Gao, Zhang, Zhang, Li, He, et al., 2010; Wang, Tang, Yang, & Gao, 2008), contributes to the electrostatic attraction with MMT. Since the charged amino acid residues are mainly located on the surface of protein molecules (Tang, Chen, & Ma, 2009), the electrostatic binding of soy proteins on MMT at pH above pI should not be excluded. Nevertheless, the protein adsorption data again suggests the significance of both coulumbic (electrostatic attraction) and non-coulumbic forces.

4.4.1.4. Zeta potential

As shown in Figure 4.5, bare MMT dispersed in phosphate buffer had negative charges at all pH conditions. Zeta potential values of the soy protein-coated MMT were less negative than those of bare ones. Soy protein had zeta potential values ranging approximately from +30 to -50 mV, being positive at pH below pI and negative at pH above pI (Malhotra & Coupland, 2004). Below pH 5.0, soy proteins are positively charged, and the adsorption of soy proteins on MMT is expected to lower the absolute value of zeta potential of MMT due to the partial charge neutralization, more apparent at a lower pH. Above pH 5.0, soy proteins are overall negatively

charged, but more than 90% were adsorbed on MMT (Table 4.2). The adsorption due to both coulumbic and non-coulumbic mechanisms, as discussed above, is reflected by increased zeta-potential value of MMT after coating. Further, the less negative charges of protein-coated MMT at alkaline pH than that of bare MMT suggests that the SPP surface-coated on MMT partially neutralized the negative charges on MMT surface by some positively-charged patches on the surface of protein molecules.

4.4.2. Effect of MMT:SPP Mass Ratio on MMT Structure Coated by SPP at pH 9.0

Because pH 9.0 was used in extraction, verified for good solubility of SPP (Table 4.2) and corresponded to the largest d-spacing (Table 4.1), this pH was used to study the impact of MMT:SPP mass ratios, shown in Figure 4.6 for XRD patterns and Table 4.3 for d-spacing values. Two diffraction peaks were detected for samples prepared with MMT:SPP mass ratios of 49:1 and 9:1: one similar to that of the pristine MMT and the other showing a left-shift to a lower 2θ angle. The corresponding d-spacing values were 2.30 and 1.24 nm at the mass ratio of 9:1 and 2.64 and 1.27 nm at the mass ratio of 49:1. When comparing to a single peak at a mass ratio of 4:1, as discussed above, the insufficient amount of soy protein only enabled partial intercalation of MMT platelets at MMT:SPP mass ratios of 49:1 and 9:1. When the MMT:SPP mass ratio was decreased to 2:1, corresponding to an increased protein mass level, the diffraction peak of pristine MMT at 2θ angle of 7.11° was no longer detected. The disappearance of the diffraction peak characteristic of pristine MMT generally can be caused by formation of either fully exfoliated or highly intercalated structures that are beyond the detection limit of the set 2θ range (Dang, Lu, Yu, Sun, & Yuan, 2010), which was 2°, corresponding to a d-spacing value of 4.41 nm.

To clarify that the disappearance of the characteristic peak was not caused by dilution of MMT with SPP (Kumar, 2009), simple mixtures of MMT and SPP at mass ratios from 2:1 to 49:1 were also characterized by XRD. All mixtures demonstrated a peak corresponding to a 2θ angle of 6.9-7.3° (Figure 4.7) with d-spacing values of 1.21-1.28 nm (Table 4.3), very similar to that of pristine MMT (Figure 4.1). Thus, the changes in XRD patterns of coated MMT at different mass ratios are due to intercalation and/or exfoliation of platelets, and the larger d-spacing at a smaller MMT:SPP mass ratio, i.e., a higher protein mass level, is likely caused by increased possibility for protein chains to penetrate into MMT galleries to separate clay platelets (Tang, Alavi, & Herald, 2008a). The results from XRD have been repeatedly verified by structures assessed by structures assessed by transmission electron microscopy (Kumar, 2009; Tang, Alavi, & Herald, 2008a) that was thus not attempted in this study.

This group of samples was also characterized for FTIR that had similar features as discussed previously (data not shown), verifying the presence of proteins on MMT after coating and the multiple interactions between MMT and proteins. Similarly, zeta potential was measured for samples prepared with various MMT:SPP mass ratios. As depicted in Figure 4.8, a higher SPP mass level corresponded to a less negative zeta potential, indicating an increased amount of soy proteins adsorbed on MMT, in turn, enhanced charge neutralization on MMT surfaces. This group of study strengthens the conclusion that the proteins coated on MMT involves both coulumbic and non-coulumbic forces.

4.5. CONCLUSION

MMT was modified from highly ordered to highly intercalated or exfoliated structures after surface coating by a sufficient amount of soy protein. The percentage of protein binding on

MMT exceeded 90% at an MMT:SPP mass ratio of 4:1, regardless of coating pH conditions. The binding was caused by both electrostatic interactions and non-coulumbic forces such as hydrogen bonding between MMT and soy protein, which was verified by complimentary results from XRD, FTIR, and zeta-potential analyses, as well as quantifications of unbound and bound proteins. The present study thus demonstrated that intercalation/exfoliation of MMT can be easily achieved by coating using low-cost soy protein. The practical approach can be integrated in preparation of various nanocomposite materials.

LIST OF REFERENCES

Arora, A., & Padua, G. W. (2010). Review: nanocomposites in food packaging. *Journal of Food Science, 75*(1), R43-R49.

Badley, R. A., Atkinson, D., Hauser, H., Oldani, D., Green, J. P., & Stubb, J. M. (1975). The structure, physical and chemical properties of the soy bean protein glycinin. *Biochim Biophys Acta, 412*, 214-428.

Cao, N., Fu, Y. H., & He, J. H. (2007). Preparation and physical properties of soy protein isolate and gelatin composite films. *Food Hydrocolloids, 21*(7), 1153-1162.

Chen, P., Tian, H. F., Zhang, L., Chen, Y., Wang, X. Y., & Do, Y. M. (2008). Structure and properties of soy protein/alumina hydrate nanocomposites fabricated via *in situ* synthesis. *Journal of Biobased Materials and Bioenergy, 2*(3), 248-257.

Chen, P., & Zhang, L. (2006). Interaction and properties of highly exfoliated soy protein/montmorillonite nanocomposites. *Biomacromolecules, 7*(6), 1700-1706.

Cuq, B., Gontard, N., & Guilbert, S. (1998). Proteins as agricultural polymers for packaging production. *Cereal Chemistry, 75*(1), 1-9.

Dang, Q. Q., Lu, S. D., Yu, S., Sun, P. C., & Yuan, Z. (2010). Silk fibroin/montmorillonite nanocomposites: effect of pH on the conformational transition and clay dispersion. *Biomacromolecules, 11*(7), 1796-1801.

de Azeredo, H. M. C. (2009). Nanocomposites for food packaging applications. *Food Research International, 42*(9), 1240-1253.

Dickinson, E. (2003). Hydrocolloids at interfaces and the influence on the properties of dipsersed systems. *Food Hydrocolloids, 17*, 25-39.

Ding, X. L., & Henrichs, S. M. (2002). Adsorption and desorption of proteins and polyamino acids by clay minerals and marine sediments. *Marine Chemistry, 77*(4), 225-237.

Essington, M. E. (2003). *Soil and water chemistry: an intergrative approach* CRC Press, LLC. Boca Raton, FL.

Feng, M., Zhao, C. G., Gong, F. L., & Yang, M. S. (2004). Study on the modification of sodium montmorillonite with amino silanes. *Acta Chimica Sinica, 62*(1), 83-87.

Gunister, E., Pestreli, D., Unlu, C. H., Atici, O., & Gungor, N. (2007). Synthesis and characterization of chitosan-MMT biocomposite systems. *Carbohydrate Polymers, 67*(3), 358-365.

Ikeda, S., & Foegeding, E. A. (1999). Dynamic viscoelastic properties of thermally induced whey protein isolate gels with added lecithin. *Food Hydrocolloids, 13*(3), 245-254.

Jahangir, S., & Leber, M. J. (2007). Biodegradable good packaging: an environmental imperative. *Industry Report*, 1-20.

Krochta, J. M., & DeMulderJohnston, C. (1997). Edible and biodegradable polymer films: challenges and opportunities. *Food Technology, 51*(2), 61-74.

Kumar, P. (2009). Development of bio-nanocomposite films with enhanced mechanical and barrier properties using extrusion processing. *North Carolina State University. Ph.D dissertation*.

Kumar, P., Sandeep, K. P., Alavi, S., Truong, V. D., & Gorga, R. E. (2010a). Effect of type and content of modified montmorillonite on the structure and properties of bio-nanocomposite films based on soy protein isolate and montmorillonite. *Journal of Food Science, 75*(5), N46-N56.

Kumar, P., Sandeep, K. P., Alavi, S., Truong, V. D., & Gorga, R. E. (2010b). Preparation and characterization of bio-nanocomposite films based on soy protein isolate and montmorillonite using melt extrusion. *Journal of Food Engineering, 100*(3), 480-489.

L'Hocine, L., Boye, J. I., & Arcand, Y. (2006). Composition and functional properties of soy protein isolates prepared using alternative defatting and extraction procedures. *Journal of Food Science, 71*(3), C137-C145.

Le Corre, D., Bras, J., & Dufresne, A. (2010). Starch nanoparticles: a review. *Biomacromolecules, 11*(5), 1139-1153.

Lin, J. J., Wei, J. C., Juang, T. Y., & Tsai, W. C. (2007). Preparation of protein−silicate hybrids from polyamine intercalation of layered montmorillonite. *Langmuir, 23*, 1995-1999.

Liu, S. H., Zhou, R. B., Tian, S. J., & Gai, J. Y. (2007). A study on subunit groups of soybean protein extracts under SDS-PAGE. *Journal of the American Oil Chemists Society, 84*(9), 793-801.

Malhotra, A., & Coupland, J. N. (2004). The effect of surfactants on the solubility, zeta potential, and viscosity of soy protein isolates. *Food Hydrocolloids, 18*(1), 101-108.

Mallakpour, S., & Dinari, M. (2011). Preparation and characterization of new organoclays using natural amino acids and Cloisite Na(+). *Applied Clay Science, 51*(3), 353-359.

Mariotti, F., Tome, D., & Mirand, P. P. (2008). Converting nitrogen into protein - Beyond 6.25 and Jones' factors. *Critical Reviews in Food Science and Nutrition, 48*(2), 177-184.

Markets, R. a. (2011). The global outlook for biodegradable packaging. Accessed by website: http://www.researchandmarkets.com/research/5e27e0/the_global_outlook. *Business Insights, June*, 110.

Maruyama, N., Katsube, T., Wada, Y., Oh, M. H., Barba De La Rosa, A. P., Okuda, E., Nakagawa, S., & Utsumi, S. (1998). The roles of the N-linked glycans and extension regions of soybean beta-conglycinin in folding, assembly and structural features. *Eur J Biochem, 258*, 854-862.

Nakasato, K., Ono, T., Ishiguro, T., Takamatsu, M., Tsukamoto, C., & Mikami, M. (2004). Rapid quantitative analysis of the major components in soymilk using fourier transform infrared spectroscopy (FT-IR). *Food Science and Technology Research, 10*(2), 137-142.

Paetau, I., Chen, C. Z., & Jane, J. L. (1994). Biodegradable plastics made from soybean products.1. effect of preparation and processings on mechanical-properties and water-absorption. *Industrial & Engineering Chemistry Research, 33*(7), 1821-1827.

Quiquampoix, H., & Burns, R. G. (2007). Interactions between proteins and soil mineral surfaces: Environmental and health consequences. *Elements, 3*(6), 401-406.

Servagent-Noinville, S., Revault, M., Quiquampoix, H., & Baron, M. H. (2000). Conformational changes of bovine serum albumin induced by adsorption on different clay surfaces: FTIR analysis. *Journal of Colloid and Interface Science, 221*(2), 273-283.

Song, F., Tang, D. L., Wang, X. L., & Wang, Y. Z. (2011). Biodegradable soy protein isolate-based materials: a review. *Biomacromolecules, 12*(10), 3369-3380.

Sorrentino, A., Gorrasi, G., & Vittoria, V. (2007). Potential perspectives of bio-nanocomposites for food packaging applications. *Trends in Food Science & Technology, 18*(2), 84-95.

Tang, X. Z., Alavi, S., & Herald, T. J. (2008). Barrier and mechanical properties of starch-clay nanocomposite films. *Cereal Chemistry, 85*(3), 433-439.

Wang, X. C., & Lee, C. (1993). Adsorption and desorption of aliphatic-amines, amino-acids and acetate by clay-minerals and marine-sediments. *Marine Chemistry, 44*(1), 1-23.

Wu, W., Zhang, C. M., Kong, X. Z., & Hua, Y. F. (2009). Oxidative modification of soy protein by peroxyl radicals. *Food Chemistry, 116*(1), 295-301.

Xiang, L. X., Tang, C. Y., Cao, J., Wang, C. Y., Wang, K., Zhang, Q., Fu, Q., & Zhao, S. G. (2009). Preparation and characterization of soy protein isolate (SPI)/montmorillonite (MMT) bionanocomposites. *Chinese Journal of Polymer Science, 27*(6), 843-849.

Yang, Y., Zhu, Z. K., Yin, J., Wang, X. Y., & Qi, Z. E. (1999). Preparation and properties of hybrids of organo-soluble polyimide and montmorillonite with various chemical surface modification methods. *Polymer, 40*(15), 4407-4414.

Zhao, R. X., Torley, P., & Halley, P. J. (2008). Emerging biodegradable materials: starch- and protein-based bio-nanocomposites. *Journal of Materials Science, 43*(9), 3058-3071.

APPENDIX

Table 4. 1. Basal spacing of MMT after coating by soy protein at an MMT:soy protein powder mass ratio of 4:1 and pH 2.0-10.0.

Coating pH	2θ(°)	d-spacing (nm)
2.0	6.63	1.33
3.0	7.07	1.25
4.0	6.96	1.27
5.0	7.08	1.25
6.0	4.23	2.09
	6.93	1.27
7.0	4.37	2.01
	6.98	1.27
8.0	4.30	2.05
9.0	4.16	2.12
10.0	4.43	1.99

Table 4. 2. Impact of pH on soy protein solubility and binding onto MMT at an MMT:soy protein powder mass ratio of 4:1.

pH	Protein Solubility (%)[1]	Unbound Protein(%)[1]	Bound Protein (%) [2]
2.0	87.07 ± 0.29^{abc}	0.72 ± 0.005^{G}	100.00 ± 1.68^{bc}
3.0	83.50 ± 0.61^{e}	0.80 ± 0.01^{F}	105.09 ± 2.33^{a}
4.0	72.77 ± 1.91^{f}	0.55 ± 0.01^{H}	93.91 ± 1.34^{cd}
5.0	80.88 ± 1.79^{de}	0.71 ± 0.01^{G}	106.71 ± 2.48^{a}
6.0	86.08 ± 1.05^{bcde}	1.15 ± 0.01^{D}	103.11 ± 1.84^{ab}
7.0	85.35 ± 0.51^{cde}	0.95 ± 0.02^{E}	97.64 ± 2.58^{bc}
8.0	86.02 ± 0.62^{abcd}	2.18 ± 0.04^{A}	90.19 ± 2.44^{d}
9.0	89.13 ± 0.68^{ab}	1.85 ± 0.03^{B}	93.29 ± 2.89^{cd}
10.0	88.45 ± 0.57^{a}	1.60 ± 0.03^{C}	92.80 ± 2.07^{cd}

[1] Different superscripts in each column indicate significant difference ($P<0.001$). Numbers are average ± standard deviations from three measurements using the BCA method.

[2] Different superscripts in this column indicate significant difference ($P<0.001$). Numbers are average ± standard deviations from three measurements using the Dumas method.

Table 4. 3. XRD characteristics of MMT coated by soy protein at pH 9.0 using different MMT:soy protein powder (SPP) mass ratios, with comparison to simple mixtures of MMT and SPP.

	MMT:SPP mass ratio	2θ (°)	d-spacing (nm)
Coated sample	2:1	Not detected	Not detected
	4:1	4.16	2.12
	9:1	3.84	2.30
		7.13	1.24
	49:1	3.35	2.64
		6.91	1.26
Simple mixture	2:1	7.29	1.21
	4:1	7.06	1.25
	9:1	6.98	1.27
	49:1	6.90	1.28

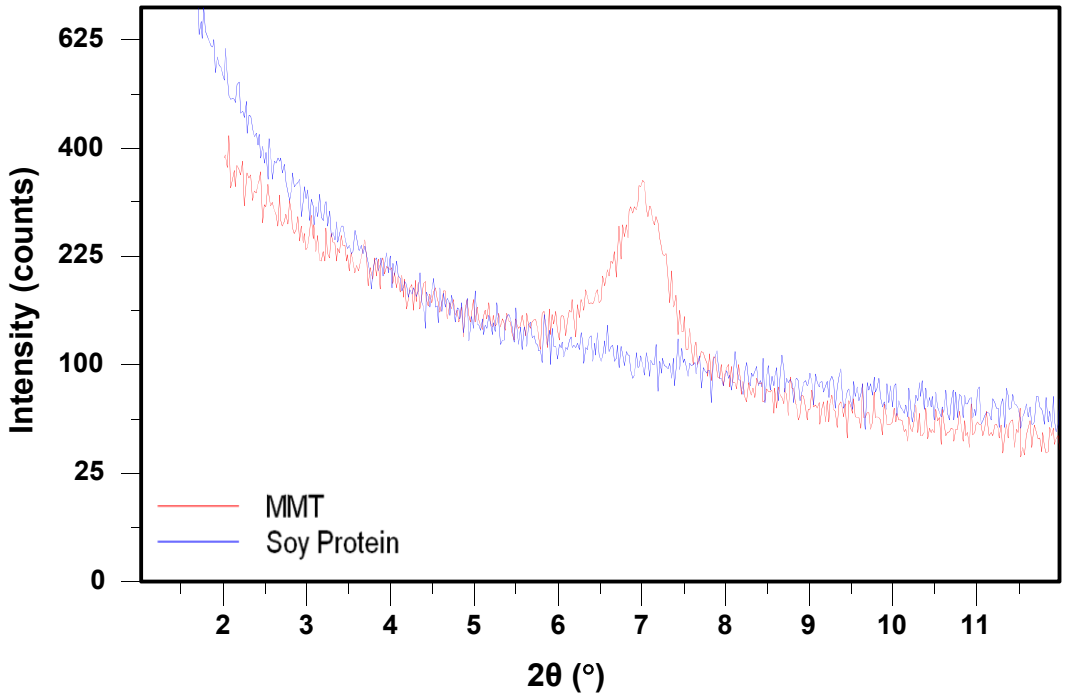

Figure 4. 1. XRD patterns of pristine MMT (red) and soy protein powder (blue).

The 2θ angle for MMT peak is 7.11°, with d-spacing of 1.24 nm.

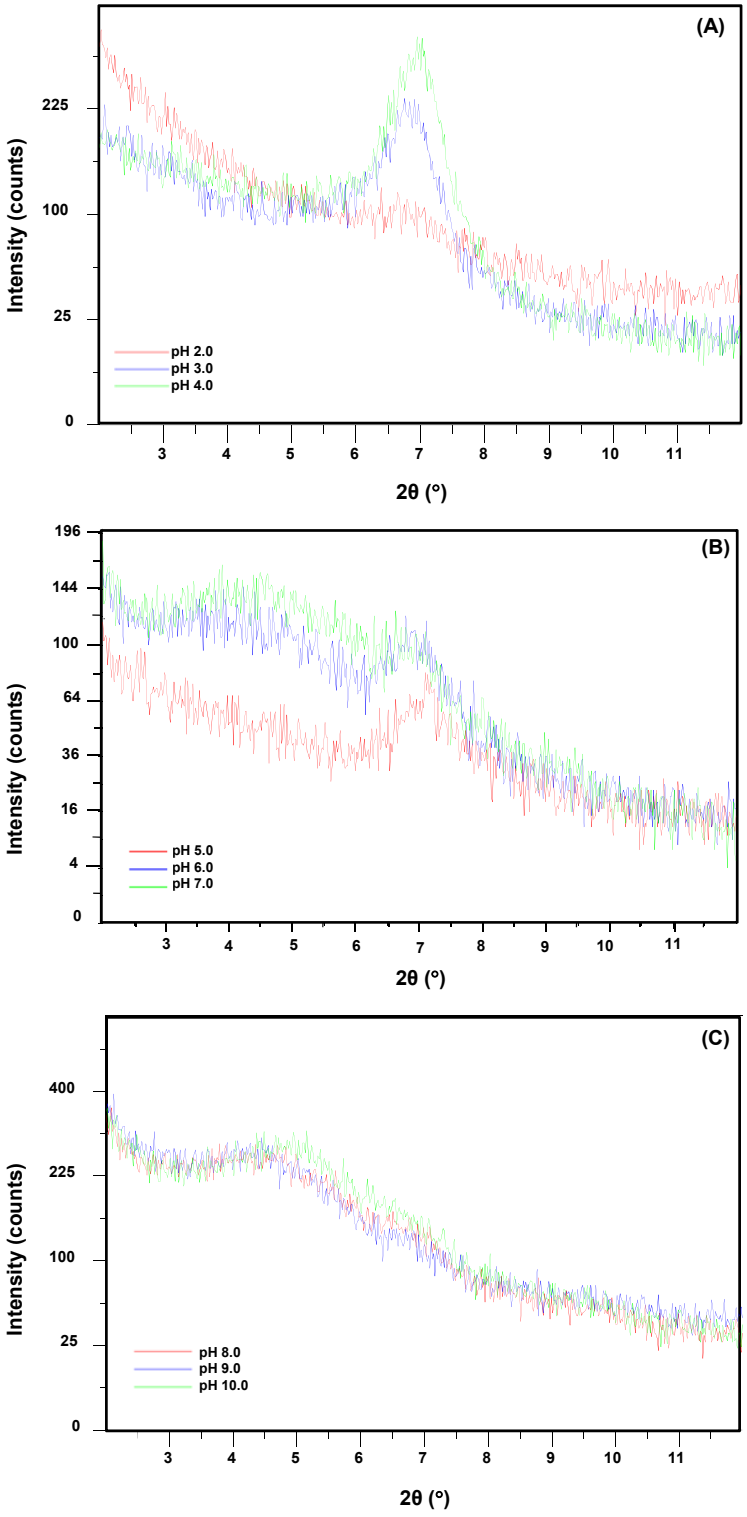

Figure 4. 2. XRD patterns of MMT coated by soy protein powder (SPP) using an MMT:SPP mass ratio of 4:1at (A) pH 2.0-4.0, (B) pH 5.0-7.0, and (C) pH 8.0-10.0.

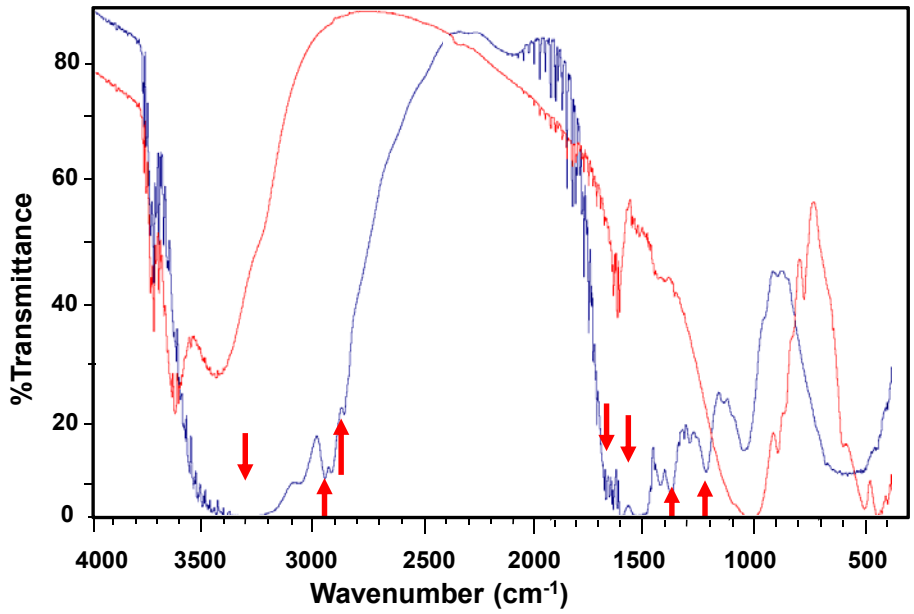

Figure 4. 3. FTIR spectra of pristine MMT (red) and soy protein powder (blue).

Arrows highlight the positions discussed in the text.

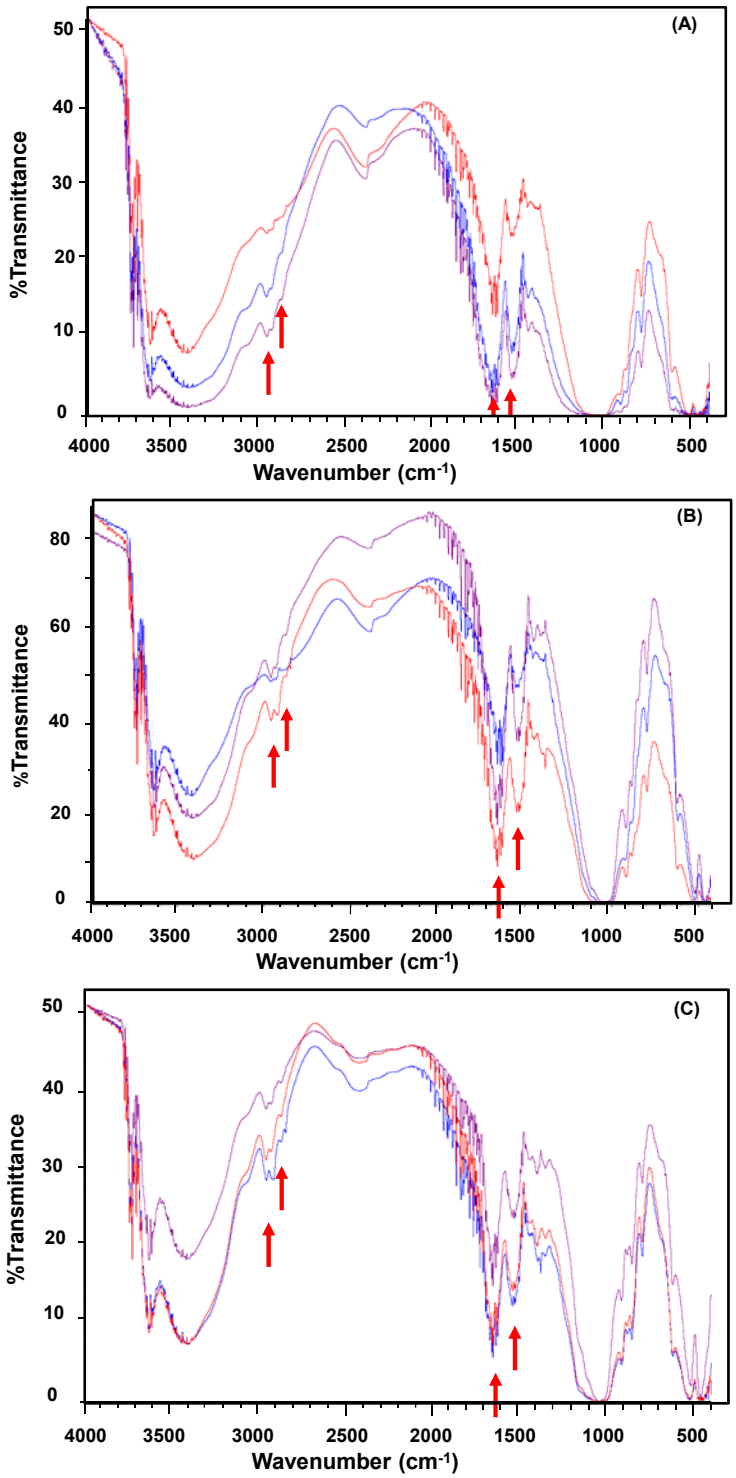

Figure 4. 4. FTIR spectra of MMT coated by soy protein at an MMT:soy protein powder mass ratio of 4:1 and (A) pH 2.0 (blue), 3.0 (purple), and 4.0 (red), (B) pH 5.0 (blue), 6.0 (purple), and 7.0 (red) and (C) pH 8.0 (blue), 9.0 (purple), and 10.0 (red).
Arrows highlight positions discussed in the text.

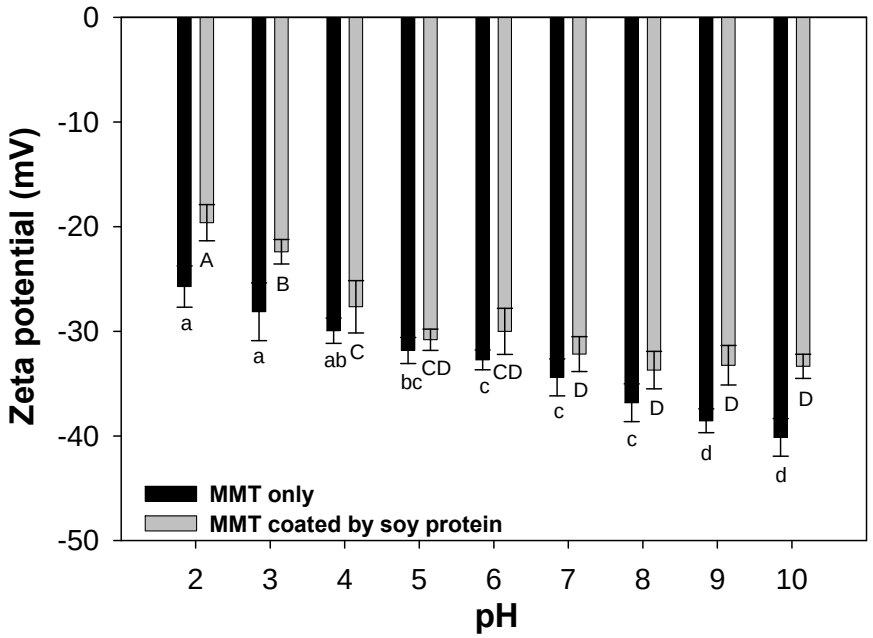

Figure 4. 5. Comparison of zeta potential of bare MMT dispersions in 10mM NaH_2PO_4 buffer and soy protein-coated MMT at pH 2.0-10.0. Coating was conducted at an MMT:SPP mass ratio of 4:1.

Error bars are standard deviations for duplicate coating experiments, each measured for three times. Different letters in each group (bare and protein-coated MMT) indicate significant difference ($P<0.001$).

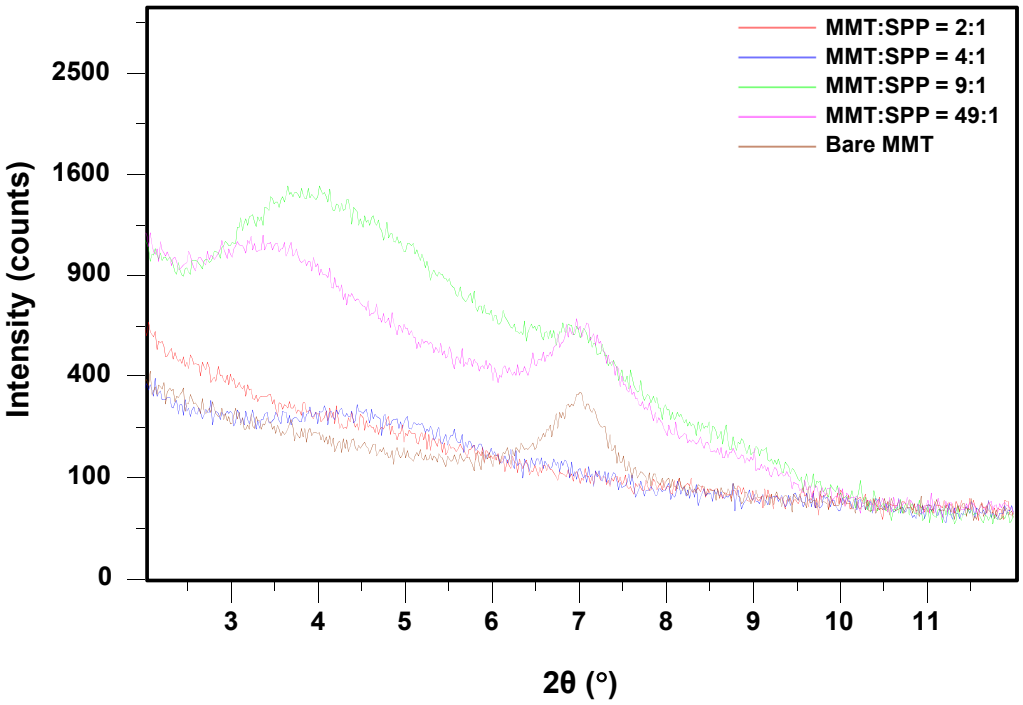

Figure 4. 6. XRD patterns of pristine MMT (brown) and MMT coated by soy protein power (SPP) at MMT:SPP mass ratios of 2:1 (red), 4:1 (blue), 9:1 (green) and 49:1 (pink) at pH 9.0. The curves at the 4:1 mass ratio and pristine MMT are repeated here for convenience of comparison.

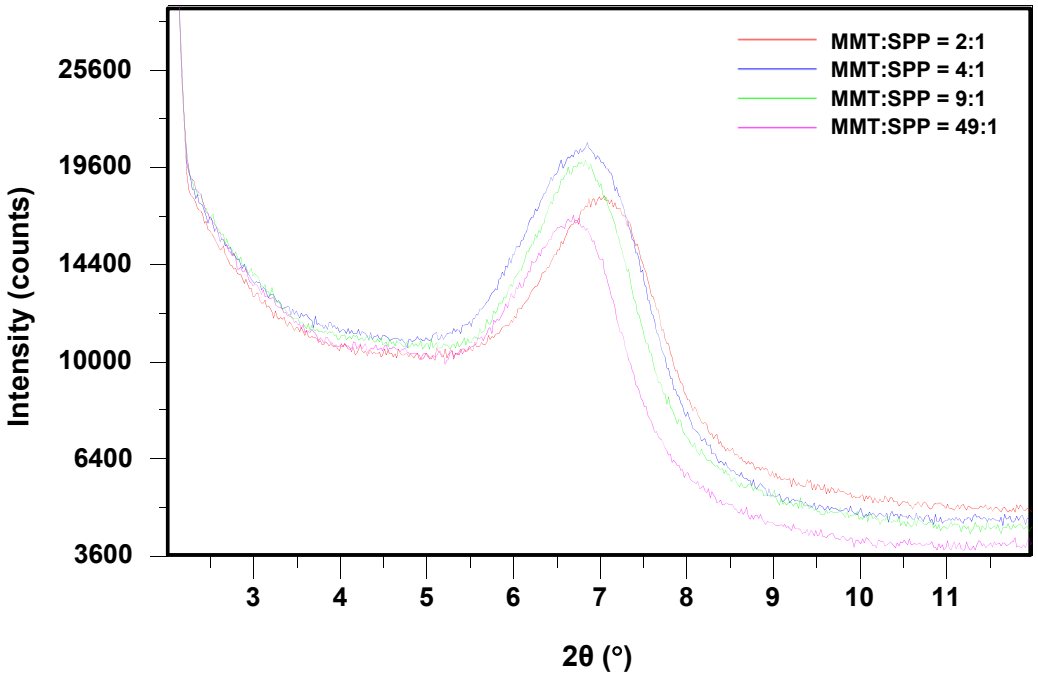

Figure 4. 7. XRD patterns of simple mixtures of MMT and soy protein powder (SPP) at MMT:SPP mass ratios of 2:1 (red), 4:1 (blue), 9:1 (green) and 49:1 (pink). The data at the 4:1 mass ratio is repeated here for convenience of comparison.

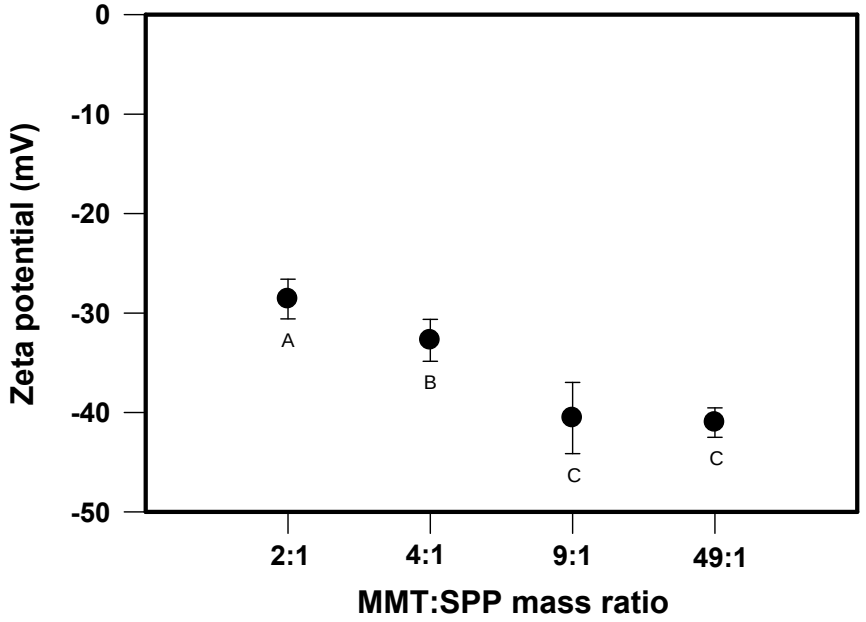

Figure 4. 8. Zeta potential of MMT coated by soy protein powder (SPP) at pH 9.0 using various MMT:SPP mass ratios.

Error bars are standard deviations for duplicate coating experiments, each measured for three times. Different letters next to symbols indicate significant difference ($P<0.001$).

CHAPTER 5 . TRANSGLUTAMINASE CROSS-LINKING OF SOY PROTEIN IN THE CONTINUOUS PHASE AND ON INTERCALATED MONTMORILLONITE NANOCLAY PROBED BY DYNAMIC RHEOLOGY

5.1. ABSTRACT

The objective of this work was to enhance interactions between layered montmorillonite (MMT) nanoclay and continuous phase biopolymer. MMT was intercalated by surface-coating with soy protein before being dispersed in soy protein suspensions for crosslinking by microbial transglutaminase (mTGase). Dynamic rheology was performed to study variables of sodium chloride and mTGase concentrations, with and without MMT. Without mTGase and MMT, the maximum storage modulus (G') was achieved at 100 mM NaCl, while the addition of MMT corresponded to an identical increase in G' at 200-1000 mM NaCl. With a higher level of mTGase, a shorter gelling time and a stronger hydrogel were observed. The addition of protein-coated MMT further increased G' and shortened the gelation time, with the highest G' observed for the treatment with 1.00%w/v mTGase and 100 mM NaCl. Our results demonstrate that mTGase cross-linking is effective in enhancing interactions between the matrix and fillers in the nanocomposite system.

Keywords: nanocomposite, enzymatic crosslinking, soy protein, protein coated nanoclay, dynamic rheology

5.2. INTRODUCTION

Bio-nanocomposites, by dispersing inorganic nanoparticles in a matrix of biopolymer, have attracted much attention as novel packaging materials for substitutions of petroleum-derived plastics due to their renewability and bio-degradability (Arora & Padua, 2010; Dang, Lu, Yu, Sun, & Yuan, 2010; de Azeredo, 2009). Proteins with good film-forming properties, such as soy protein (SP), wheat gluten, pea protein and gelatin, have been extensively studied for bio-derived packaging materials, with several recent studies investigating the improvement of mechanical and barrier properties of nanocomposite films after incorporating nanoclays such as montmorillonite (MMT) (Arora & Padua, 2010; Chang, Yang, Huang, Xia, Feng, & Wu, 2009; Chen & Zhang, 2006; Guilherme, Mattoso, Gontard, Guilbert, & Gastaldi, 2010; Kumar, Sandeep, Alavi, Truong, & Gorga, 2010a, 2010b; Lee & Kim, 2010; Martucci & Ruseckaite, 2010). Soy protein isolate (SPI)/MMT nanocomposite films have been reported for improved vapor permeability and mechanical properties than those without nanofillers (Chen & Zhang, 2006; Kumar, Sandeep, Alavi, Truong, & Gorga, 2010a, 2010b; Lee & Kim, 2010). However, water vapor permeability of SPI-based nanocomposite films, because of the hydrophilic nature of SP, still requires substantial improvement when compared to petrochemical-based plastics (Kumar, Sandeep, Alavi, Truong, & Gorga, 2010a).

It is well established that achieving either intercalation or exfoliation of layered nanoclay is critical to improve mechanical and barrier properties of nanocomposite materials (Le Corre, Bras, & Dufresne, 2010; Tang, Alavi, & Herald, 2008a). Modification of nanoclays by increasing basal spacing with intercalated and/or exfoliated structures prior to incorporation into the polymer matrix is a viable approach in improving structure and properties of final nanocomposite materials (Feng, Zhao, Gong, & Yang, 2004; Lin, Wei, Juang, & Tsai, 2007;

Mallakpour & Dinari, 2011). In our separate study, surface coating of MMT via solution intercalation by SP was observed to have enlarged basal spacing of MMT platelets that corresponded to highly intercalated and/or exfoliated layers. In this study, the major objective was to improve the interaction between protein-coated MMT and matrix SP so as to develop nanocomposite materials with enhanced mechanical and barrier properties.

Crosslinking proteins coating MMT and those in the continous matrix is a logical approach to enhance the interactions of the nanocomposite system. Enzymatic and chemical cross-linking approaches have been studied for soy proteins (Caillard, Remondetto, & Subirade, 2009, 2010; de Carvalho & Grosso, 2004; Gan, Latiff, Cheng, & Easa, 2009; Jiang, Tang, Wen, Li, & Yang, 2007; Yildirim & Hettiarachchy, 1998). The focus of this study was the enzymatic method because it has been used in food production, which reduces possible regulatory issues when applying to nanocomposite materials for applications such as food packaging films. Transglutaminase (EC 2.3.2.13, protein-glutamine γ-glutamyltransferase, TGase) is an enzyme with the capability of catalyzing crosslinking reactions between protein molecules, peptides, and primary amines through acyl transfer reactions to form inter- or intramolecular ε-(γ-glutamyl)lysine isopeptidic bond (Seguro, Nio, & Motoki, 1996; Zhu, Bol, Rinzema, Tramper, & Wijngaards, 1999). TGase is ubiquitous, and the morden biotechnology has made it possible to produce microbial TGase (mTGase) for commercial applications. The mTGase has been studied extensively to improve functional properties of food proteins and protein-containing products such as meat (Motoki & Seguro, 1998; Seguro, Nio, & Motoki, 1996). Reduced solubility and increased surface hydrophobicity of SP was observed after treatment by mTGase, and the films prepared from mTGase-treated SP had decreased solubility and improved mechanical properties such as tensile strength and elongation at break (Gan, Latiff, Cheng, & Easa, 2009). Thus,

mTGase has the potential to improve the interactions of the nanocomposite system studied in this work.

Specifically in this work, dynamic rheological tests were applied as a non-destructive method to investigate interactions of SP dispersions with protein-coated MMT during cross-linking by mTGase and the subsequent thermal treatment steps to additionally improve network strength. Variables in enzymatic cross-linking included the concentrations of sodium chloride and mTGase, and the presence or absence of protein-coated MMT.

5.3. MATERIALS AND METHODS

5.3.1. Materials

Cloisite® Na^+-montmorillonite was purchased from Southern Clay Products, Inc. (Gonzales, TX). Soy flour was a commercial product from MP Biomedicals, LLC (Solon, OH). The mTGase (ACTIVA® TI) was a product of Ajinomoto Food Ingredients, LLC (Chicago, IL). Other chemicals were from Sigma-Aldrich Corp. (St. Louis, MO) or Fisher Scientific (Fair Lawn, NJ). All reagents were used without further purification.

5.3.2. Extraction of SP

SP was extracted from soy flour using the modified protocol for preparation of SPI (L'Hocine, Boye, & Arcand, 2006). Soy flour was finely ground by a coffee grinder (Hamilton Beach Proctor-Silex, Inc., Southern Pines, NC), suspended in deionized water at a solid:liquid mass ratio of 1:10, adjusted to pH 9.0 by 4 N NaOH, and constantly stirred for 3 h at 48 °C (model Isotemp®, Fisher Scientific, Fair Lawn, NJ). The dispersion was then centrifuged (Sorvall RC 5B Plus, Newtown, CT) at 3,778*g* for 30 min at ambient temperature, and the supernatant was filtered twice using the #1 filter paper and then twice using the #2 filter paper

(Whatman®, Lawrence, KS). The extraction was repeated three times. The three permeate fractions were combined and acidified to pH 4.5 using 6 N HCl to precipitate protein followed by centrifugation (3,778*g* for 15 min). The precipitate was re-dispersed in deionized water and adjusted to pH 9.0, followed by acidic precipitation at pH 4.5 and centrifugation as above. The re-dispersion and re-precipitation were repeated for a third time. The final precipitate was dispersed in deionized water, adjusted to pH 6.5, and spray-dried utilizing a B-290 Mini Spray Dryer (BÜCHI Labortechnik AG, Postfach, Switzerland) at a feed rate of 6.67 mL/min and inlet and outlet temperatures of 150 and 55-65 °C, respectively. The spray-dried soy protein powder (SPI) was collected and stored in a -20 °C freezer.

5.3.3. Determination of Total Protein Content of SPI

The total solid in SPI was measured using the method of AOAC 925.23. The total protein content of SPI was determined for the total nitrogen content using the combustion (Dumas) method by the Atlantic MicroLab, Inc. (Norcross, GA). The nitrogen content was converted to protein content by multiplying with the Jones' factor, which is 6.25 for soy protein (Mariotti, Tome, & Mirand, 2008).

5.3.4. Preparation of Protein-coated MMT

MMT was surface-coated with SP using a solution intercalation method (Chen & Zhang, 2006). Surface-coating conditions were optimized for the mass ratio of MMT:SPI and pH in our separate study. At an MMT:SPI mass ratio of 4:1 and pH 9.0, the X-ray diffraction results demonstrated highly intercalated/fully exfoliated nanoclay platelets. Experimentally, dispersions containing 0.5% w/v SPI or 2% w/v MMT were separately prepared at an equal volume in the 10 mM NaH_2PO_4 buffer, adjusted to pH 9.0, heated at 60 °C, and stirred at 300 rpm for 30 min using a magnetic stirring hot plate (model Isotemp®, Fisher Scientific, Fair Lawn, NJ). The

MMT dispersion was slowly added to the SPI dispersion to reach an MMT:SPI mass ratio of 4:1, while being agitated at 1000 rpm and maintained at 60 °C. After 3-h agitation, the resultant slurry was ready for incorporation of SPI for mTGase cross-linking.

5.3.5. Determination of mTGase Activity

The activity of mTGase was determined using the enzymatic assay of TGase (EC 2.3.2.13) from Sigma-Aldrich Corp., with all solutions adjusted to pH 6.0 at 37 °C. The fresh enzyme solution was prepared immediately before use by dissolving enzyme powder at a concentration of 1 mg/mL in cold deionized water at ca. 4 °C. After mixing with the reaction cocktail of reagents, incubating the test sample containing mTGase at 37 °C for 10 min, and centrifugation (10,000*g*) for 5 min, the absorbance was recorded at a wavelength of 525 nm using a UV/Vis spectrophotometer (model Biomate 5, Thermo Electron Corporation, Woburn, MA). One unit of enzyme was defined as the amount of enzyme that catalyzed the formation of 1.0 μmole per min of hydroxamate from Na-CBZ-Glutaminylglycine and hydroxylamine at pH 6.0 and 37 °C. Triplicate measurements were conducted for each sample.

5.3.6. Dynamic Rheological Tests

5.3.6.1. Sample preparation

SPI was hydrated at 6% w/v in the 10 mM NaH_2PO_4 buffer or protein-coated MMT slurry overnight, with pH maintained at 6.5. Immediately before the rheological test, NaCl and mTGase were added to the dispersions to various combinations of NaCl (0, 50, 100, 200, 500, 750, and 1000 mM) and mTGase (0, 0.12, 0.16, 0.30, 0.40, and 1.00% w/v in the entire sample) concentrations. A pH value of 6.5 was chosen for cross-linking studies because (1) high protein solubility is needed for the formation of homogeneous hydrogel network (Lakemond, de Jongh, Hessing, Gruppen, & Voragen, 2000), (2) soy protein had drastically improved solubility at pH

6.5 than that at pH 6.0 (Wolf, 1970), and (3) mTGase has an optimal activity at pH 6.0 and is very stable at pH 5.0-7.0 (Ho, Leu, Hsieh, & Jiang, 2000; Tsai, Lin, & Jiang, 1996).

5.3.6.2. Rheological tests

An AR2000 rheometer (TA Instruments, New Castle, DE) equipped with a concentric cylinder geometry consisting of a bob with an outer diameter of 28 mm and a cup with an inner diameter of 30 mm was utilized to monitor cross-linking and subsequent thermal treatments of dispersions. Approximately 15 mL of the dispersion was carefully transferred into the cup. After positioning the bob and removing the excess sample, a layer of mineral oil was applied above the sample to prevent moisture loss during measurement. The oscillatory tests consisted of these sequential steps: (1) an isothermal step at 45 °C for 2 h, (2) a heating ramp from 45 to 90 °C at 2 °C/min, (3) an isothermal step at 90 °C for 1 h, (4) a cooling ramp from 90 to 25 °C at 3 °C/min, and (5) a strain sweep at 25 °C using a strain range of 0.001-1 and a frequency of 1 Hz. Except for strain sweep tests, a strain of 0.01 and a frequency of 1 Hz were used. Each sample was measured in duplicate and averages from two tests were reported.

5.4. RESULTS AND DISCUSSION

5.4.1. Representative Rheological Profiles Showing Impacts of NaCl, MMT, and mTGase

The storage modulus (G') and loss modulus (G'') of SPI dispersions developed during holding at 45 °C for 2 h for enzymatic cross-linking (step 1), heating to 90 °C (step 2), holding at 90 °C for 1 h (step 3), and cooling to 25 °C (step 4). The holding step at 45 °C was shortened to 10 min for the SPI samples added with NaCl only because protein aggregation and cross-linking is not expected. The end point at each step of the thermal profile was denoted as P1, P2, P3, or

P4, respectively. While representative rheological profiles are presented in this section, rheological properties at four end points are discussed in following sections to describe the impacts of the studied variables. The time corresponding to the cross-over of G' and G'' was used as the gelation time.

For treatments without MMT and mTGase, the G' and G'' values were small (<0.1 Pa) during heating to 90 °C but drastically increased and crossed immediately during the holding at 90 °C for samples with 50-1000 mM NaCl, demonstrated in Figure 5.1A for the 100 mM NaCl treatment, implying the formation of a hydrogel network. The insignificant development of structures during the heating step is consistent with the denaturation temperatures of two major soy protein fractions β-conglycinin and glycinin, which are 76.7 and 94.1 °C, respectively (C. H. Tang, Choi, & Ma, 2007). During holding (step 3), gelation was obtained from the gradual aggregation of denatured protein (Lakemond, de Jongh, Paques, van Vliet, Gruppen, & Voragen, 2003). As illustrated in Figure 5.1B, the addition of coated MMT gradually enhanced the G' value that was already larger than G'' at the beginning of the measurement, presumably due to both the increased volume fraction of the dispersed phase (van Vliet, 1988) and enhanced interactions between MMT-bound protein and protein molecules in dispersions. Although samples with MMT contained additional 0.25% SPI (used in coating), this increase in protein concentration (6%w/v vs. 6.25%w/v) is not sufficient to impact rheological characteristics discussed below for variables during cross-linking.

Rheological profiles of samples treated by mTGase are demonstrated in Figure 5.2. Both G' and G'' gradually increased during step 1, because of the formation of covalent bonds catalyzed by mTGase, and step 2, caused by heat-induced aggregation of protein. Figures 2A and

2B present a comparison between the absence and presence of coated MMT in combination with mTGase. In the absence of coated MMT (Figure 5.2A), G' increased more rapidly than G'' during step 1, with a cross-over indicating the formation of hydrogel network. The rates of G' and G'' developments increased upon heating over 45 °C up to around 53 °C, followed by significant decrease upon further heating up to approximately 80 °C in step 2. The quick increase in the former was probably associated with the increased rate of enzymatic crosslinking, while the latter decrease coincided with the ca. 55 °C deactivation temperature of mTGase (Nury, Meunier, & Mouranche, 1989) and may have resulted from dissociated structures due to excessive heating. The re-increase in G' when the temperature exceeded 80 °C was mainly caused by the denaturated β-conglycinin aggregation. When MMT was incorporated into SPI dispersions treated with mTGase (Figure 5.2B), G' and G'' steadily increased, contrasting the fluctuation of G' in step 2 observed for the treatment without MMT (Figure 5.2A), but the rate of increase appeared to be slower than the one without MMT. This phenomenon can be explained by the interfering between the hydrogel network and MMT, in which newly formed hydrogel network was further fortified by the intercalated MMT that behaved as rigid fillers (van Vliet, 1988). The slow crosslinking rate further favored the formation of compact gel network (Jiang, Tang, Wen, Li, & Yang, 2007a).

When NaCl was present during mTGase cross-linking, Figure 5.2C (without coated-MMT) and Figure 5.2D (with coated-MMT) both show fast increases of G' in the early stage of step 1 and gradual increases afterwards. When comparing to treatments with NaCl (Figure 5.1A) or mTGase only (Figure 5.2A), Figure 5.2C demonstrates synergistic effects of ionic strength and enzymatic cross-linking on hydrogel network development. Once MMT was incorporated in

the dispersion treated with both 100 mM NaCl and mTGase (Figure 5.2D), G' began with a high value and continuously increased during step 1 and 2. The almost constant G' in step 3 indicates that the incorporation of surface-coated MMT into SPI dispersions improved heat-resistant property of the formed hydrogel network.

During cooling (step 4), hydrogels formed under all treatments were further strengthened, evidenced by continuous increases of G' and G'', due to the formation of hydrogen bonds (Song, Tang, Wang, & Wang, 2011). Upon cooling to 25 °C, the strain sweep tests verified that the oscillatory deformation using a frequency of 1 Hz and a strain of 0.01 was within the limit of linear viscoelastic regime.

5.4.2. Effects of Ionic Strength and MMT on Rheological Properties of SPI Dispersions without mTGase Cross-linking

For treatments without mTGase and NaCl, SPI dispersions did not show significant changes in the moduli throughout step 1-step 4, indicating the SPI at 6% w/v alone is insufficient to form a hydrogel network. After supplementing 50-1000 mM NaCl, G' values at the end of each step are presented in Figure 5.3 for treatments with and without coated-MMT. For those without MMT, the magnitude of G' did not change significantly at all NaCl concentrations during heating from 45 to 90 °C, showing almost identical G' at P1 and P2 (Figure 5.3A). As mentioned previously, SPI dispersions formed hydrogels immediately after the temperature reached 90 °C, followed by drastic increase of G' and G'' during 1-h holding at 90 °C that showed dependence on the ionic strength. The G' at P3 remarkably increased when NaCl concentration increased from 50 to 100 mM but decreased at higher ionic strengths. At pH 6.5, soy proteins are net negatively-charged (Malhotra & Coupland, 2004). Due to electrostatic

repulsion between protein molecules, the probability of aggregation between two protein molecules is relatively low at low ionic strengths. An increase in the ionic strength is expected to facilitate aggregation between protein molecules since the charges on protein molecules are shielded to a greater extent. It has been established that protein hydrogel networks become coarser and mechanically weaker with increasing rate of aggregation at high ionic strengths (Ikeda, Foegeding, & Hagiwara, 1999). The present results suggest that 100 mM is the optimum NaCl concentration for maximizing the mechanical strength of the formed hydrogel networks. Significant increases in G' were observed at relatively low NaCl concentrations of 50-200 mM after SPI dispersions were cooled to 25 °C. It was confirmed that the maximum G' at P4 was obtained at 100 mM NaCl, consistent with the optimum NaCl concentration for heat-induced gelation of whey protein isolate (Ikeda & Foegeding, 1999).

In contrast to Figure 5.3A, SPI dispersions containing surface-coated MMT exhibited different trends: G' increased with an increase in NaCl concentration up to 200 mM before reaching a plateau (Figure 5.3B). As discussed above, the addition of coated-MMT changes interactions among protein molecules in the continuous phase and increases the overall volume fraction of the dispersed phase and thus G' (van Vliet, 1988). At 50-200 mM NaCl, MMT appeared to interfere with protein-protein aggregation and the development of hydrogel networks, demonstrating lower G' than the samples without MMT (Figure 5.3A). Above 200 mM NaCl, G' was not impacted by ionic strength, indicating the network-weakening at high ionic strengths in MMT-free systems (Figure 5.3A) was not significant when comparing to the impacts on overall network structures due to addition of surface-coated MMT. It was previously suggested that fillers strengthen the hydrogel moduli only for the case of strong interactions between fillers and matrix polymer molecules (van Vliet, 1988). The results in Figure 5.3 suggest that the coated-

MMT silicates are active fillers improving the mechanical strength of hydrogel networks but inhibited the effect of ionic strength on protein-protein aggregations. The impacts of mTGase cross-linking on hydrogel strengths of SPI dispersions with coated-MMT are presented below for the strongest and weakest systems in Figure 5.3, corresponding to 0 and 100 mM NaCl.

5.4.3. Rheological Properties of SPI Dispersions Cross-linked by mTGase at 0 mM NaCl

The enzyme activity of mTGase was determined as 0.0314 U/mg powder, while SPI contained 83.85% protein wet-based, with 92.11% total solid. Treatments with mTGase powder used at 0.00, 0.12, 0.16, 0.30, 0.40, and 1.00% w/v in SPI dispersions thus corresponded to enzyme levels of 0.00, 0.75, 1.00, 1.88, 2.50, and 6.25 U/g protein, respectively. For simplicity of description, the mass/volume concentrations of mTGase powder are still used.

Figure 5.4A reveals that G' at the end of each step monotonically increased with an increase in mTGase concentration. During step 1, a shorter gelation time was observed at a higher level of mTGase (Figure 5.5), consistent to the trend in a literature study (Song & Zhang, 2008). The addition of protein-coated MMT was found to remarkably increase G' at all examined mTGase concentrations (Figure 5.4B), and the short gelation time (Figure 5.5) corresponded to the observations that G' was already higher than G'' at the beginning of data collection. It is known that G' of composite gles increases since interactions between the matrix and filler particles favor network formation but decreases otherwise (van Vliet, 1988). The drastic increase in G' when compared to mTGase- (Figure 5.4A) or MMT-only (no gelation) treatments illustrates the occurrence of cross-linking between proteins coating MMT and those in the continuous phase and the significance of our approach in strengthening the interactions of the studied system.

5.4.4. Rheological Properties of SPI Dispersions Cross-linked by mTGase at 100 mM NaCl

The combined effects of 100 mM NaCl, mTGase, and MMT on G' of SPI dispersions were further studied. For systems without MMT, the synergistic effects of NaCl and mTGase on G' development discussed above were observed for all mTGase levels (Figure 5.6A). It is worth noting that the SPI dispersion treated with 1.00% mTGase showed a lower G' at P2 and P3 than at P1, indicating that the highest mTGase level resulted in the formation of a well-developed network during the 2-h cross-linking (step 1) and the restructuring of network at elevated temperatures weakened the hydrogel strength. Similar to the samples without NaCl (Figure 5.5), a shorter gelation time was observed at a higher level of mTGase during step 1 (Figure 5.7). Furthermore, the addition of 100 mM NaCl shortened the gelation time to some extent at the same mTGase level (Figure 5.5 vs. 5.7), presumably due to the synergistic effects of ionic strength- induced protein-protein aggregations.

The weaker structures at P2 and P3 than that at P1 for systems in the absence of MMT were not observed when protein-coated MMT was incorporated in SPI dispersions for mTGase cross-linking with 1.00% mTGase (Figure 5.6B). The addition of MMT caused consistent increases in G' at all examined mTGase concentrations. The MMT-filled SPI dispersion containing 100 mM NaCl and treated with 1.00%w/v mTGase developed the highest G' at P4. However, the effect of mTGase level at P4 was not linear: G' increased from 72 to 907 Pa with an increase of mTGase from 0.00 to 0.16%, and increased to 1099 Pa after a further increase of mTGase concentration to 1.00%. The data suggests that the combination of 100 mM NaCl, 0.16%w/v mTGase, and 1% protein-coated MMT may be a cost-effective option in production, because 82.5% of the maximum G' value, corresponding to the 1.00%w/v mTGase treatment, was obtained at a much lower level of mTGase.

5.4.5. Rheological Interpretation of Hydrogel Network Impacted by MMT

To understand the mechanism of the formed hydrogel structures requires other techniques to complement rheology, e.g., transmission electron microscopy to investigate the occurrence of segregation of protein-coated MMT at the studied conditions, especially after thermal treatments. Nevertheless, the network structures as impacted by MMT are discussed for strain sweep results at 25°C, after step 4, in this section. For samples without mTGase crosslinking, G' was almost constant at the low strain regime, but strain-stiffening (higher G' at larger strains) was observed before yielding at a strain of ca. 1 for treatments with 50-1000 mM NaCl (shown in Figure 5.8 for the 100 mM NaCl sample), demonstrating that these hydrogel networks are elastic. In contrast, nonlinear regimes were readily observed at lower strains for treatments with MMT, e.g., ca. 0.03 for the 100 mM NaCl treatment (Figure 5.8), indicating a typical filler system. The strain sweep data confirmed that MMT screened the effect of ionic strength on get network formation, as discussed previously.

The similar trend was observed for the dispersions treated by mTGase only, demonstrated in Figure 5.9 for the 0.30%w/v mTGase treatment. For the sample without MMT, the strain-stiffening also was observed (Figure 5.9), implying semi-flexible or rigid aggregates (Chen, Wen, Janmey, Crocker, & Yodh, 2010) of covalent-bonded protein molecules catalyzed by mTGase. The hydrogel containing MMT did not show the strain-stiffening property (Figure 5.9), possibly due to a less homogenous network than the protein network cross-linked by mTGase without the filler. The improved gel strength for the MMT-containing sample indicates the contribution from cross-links created between proteins bound on MMT and those in the matrix, as well as the role of MMT being rigid fillers, as discussed previously.

When mTGase cross-linking was conducted at 100 mM NaCl, the straining stiffening was observed for the samples with and without MMT (Figure 5.10). The parallel G' and G'' curves indicate both are stronger and more elastic hydrogels than comparable treatments in Figures 5.8 and 5.9. The stronger and more elastic hydrogel containing mTGase, 100 mM NaCl, and 1%w/v MMT than other comparable treatments are synergistically contributed by impacts of ionic strength on protein aggregations, mTGase crosslinking of proteins in the continuous phase and/or bound on MMT, and the addition of rigid fillers – protein-coated MMT, as discussed above.

5.5. CONCLUSION

Dynamic rheological properties of soy protein dispersions with protein-coated MMT were highly affected by variables during enzymatic crosslinking induced by mTGase and were further strengthened by subsequent heating and cooling processes. Concentrations of NaCl and mTGase were critical in developing hydrogel strength during crosslinking, with a higher G' observed at 100 mM NaCl and a higher level of mTGase. Overall, the non-gelling 6%w/v SPI dispersion was transformed to a hydrogel with G' of 1099 Pa after addition of 100 mM NaCl and 1% protein-coated MMT and treatments by 1%w/v mTGase for 2 h and a heating-cooling cycle. The much strengthened interactions between the nanofillers and matrix biopolymer can be used to direct the manufacturing of biodegradable nanocomposite materials with superior functional performances.

LIST OF REFERENCES

Arora, A., & Padua, G. W. (2010). Review: nanocomposites in food packaging. *Journal of Food Science, 75*(1), R43-R49.

Caillard, R., Remondetto, G. E., & Subirade, M. (2009). Physicochemical properties and microstructure of soy protein hydrogels co-induced by Maillard type cross-linking and salts. *Food Research International, 42*(1), 98-106.

Caillard, R., Remondetto, G. E., & Subirade, M. (2010). Rheological investigation of soy protein hydrogels induced by Maillard-type reaction. *Food Hydrocolloids, 24*(1), 81-87.

Chang, P. R., Yang, Y., Huang, J., Xia, W. B., Feng, L. D., & Wu, J. Y. (2009). Effects of layered silicate structure on the mechanical properties and structures of protein-based bionanocomposites. *Journal of Applied Polymer Science, 113*(2), 1247-1256.

Chen, D. T. N., Wen, Q., Janmey, P. A., Crocker, J. C., & Yodh, A. G. (2010). Rheology of soft materials. *Annu. Rev. Condens. Matter Phys., 1*, 301-322.

Chen, P., & Zhang, L. (2006). Interaction and properties of highly exfoliated soy protein/montmorillonite nanocomposites. *Biomacromolecules, 7*(6), 1700-1706.

Dang, Q. Q., Lu, S. D., Yu, S., Sun, P. C., & Yuan, Z. (2010). Silk fibroin/montmorillonite nanocomposites: effect of pH on the conformational transition and clay dispersion. *Biomacromolecules, 11*(7), 1796-1801.

de Azeredo, H. M. C. (2009). Nanocomposites for food packaging applications. *Food Research International, 42*(9), 1240-1253.

de Carvalho, R. A., & Grosso, C. R. F. (2004). Characterization of gelatin based films modified with transglutaminase, glyoxal and formaldehyde. *Food Hydrocolloids, 18*(5), 717-726.

Feng, M., Zhao, C. G., Gong, F. L., & Yang, M. S. (2004). Study on the modification of sodium montmorillonite with amino silanes. *Acta Chimica Sinica, 62*(1), 83-87.

Gan, C. Y., Latiff, A. A., Cheng, L. H., & Easa, A. M. (2009). Gelling of microbial transglutaminase cross-linked soy protein in the presence of ribose and sucrose. *Food Research International, 42*(10), 1373-1380.

Guilherme, M. R., Mattoso, L. H. C., Gontard, N., Guilbert, S., & Gastaldi, E. (2010). Synthesis of nanocomposite films from wheat gluten matrix and MMT intercalated with different quaternary ammonium salts by way of hydroalcoholic solvent casting. *Composites Part a-Applied Science and Manufacturing, 41*(3), 375-382.

Ho, M. L., Leu, S. Z., Hsieh, J. F., & Jiang, S. T. (2000). Technical approach to simplify the purification method and characterization of microbial transglutaminase produced from Streptoverticillium ladakanum. *Journal of Food Science, 65*(1), 76-80.

Ikeda, S., & Foegeding, E. A. (1999). Dynamic viscoelastic properties of thermally induced whey protein isolate gels with added lecithin. *Food Hydrocolloids, 13*(3), 245-254.

Ikeda, S., Foegeding, E. A., & Hagiwara, T. (1999). Rheological study on the fractal nature of the protein gel structure. *Langmuir, 15*(25), 8584-8589.

Jiang, Y., Tang, C.-H., Wen, Q.-B., Li, L., & Yang, X.-Q. (2007). Effect of processing parameters on the properties of transglutaminase-treated soy protein isolate films. *Innovative Food Science and Emerging Technologies, 8*(2), 218-225.

Jiang, Y., Tang, C. H., Wen, Q. B., Li, L., & Yang, X. Q. (2007). Effect of processing parameters on the properties of transglutaminase-treated soy protein isolate films. *Innovative Food Science & Emerging Technologies, 8*(2), 218-225.

Kumar, P., Sandeep, K. P., Alavi, S., Truong, V. D., & Gorga, R. E. (2010a). Effect of type and content of modified montmorillonite on the structure and properties of bio-nanocomposite films based on soy protein isolate and montmorillonite. *Journal of Food Science, 75*(5), N46-N56.

Kumar, P., Sandeep, K. P., Alavi, S., Truong, V. D., & Gorga, R. E. (2010b). Preparation and characterization of bio-nanocomposite films based on soy protein isolate and montmorillonite using melt extrusion. *Journal of Food Engineering, 100*(3), 480-489.

L'Hocine, L., Boye, J. I., & Arcand, Y. (2006). Composition and functional properties of soy protein isolates prepared using alternative defatting and extraction procedures. *Journal of Food Science, 71*(3), C137-C145.

Lakemond, C. M. M., de Jongh, H. H. J., Hessing, M., Gruppen, H., & Voragen, A. G. J. (2000). Soy glycinin: Influence of pH and ionic strength on solubility and molecular structure at ambient temperatures. *Journal of Agricultural and Food Chemistry, 48*(6), 1985-1990.

Lakemond, C. M. M., de Jongh, H. H. J., Paques, M., van Vliet, T., Gruppen, H., & Voragen, A. G. J. (2003). Gelation of soy glycinin; influence of pH and ionic strength on network structure in relation to protein conformation. *Food Hydrocolloids, 17*(3), 365-377.

Le Corre, D., Bras, J., & Dufresne, A. (2010). Starch nanoparticles: a review. *Biomacromolecules, 11*(5), 1139-1153.

Lee, J. E., & Kim, K. M. (2010). Characteristics of Soy Protein Isolate-Montmorillonite Composite Films. *Journal of Applied Polymer Science, 118*(4), 2257-2263.

Lin, J. J., Wei, J. C., Juang, T. Y., & Tsai, W. C. (2007). Preparation of protein-silicate hybrids from polyamine intercalation of layered montmorillonite. *Langmuir, 23*(4), 1995-1999.

Malhotra, A., & Coupland, J. N. (2004). The effect of surfactants on the solubility, zeta potential, and viscosity of soy protein isolates. *Food Hydrocolloids, 18*(1), 101-108.

Mallakpour, S., & Dinari, M. (2011). Preparation and characterization of new organoclays using natural amino acids and Cloisite Na(+). *Applied Clay Science, 51*(3), 353-359.

Mariotti, F., Tome, D., & Mirand, P. P. (2008). Converting nitrogen into protein - Beyond 6.25 and Jones' factors. *Critical Reviews in Food Science and Nutrition, 48*(2), 177-184.

Martucci, J. F., & Ruseckaite, R. A. (2010). Biodegradable three-layer film derived from bovine gelatin. *Journal of Food Engineering, 99*(3), 377-383.

Motoki, M., & Seguro, K. (1998). Transglutaminase and its use for food processing. *Trends in Food Science & Technology, 9*(5), 204-210.

Nury, S., Meunier, J. C., & Mouranche, A. (1989). The kinetics of the thermal deactivation of transglutaminase from guinea-pig liver. *European Journal of Biochemistry, 180*(1), 161-166.

Seguro, K., Nio, N., & Motoki, M. (1996). Some characteristics of a microbial protein cross-linking enzyme: Transglutaminase. In N. K. A. C. L. K. P. J. Parris (Ed.), *Macromolecular Interactions in Food Technology*, vol. 650 (pp. 271-280).

Song, F., Tang, D. L., Wang, X. L., & Wang, Y. Z. (2011). Biodegradable soy protein isolate-based materials: a review. *Biomacromolecules, 12*(10), 3369-3380.

Song, F., & Zhang, L. M. (2008). Enzyme-catalyzed formation and structure characteristics of a protein-based hydrogel. *Journal of Physical Chemistry B, 112*(44), 13749-13755.

Tang, C. H., Choi, S. M., & Ma, C. Y. (2007). Study of thermal properties and heat-induced denaturation and aggregation of soy proteins by modulated differential scanning calorimetry. *International Journal of Biological Macromolecules, 40*(2), 96-104.

Tang, X. Z., Alavi, S., & Herald, T. J. (2008). Barrier and mechanical properties of starch-clay nanocomposite films. *Cereal Chemistry, 85*(3), 433-439.

Tsai, G. J., Lin, S. M., & Jiang, S. T. (1996). Transglutaminase from Streptoverticillium ladakanum and application to minced fish product. *Journal of Food Science, 61*(6), 1234-1238.

van Vliet, T. (1988). Rheological properties of filled gels. Influence of filler matrix interaction *Colloid and Polymer Science, 266*(6), 518-524.

Wolf, W. J. (1970). Soybean protiens - their functional, chemical, and physical properties. *Journal of Agricultural and Food Chemistry, 18*(6), 969-&.

Yildirim, M., & Hettiarachchy, N. S. (1998). Properties of films produced by cross-linking whey proteins and 11S globulin using transglutaminase. *Journal of Food Science, 63*(2), 248-252.

Zhu, Y., Bol, J., Rinzema, A., Tramper, J., & Wijngaards, G. (1999). Transglutaminase as a potential tool in developing novel protein foods. *Agro Food Industry Hi-Tech, 10*(1), 8-10.

APPENDIX

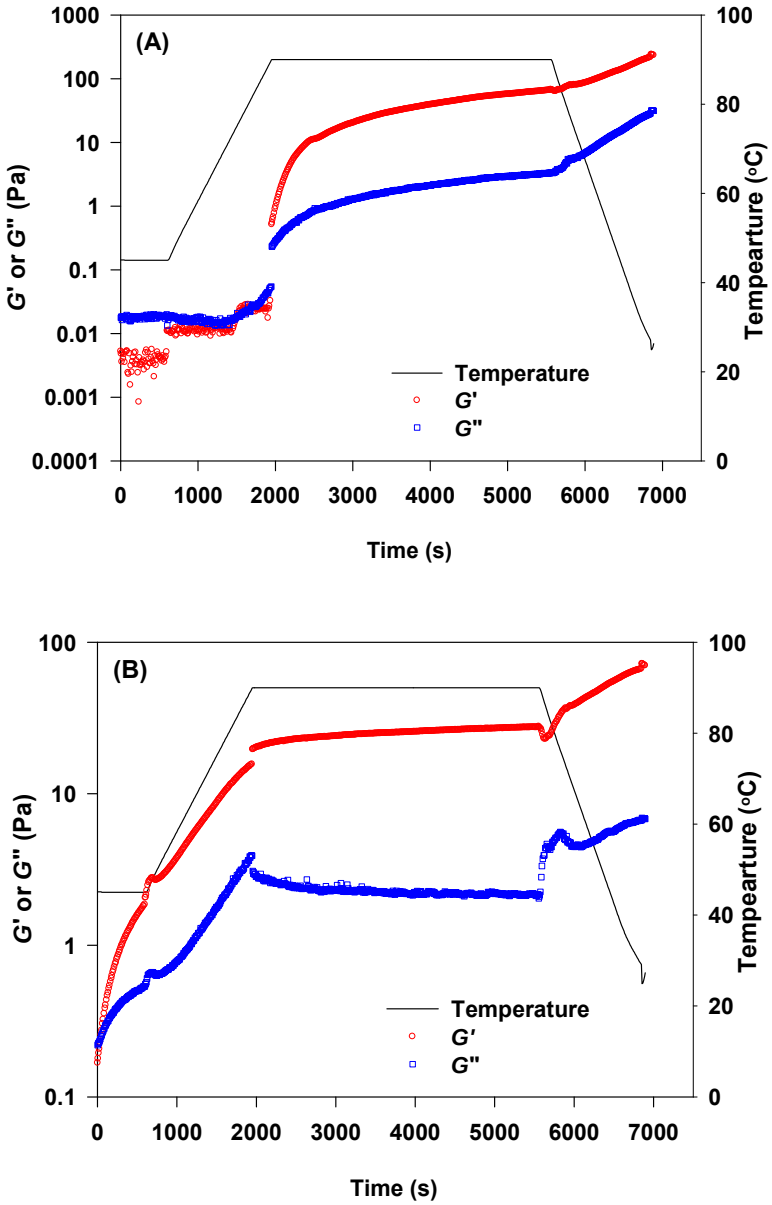

Figure 5. 1. Rheological profiles demonstrated for dispersions containing 6% w/v SPI with 100 mM NaCl, (A) without and (B) with 1%w/v protein-coated MMT during (1) a holding step at 45 °C for 10 min; (2) a heating step from 45 to 90 °C at 2 °C/min; (3) a holding step at 90 °C for 1 h; (4) a cooling step from 90 to 25 °C at 3 °C/min.

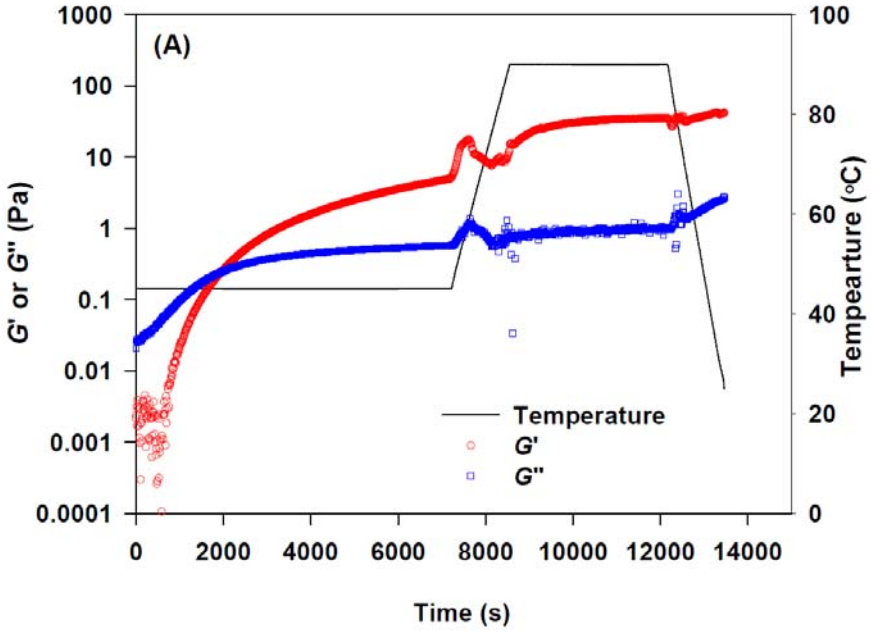
(A)
G' or G'' (Pa)
Tempearture (°C)
Time (s)
Temperature
G'
G''
1000
100
10
1
0.1
0.01
0.001
0.0001
0
2000
4000
6000
8000
10000
12000
14000
100
80
60
40
20
0

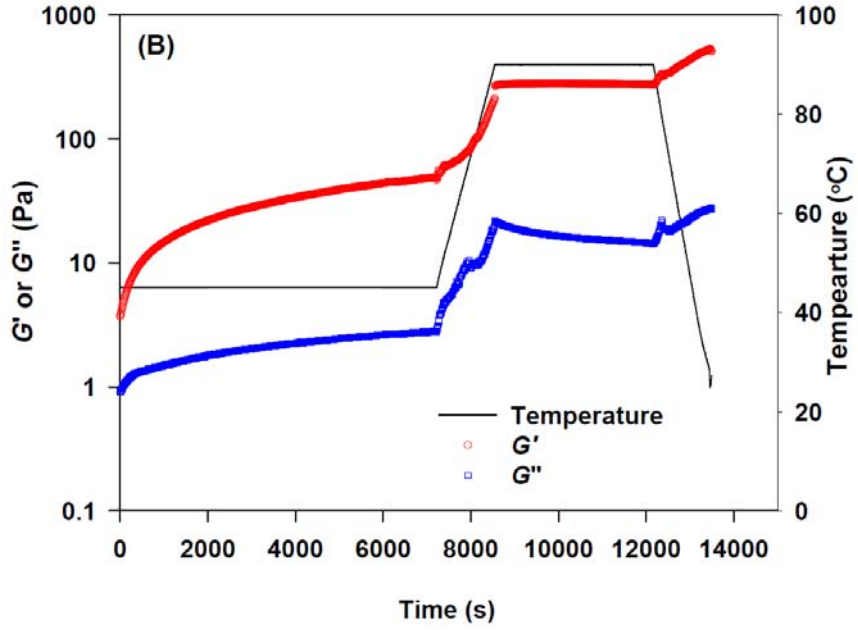
(B)
G' or G'' (Pa)
Tempearture (°C)
Time (s)
Temperature
G'
G''
1000
100
10
1
0.1
0
2000
4000
6000
8000
10000
12000
14000
100
80
60
40
20
0

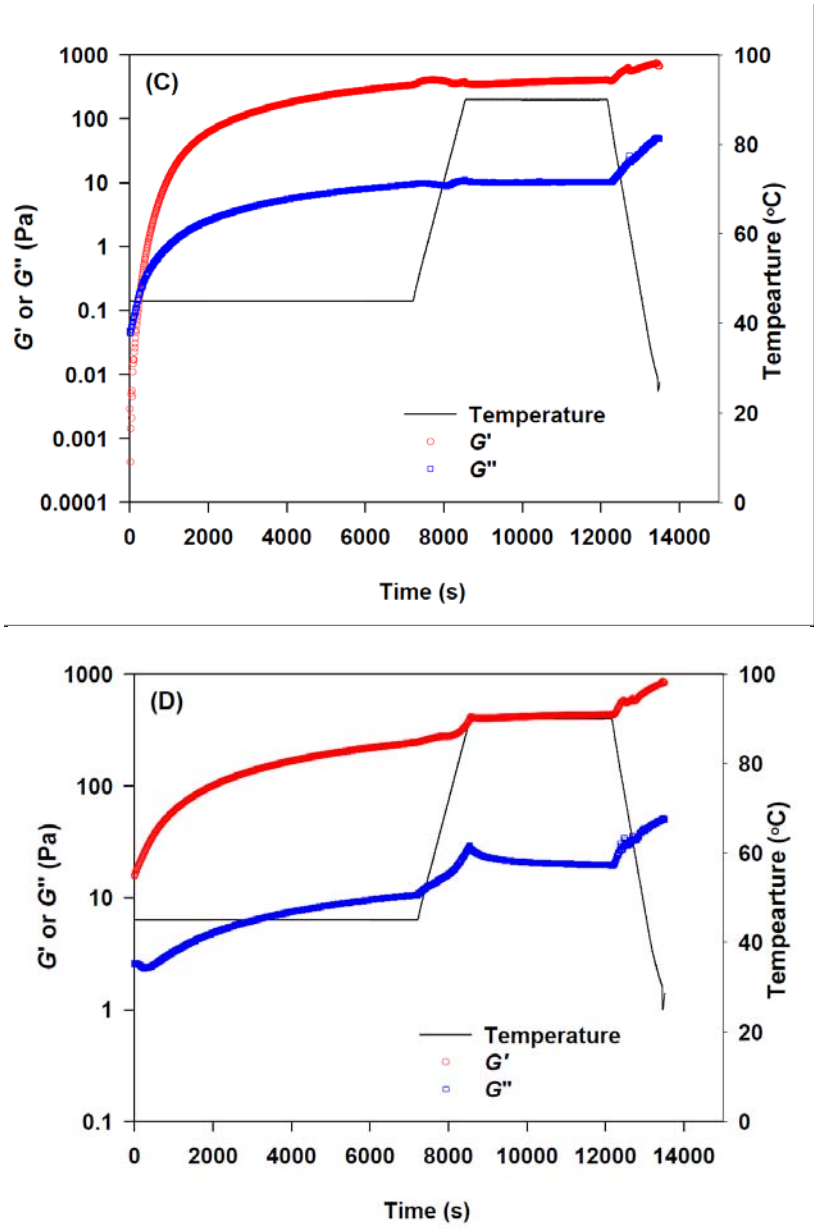

Figure 5. 2. Rheological profiles demonstrated for dispersions containing 6% w/v SPI with (A) 0.3%w/v mTGase, (B) 0.3%w/v mTGase and 1%w/v protein-coated MMT, (C) 0.4%w/v mTGase and 100 mM NaCl, and (D) 0.4%w/v mTGase, 100 mM NaCl and 1%w/v protein-coated MMT during (1) a holding step at 45 °C for 2 h; (2) a heating step from 45 to 90 °C at 2 °C/min; (3) a holding step at 90 °C for 1 h; (4) a cooling step from 90 to 25 °C at 3 °C/min.

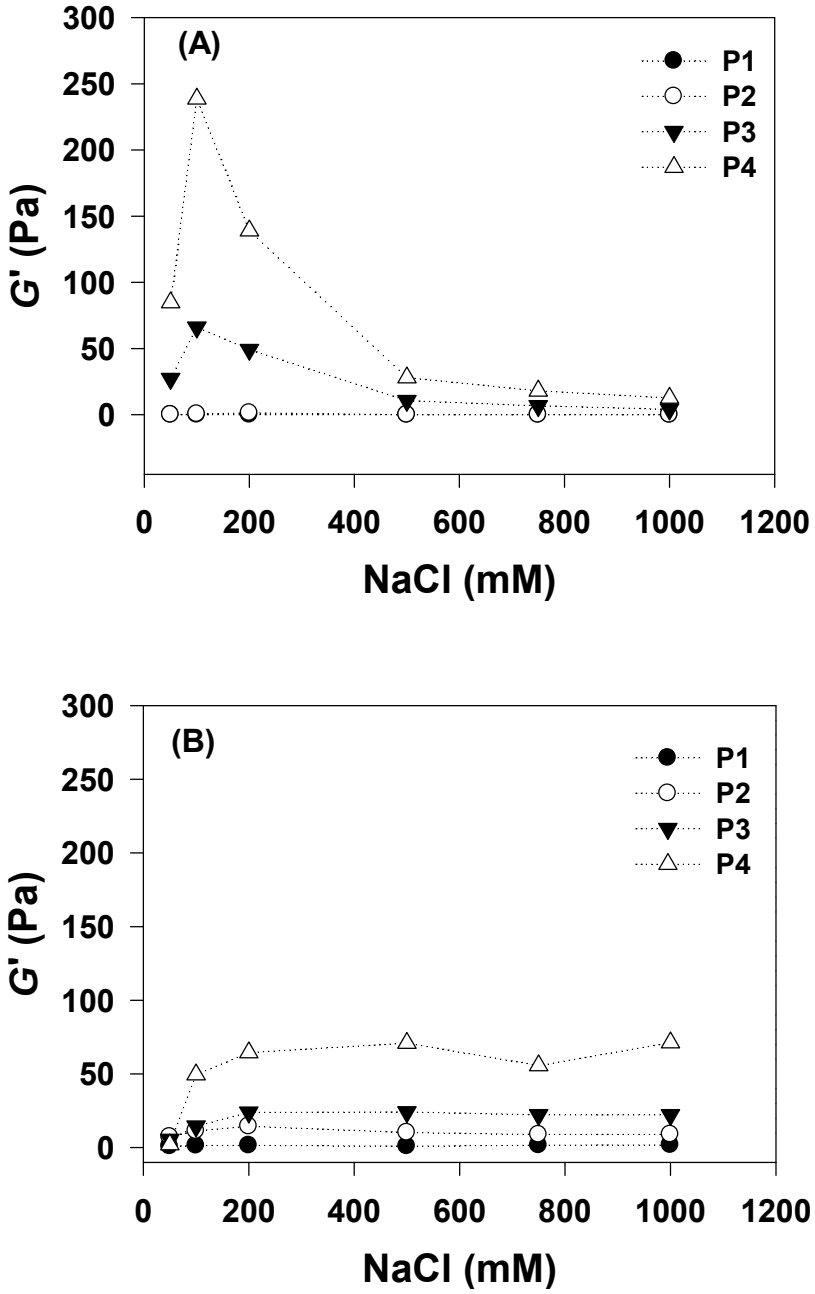

Figure 5. 3. The storage moduli (G') of 6%w/v dispersions, containing 50-1000 mM NaCl, (A) without and (B) with 1%w/v protein-coated MMT after 10-min holding at 45 °C (P1), heating to 90 °C at 2 °C/min (P2), 1-h holding at 90 °C (P3), and cooling to 25 °C at 3 °C/min (P4).

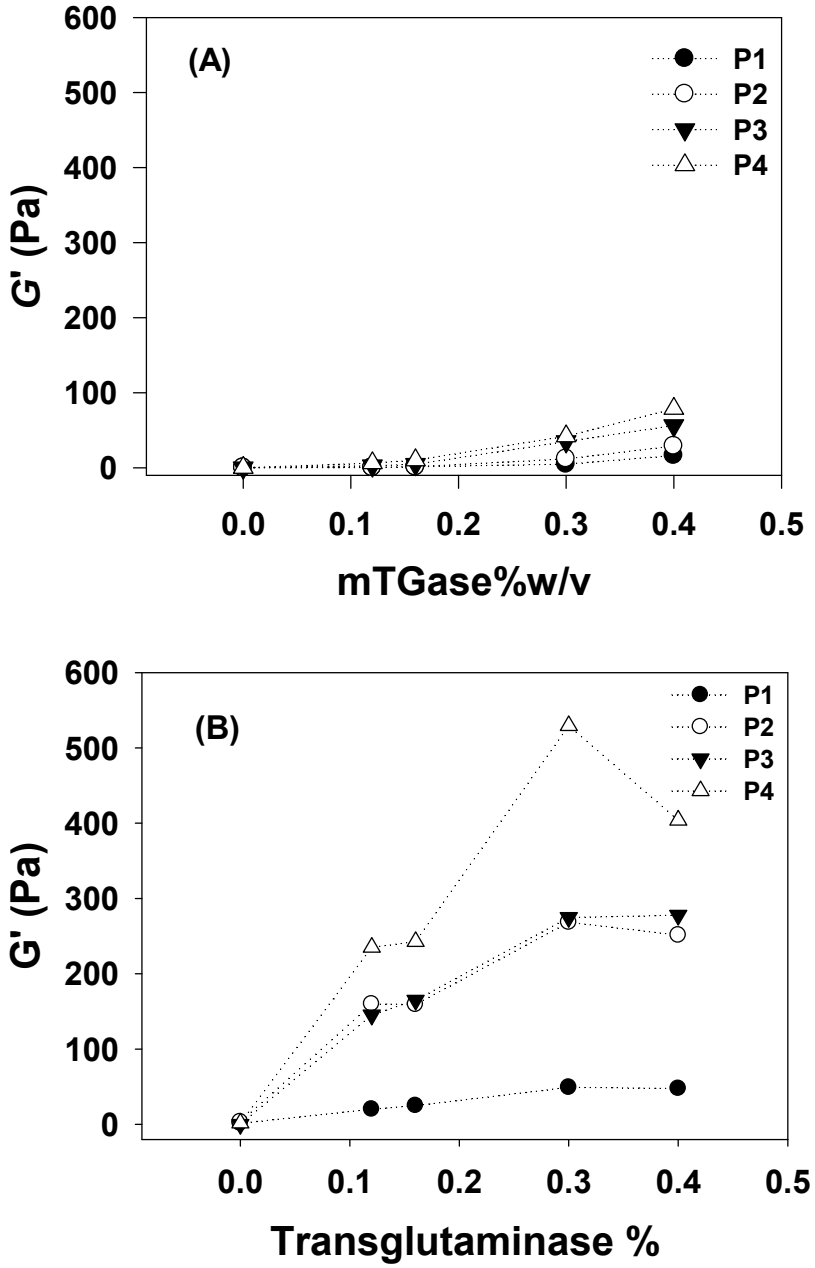

Figure 5. 4. The storage moduli (*G'*) of 6%w/v SPI dispersions, containing varied mTGase concentrations, (A) without and (B) with 1%w/v protein-coated MMT after 2-h holding at 45 °C (P1), heating to 90 °C at 2 °C/min (P2), 1-h holding at 90 °C (P3), and cooling to 25 °C at 3 °C/min (P4).

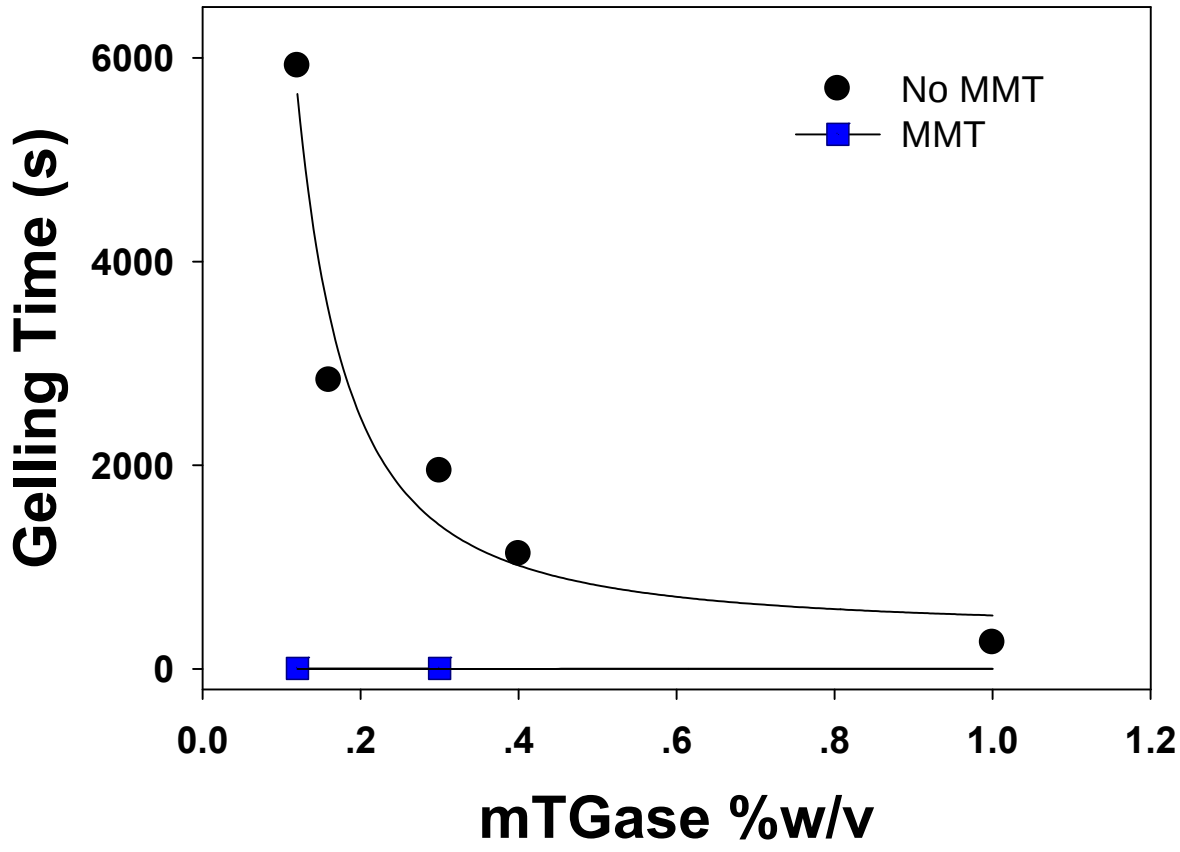

Figure 5. 5. Effects of mTGase concentration on gelation time during crosslinking 6%w/v SPI dispersions with and without 1%w/v protein-coated MMT.

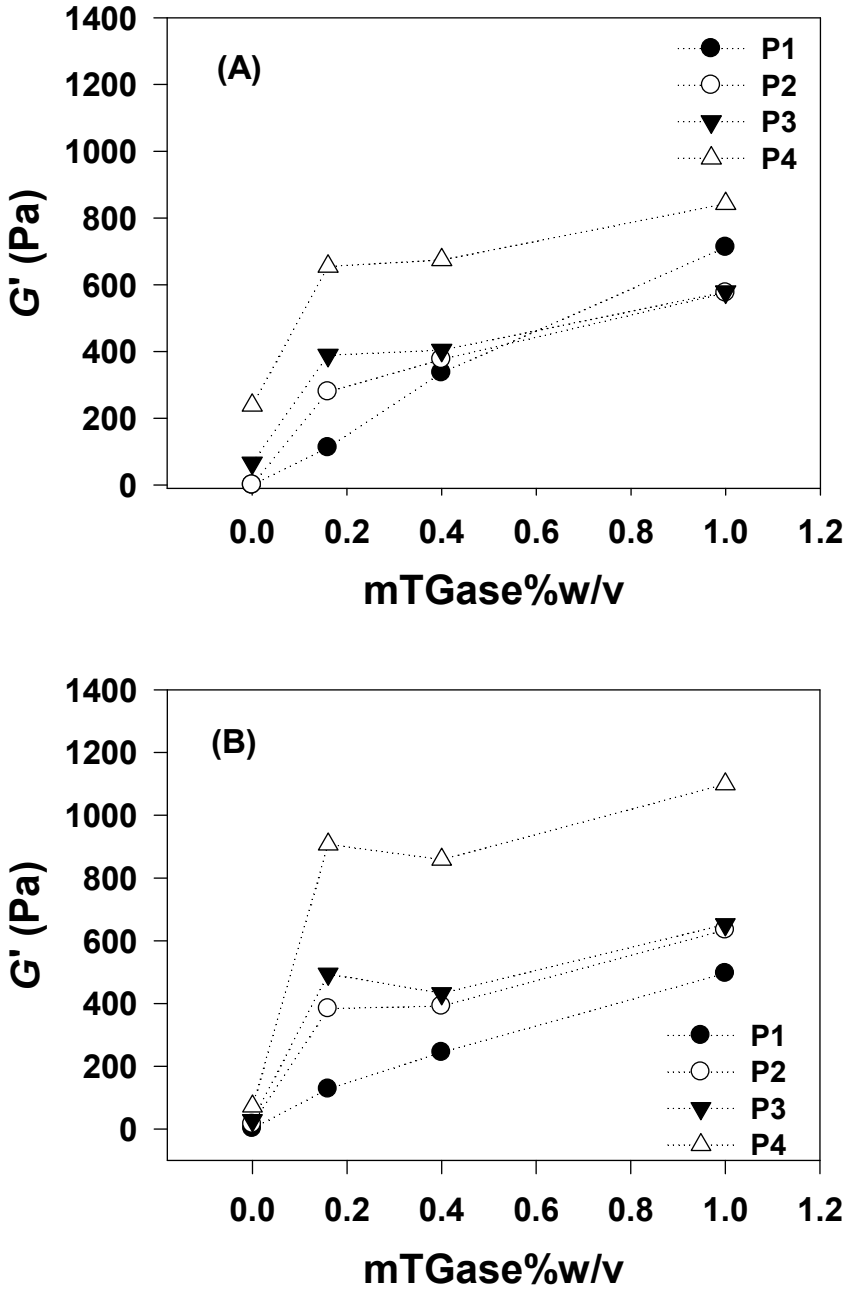

Figure 5. 6. The storage moduli (*G*′) of 6%w/v SPI dispersions, containing 100 mM NaCl and varied mTGase concentrations, (A) without and (B) with 1%w/v protein-coated MMT after 2-h holding at 45 °C (P1), heating to 90 °C at 2 °C/min (P2), 1-h holding at 90 °C (P3), and cooling to 25 °C at 3 °C/min (P4).

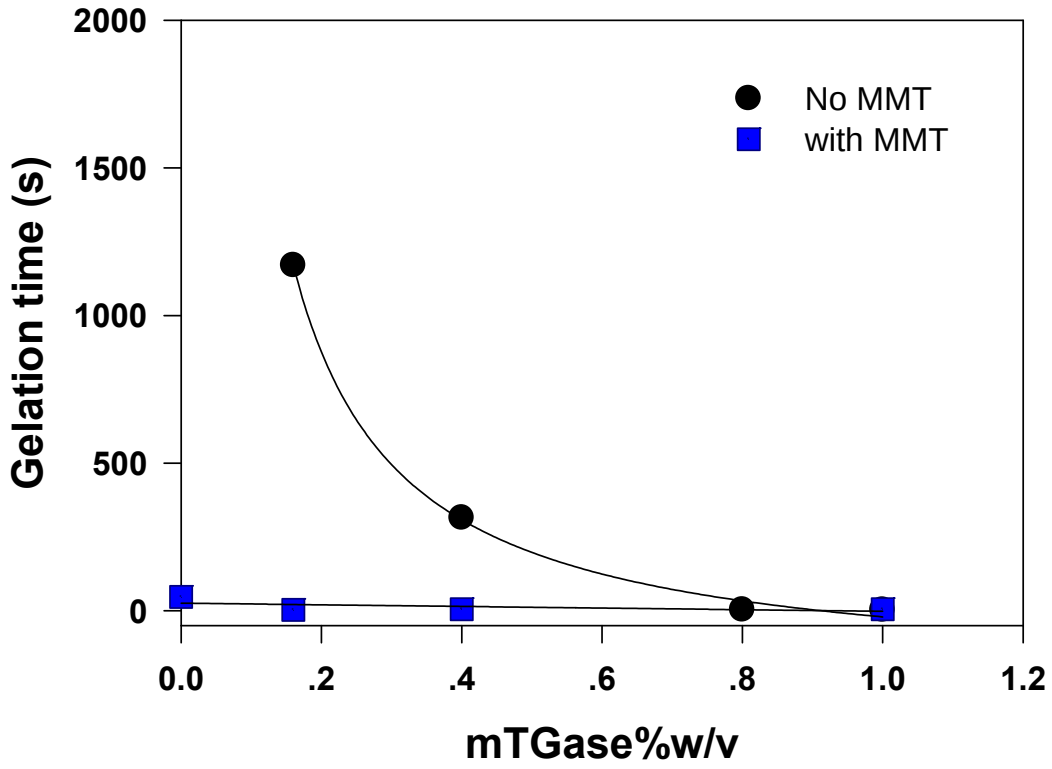

Figure 5. 7. Effects of mTGase concentration on gelation time during crosslinking 6%w/v SPI dispersions with and without 1%w/v protein-coated MMT.

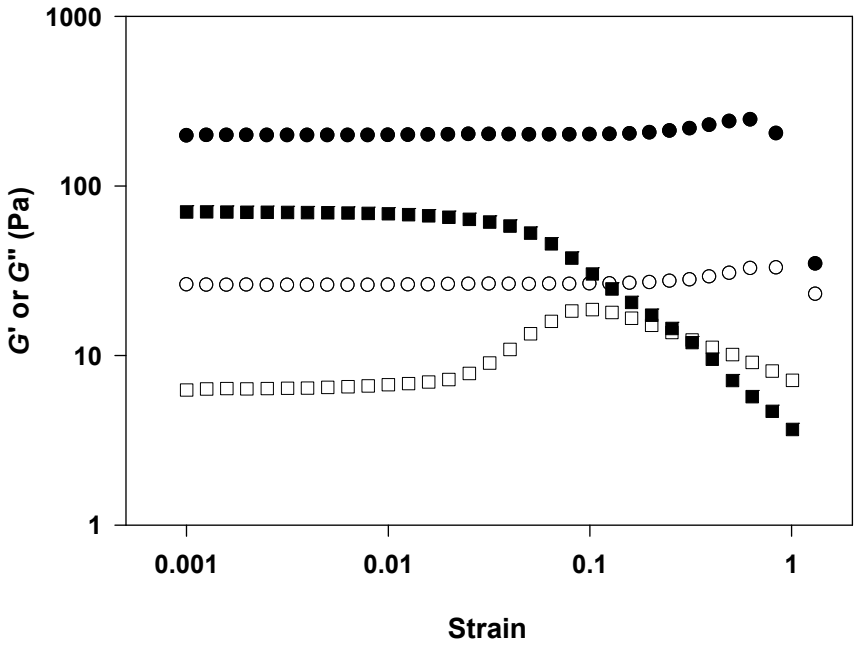

Figure 5. 8. Strain sweep profiles at 25 °C, after a heating-cooling cycle as in Figure 1, for SPI gels formed with 100 mM NaCl and the absence (circles) or presence (squares) of 1%w/v protein-coated MMT.

Filled and open symbols represent storage (G') and loss (G'') moduli, respectively.

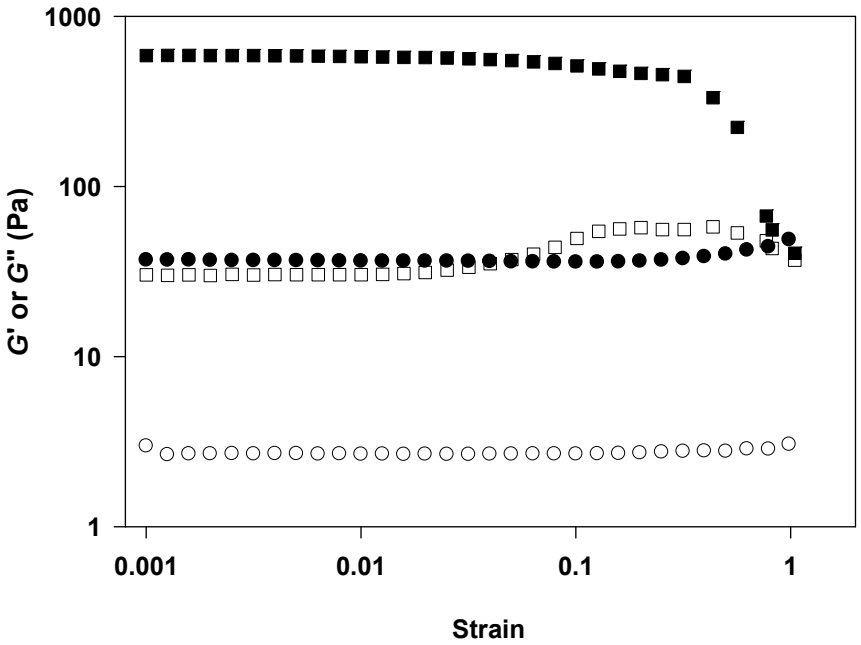

Figure 5. 9. Strain sweep profiles at 25 °C, after a heating-cooling cycle as in Figure 2, for SPI gels cross-linked by 0.30%w/v TGase in the absence (circles) or presence (squares) of 1%w/v protein-coated MMT.

Filled and open symbols represent storage (G') and loss (G'') moduli, respectively.

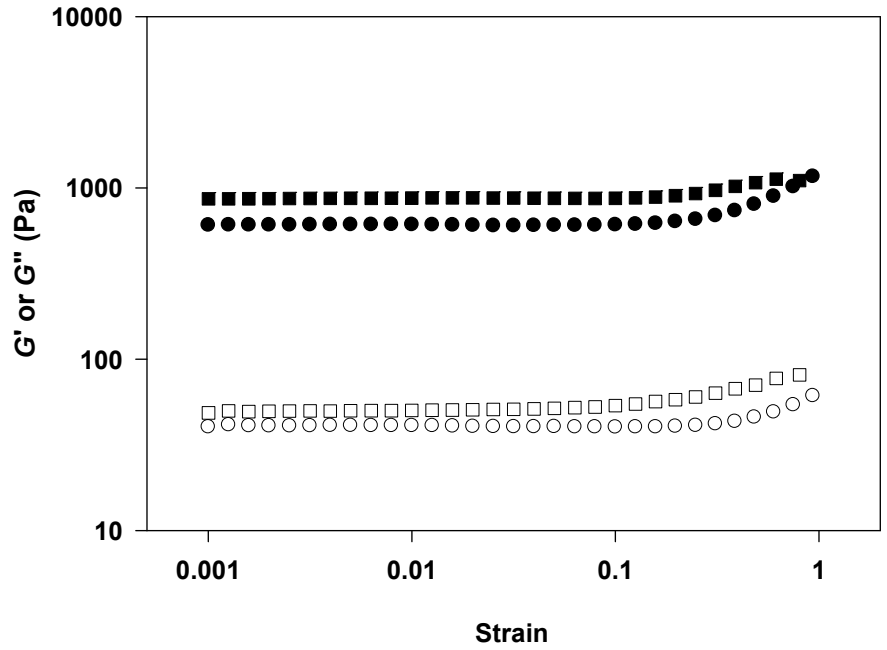

Figure 5. 10. Strain sweep profiles at 25 °C, after a heating-cooling cycle as in Figure 2, for SPI gels cross-linked by 0.40%w/v TGase at 100 mM NaCl in the absence (circles) or presence (squares) of 1%w/v protein-coated MMT. Filled and open symbols represent storage (G') and loss (G'') moduli, respectively.

CHAPTER 6 . EFFECTS OF GLUTARALDEHYDE CONCENTRATION, pH AND TEMPERATURE ON RHEOLOGICAL PROPERTIES OF NANOCOMPOSITES CONSISTING OF INTERCALATED MONTMORILLONITE DISPERSED IN SOY PROTEIN MATRIX

6.1. ABSTRACT

Cross-linking of proteins between matrix protein polymers and protein-coated montmorillonite (MMT) may strengthen the interactions of relevant bio-nanocomposite systems, besides the well-established concept that material properties are improved by the incorporation of highly intercalated or exfoliated nanoclays. Dynamic rheological tests were utilized as a non-destructive method to illustrate the formation of hydrogel network and the strength during chemical crosslinking by glutaraldehyde (GA), impacted by GA concentration, pH, cross-linking temperature, and the absence and presence of coated MMT. In the absence of MMT, the storage modulus (G') gradually increased with an increase in GA concentration, while the incorporation of MMT further increased G' to a high order of magnitude. At a GA concentration equal to 10% mass of soy protein, increased chemical crosslinking rates and G' were observed at ambient temperature than those at 90 °C, while results were opposite at lower additions of GA. At pH 5.5, the strength of soy protein nanocomposite gel network was greatly improved with the existence of particulate aggregates. The results showed that the interactions in cross-linked soy protein gel system were enhanced by the incorporation of protein-coated MMT and the synergetic impacts of GA concentration, pH, and crosslinking temperature. The established chemical cross-linking method between fillers and matrix and conditions can be beneficial for preparing bionanocomposite materials with enhanced mechanical properties.

Keywords: nanocomposite, chemical crosslinking, soy protein, protein-coated montmorillonite, dynamic rheology

6.2. INTRODUCTION

The modification of nanofillers to obtain good dispersibility has been demonstrated for improving material properties of nanocomposite systems (Arora & Padua, 2010; Lin, Wei, Juang, & Tsai, 2007; Spirkova, Duchek, Strachota, Poreba, Kotek, Baldrian, et al., 2011). Montmorillonite (MMT) is an intensively-studied nanofiller because of the abundance, availability, low cost, and the specific characteristics of high elastic modulus (178 GPa), high surface area (750 m^2/g) and large aspect ratio (50-1000) (Kumar, 2009). The specific characteristics of MMT contribute to enhanced mechanical and barrier properties of nanocomposite materials (de Azeredo, 2009; Essington, 2003; Gunister, Pestreli, Unlu, Atici, & Gungor, 2007; Le Corre, Bras, & Dufresne, 2010). Chemical or physical modifications of MMT have been demonstrated for enlarging the basal spacing between platelets and modifying the clay layers from highly ordered to intercalated and/or exfoliated structures (Feng, Zhao, Gong, & Yang, 2004; Mallakpour & Dinari, 2011; Yang, Zhu, Yin, Wang, & Qi, 1999). The affinity of proteins and amino acids on soil minerals indicates the possibility of surface coating MMT with naturally-existing proteins (Ding & Henrichs, 2002; Quiquampoix & Burns, 2007). MMT modified with proteins can thus potentially further improve the interactions within the bio-composite system by enhancing interactions between biopolymer molecules in the interphase layer formed between the MMT and those in the bulk (Shenoy, 1999). Our studies in Chapters 3 and 4 identified the feasibility of surface-coating MMT with extracted plant proteins, i.e., water soluble hominy protein and soy protein, to obtain the enlarged basal spacing and intercalated/exfoliated structures of MMT with a sufficient MMT:protein mass ratios and coating pH.

Crosslinking is a potential method for further strengthening the interaction among our protein-based nanocomposite system because of the possibility to form covalent bonds between proteins on MMT and those in the continuous phase. Enzymatic and chemical cross-linking approaches have been studied for soy proteins to enhance the hydrogel, polymer, and film properties (Caillard, Remondetto, & Subirade, 2009, 2010; de Carvalho & Grosso, 2004; Gan, Latiff, Cheng, & Easa, 2009; Jiang, Tang, Wen, Li, & Yang, 2007b; Yildirim & Hettiarachchy, 1998). Cross-linkers containing aldehyde groups include glutaraldehyde, formaldehyde, glyxoal, dialdehyde starch, hexanedial, biacetyl, and cyclopentane-dione and have been widely utilized for protein crosslinking (Gerrard, et al., 2005). This type of crosslinking reaction is called "Maillard-type" crosslinking (Caillard, Remondetto, & Subirade, 2009, 2010) because covalent amide (CO-NH) bonds are formed between lysine residues on protein molecules and aldehyde groups on cross-linkers, resulting in the loss of lysine residues on proteins (Gerrard, Brown, & Fayle, 2003). Soy proteins cross-linked by glutaraldehyde had a lowered solubility, lowered emulsifying properties and improved foaming stabilities. Meanwhile, glutaraldehyde-treatment enhanced tensile strength and elongation at break of soy protein isolate (SPI) films, more significantly at increased glutaraldehyde concentrations (Park, Bae, & Rhee, 2000). Increased tensile properties and improved processability as a resin of soy protein concentrate were also obtained by crosslinking with glutaraldehyde to manufacture flax fabric-reinforced composites (Chabba & Netravali, 2005).

Soy protein, as an abundant plant supply resource with good film-forming properties, has been frequently studied to develop either protein coatings/films alone or clay-incorporated nanocomposite films (Chen, Tian, Zhang, Chen, Wang, & Do, 2008; Kumar, Sandeep, Alavi, Truong, & Gorga, 2010a, 2010b; Nayak, Sasmal, Nayak, Sahoo, Mishra, Kang, et al., 2008;

Zhao, Torley, & Halley, 2008). In this dissertation research, our objective was to improve the interaction between the matrix biopolymer – soy protein and protein-coated MMT for potentially developing protein-based nanocomposites with further enhanced mechanical and barrier properties. In Chapter 5, enzymatic crosslinking induced by transglutaminase was investigated and demonstrated that the incorporation of protein-coated MMT further increased the storage modulus and hydrogel network strength at the optimized ionic strength. In this study, chemical crosslinking was utilized to strengthen the interactions between protein-coated MMT and bulk soy proteins. Formaldehyde, glutaraldehyde, and glyxoal were studied in our preliminary tests. Results showed that the best crosslinking effect, evident by highest rheological moduli, was obtained by utilizing glutaraldehyde, consistent with the literatures that glutaraldehyde was the most reactive cross-linker among these three (Gerrard, Brown, & Fayle, 2003). Small-deformation rheological analyses were performed as a non-destructive method to illustrate the development of rheology moduli and the formation of hydrogel network, impacted by pH (5.5, 6.5, and 10.0), cross-linking temperature (23, 60, and 90°C), glutaradehyde concentration (2.0, 4.0, and 10.0% mass of spray-dried soy protein powder, and the absence and presence of protein-coated MMT.

6.3. MATERIALS AND METHODS

6.3.1. Materials

Na^+-montmorillonite (Cloisite® Na^+ Nanoclay) used in the present study was supplied from Southern Clay Products, Inc. (Gonzales, TX). Commercial soy flour was obtained from MP Biomedicals, LLC (Solon, OH). Glutaraldehyde (50 wt% solution in water) was purchased from Sigma-Aldrich Corp. (St. Louis, MO), used as received. Mineral oil and other chemicals were of

analytical grade and purchased from Fisher Scientific (Fair Lawn, NJ) and Sigma-Aldrich Corp. (St. Louis, MO).

6.3.2. Extraction of Soy Protein

Soy protein used in present study was extracted from commercial soy flour using a modified protocol for preparing SPI (L'Hocine, Boye, & Arcand, 2006). Soy flour was finely ground utilizing a coffee grinder (Hamilton Beach Proctor-Silex, Inc., Southern Pines, NC), suspended in deionized water at a solid:liquid mass ratio of 1:10, adjusted to pH 9.0, and vigorously stirred at 48 °C for 3 h using a magnetic stirring hot plate (model Isotemp®, Fisher Scientific, Fair Lawn, NJ). The suspension was then centrifuged (Sorvall RC 5B Plus, Newtown, CT) at 3,778*g* for 30 min at ambient temperature. The extraction in alkaline condition was repeated three times to increase the protein extraction yield on each batch of soy flour. The supernatants were filtered twice using a #1 filter paper and then twice with a #2 filter paper (Whatman®, Lawrence, KS), followed by adjustment to pH 4.5 for acidic precipitation of soy proteins. The precipitate was separated by centrifugation (3,778*g* for 15 min), re-suspended in deionized water and adjusted to pH 9.0, re-precipitated at pH 4.5 and centrifuged as above. The re-suspension and re-precipitation procedures were repeated for a third time. The final protein precipitate was suspended in deionized water, adjusted to pH 6.5, and spray-dried by using a B-290 Mini Spray Dryer (BÜCHI Labortechnik AG, Postfach, Switzerland). The spray drying parameters were as below: a feed rate of 6.67 mL/min and inlet and outlet temperatures of 150 and 55-65 °C, respectively. Afterwards, the spray-dried soy protein powder (SPI) was collected and stored at a -20 °C freezer.

6.3.3. Preparation of Protein-coated MMT

Surface-coated MMT by SPI was prepared via solution intercalation (Chen & Zhang, 2006). In Chapter 4, surface-coating conditions were optimized at an MMT:SPI mass ratio of 4:1 and pH 9.0, at which the X-ray diffraction test illustrated highly intercalated nanoclay platelets that are expected to improve the interaction with biopolymer matrix. Practically, dispersions of 0.5% w/v SPI or 2% w/v MMT were prepared in 10 mM NaH_2PO_4 buffer, adjusted to pH 9.0, heated at 60 °C, and stirred at 300 rpm for 30 min using a magnetic stirring hot plate, respectively. The MMT dispersion was slowly added to the same volume of SPI dispersion, while being vigorously agitated at 1000 rpm and heated at 60 °C. The resultant slurry was agitated for 3 h and then ready for hydrating SPI for chemical cross-linking.

6.3.4. Sample Preparation for Rheological Measurement

Dispersions containing 8% w/v SPI were prepared in 10 mM NaH_2PO_4 buffer or protein-coated MMT slurry overnight, and adjusted to a pH of 5.5, 6.5 or 10.0. Immediately before the rheological test, predetermined amounts of glutaraldehyde were added to the SPI dispersions to achieve the final concentrations of 2.0, 4.0, and 10.0% mass of SPI.

6.3.5. Dynamic Rheological Analyses

Small-deformation rheological analyses were performed with an AR2000 rheometer (TA Instruments, New Castle, DE). A concentric cylinder geometry consisting of a bob with an outer diameter of 28 mm and a cup with an inner diameter of 30 mm was applied for measuring the storage modulus (G') and loss modulus (G'') during cross-linking. Approximately 15 mL of the prepared SPI dispersion were carefully added into the cup. After positioning the bob and removing the excess sample, a thin layer of mineral oil was applied to the top of the sample to minimize moisture evaporation during monitoring. The small-deformation tests included the

following sequential steps: (1) an isothermal step at a designed temperature of 23, 60, or 90 °C for 5 h, at a strain of 0.01 and a frequency of 1 Hz and (2) a strain sweep test at 23 °C at a strain range of 0.001-1 and a frequency of 1 Hz. All experiments were performed in duplicate and the averages were reported.

6.4. RESULTS AND DISCUSSION

6.4.1. Effects of Glutaraldehyde Concentration and MMT

Soy proteins having an isoelectric point around pH 4.5 are partially unfolded in alkaline conditions and a greater number of lysine residues are available for the crosslinking reaction catalyzed by glutaraldehyde (Jiang et al. 2009). Therefore, effects of the glutaraldehyde concentration were investigated at pH 10.0 in this section. Figure 6.1 presents developments of G' and G'' during the isothermal treatment at 23 °C and pH 10.0 for up to 5 hours as affected by different levels of glutaraldehyde and the absence and presence of protein-coated MMT. In the absence of protein-coated MMT (Figure 6.1A), 2.0% glutaraldehyde was insufficient to cause gelation. The G' appears to increase somewhat faster than G'' but G'' was still larger than G' at the end of the treatment. When treated with 4.0 and 10.0% glutaraldehyde, G' was already larger than G'' at the beginning of the treatment, indicating that glutaraldehyde is a very reactive cross-linker (Gerrard, et al., 2005). The addition of surface coated MMT resulted in remarkable increases in both G' and G'' at all examined glutaraldehyde concentrations (Figure 6.1B).

Figure 6.2 shows the strain dependence of G' and G'' after the isothermal treatment at 23 °C. The all examined samples showed a limit of linear viscoelastic regime (LLVR) greater than approximately 0.05, verifying that the strain amplitude used in oscillatory shear tests (0.01) was

within the linear viscoelastic regime. Within LLVR, the storage modulus was significantly larger than the loss modulus, indicating predominantly elastic response of the samples. For samples without containing MMT (Figure 6.2A), G' was almost constant at low strains and the samples treated with 4.0 or 10.0% glutaraldehyde showed strain-stiffening around a strain of 1.0, indicating that theses hydrogel networks are elastic. The gel stiffness increases with the increases in glutaraldehyde concentrations. In the presence of protein-coated MMT (Figure 6.2B), G' remained almost constant at first and then started to decrease around a strain magnitude of 0.1. The decrease in G' indicates a shear-induced loss in the connectivity between filler particles in the composite materials, which is commonly referred to as the Payne effect (Payne & Whittaker, 1971). The loss modulus also remained constant at first and then increased around a strain magnitude of 0.1 and reached a maximum. The broad peak in G'' is considered to originate from increasing dissipation of energy accompanying the structural rearrangement such as energy dissipation due to friction between mutually sliding MMT particles in contact. The presence of similar broad peaks in G'' has been reported for composites consisting of carbon black particles dispersed in butyl rubber (Payne & Whittaker, 1971).

In the absence of protein-coated MMT, G' and G'' at the end of the treatment increased with increasing glutaraldehyde concentration (Figure 6.3), consistent with the results from literature studies (Caillard, Remondetto, & Subirade, 2009, 2010). In the presence of MMT, remarkably larger values of G' and G'' were observed at all examined glutaraldehyde concentrations. This is a well-known effect of 'active' fillers that are capable of interacting with the matrix and reinforcing mechanical strengths of the entire system (van Vliet, 1988). The MMT particles used in the present study were coated with soy proteins. Treatments with glutaraldehyde are expected to induce the formation of crosslinks between protein molecules

coating MMT and those consisting of the matrix, resulting in strengthened interactions between the fillers and the matrix. A substantially darker color was also observed at a higher glutaraldehyde concentration, similar to the study of cross-linked soy protein films that an increased glutaraldehyde concentration resulted in increased turbidity and yellow color intensity (Park, Bae, & Rhee, 2000).

6.4.2. Effects of pH and MMT

Properties of soy protein hydrogels depend on pH because the degree of denaturation and the strength of electrostatic repulsions between protein molecules depend on pH (Renkema, Gruppen, & van Vliet, 2002). Figure 6.4 shows G' and G'' values of SPI dispersions after treatment with 10% glutaraldehyde for 5 hours at the ambient temperature and varied pH conditions, i.e., pH 5.5, 6.5 and 10.0. In the absence of protein-coated MMT, the highest G' was observed at pH 5.5, consistent with the results from the previous study that reported steep drops in G' at pH 6.0 with increasing pH (Renkema, Gruppen, & van Vliet, 2002). These results are considered to reflect the complexity of the association-dissociation equilibrium of the subunits of soy proteins occurring at different pH (Renkema, Knabben, & van Vliet, 2001). Soy proteins have two major fractions, i.e., β-conglycinin (7S) and glycinin (11S). β-conglycinin is a trimeric glycoprotein with a molecular weight of 180 kDa, consisting of three types of subunits, i.e., α', α and β subunits, corresponding to molecular weights of 60, 67 and 71 kDa, respectively (Maruyama, et al., 1998). Glycinin, having a molecular weight of ca. 360 kDa, is composed of 6 acidic and 6 basic polypeptides, linked by disulfide bonds (Badley, Atkinson, Hauser, Oldani, Green, & Stubb, 1975). At pH 5.5, soy proteins show an intermediate solubility and are partially aggregated (Wolf, 1970). The aggregated soy globulins are considered as "particulate aggregates" that further aggregate to form a gel network. Particulate aggregates of soy globulins

are much larger than individual protein molecules. Gel networks formed from such particulate aggregates are expected to be much thicker and hence mechanically stronger than those formed from individual protein molecules. At alkaline pH conditions, proteins have a strong net negative charge. β-Conglycinin trimers dissociate into individual subunits and glycinin is dissociated into acidic and basic polypeptides (Petruccelli & Anon, 1995). Most of acidic polypeptides do not participate in the formation of protein gel network, resulting in a weak gel structure at an alkaline condition, corresponding to a low G' (Renkema, Gruppen, & van Vliet, 2002). Meanwhile, the higher degree of dissociation in soy protein at a higher pH (10.0) may generate more available lysine residues to be crosslinked with glutaraldehyde in the formation of the crosslinked gel network, leading to a slightly enhanced G' at pH 10.0 in comparison to that at pH 6.5.

When protein-coated MMT was present, much improved G' and G'' values were obtained at all three studied pH conditions (Figure 6.4), confirming that the protein-coated MMT functions as an active filler at all examined pH conditions. Comparing to the very low G' and G'' values for samples with only MMT (data not shown), this result shows that the enhanced rheology moduli resulted from both the increased volume fractions of rigid particles in the matrix and the improved interactions between proteins in the continuous phase and those bound on MMT via crosslinking.

6.4.3. Effects of Temperature and MMT

β-conglycinin and glycinin have peak denaturation temperatures of 76.7 and 94.1 °C, respectively (Tang, Choi, & Ma, 2007). Temperature is a critical factor for determining the degree of protein denaturation and hence the probability of the formation of crosslink between protein molecules upon contact. The rate of diffusion of protein molecules and hence the frequency of contact between protein molecules are also functions of temperature. Both the

probability of crosslinking and the frequency of contact between protein molecules are expected to increase with increasing temperature. Furthermore, the rate of crosslinking reaction catalyzed by glutaraldehyde is also expected to increase with increasing temperature. The SPI sample used in this study formed gels only at pH 5.5 when it was heated at 90 °C (data not shown). Therefore, effects of temperature on gel properties were investigated at pH 5.5.

Figure 6.5A presents the effect of crosslinking temperatures in the presence of 2.0% glutaraldehyde with and without the addition of protein-coated MMT. Regardless of the presence or absence of MMT, both G' and G'' increased with increasing temperature. Heating at a higher temperature is expected to promote unfolding, dissociation, and denaturation of soy proteins and hence facilitate the cross-linking by glutaraldehyde. Simultaneously, heat-induced aggregation between protein molecules occurs at temperatures higher than the denaturation temperature without involving enzyme catalysis. The heat-induced gelation is contributed to the dissociation of soy proteins and the re-formation of disulfide bonds between protein molecules, defined as intermolecular disulfide bonding (Renkema, Gruppen, & van Vliet, 2002). The positive impacts of temperature on G' and G'' are thus considered to result from more enhanced crosslinking between proteins bound on MMT and in the continuous matrix as well as protein crosslinking within the matrix. The incorporation of protein-coated MMT had positive impacts on G' and G'' at all temperatures, confirming that protein-coated MMT particles played a role as active fillers in all examined conditions.

When a greater amount of glutaraldehyde corresponding to the 10% mass of SPI was applied, G' increased with increasing temperature without the addition of MMT (Figure 6.5B), similar to the results shown in Figure 6.5A. However, the opposite trend was observed in the presence of protein-coated MMT: G' decreased with increasing temperature although the

addition of MMT still resulted in one to two decades of magnitude of increases in G' and G''. These results indicate that the chemical crosslinking catalyzed by glutaraldehyde had predominant effects over the heat-induced intermolecular disulfide bonding and hydrophobic interactions between protein molecules on the determination of G' and G'' of soy protein gels in the presence of protein-coated MMT particles.

It has been reported that the elastic modulus of heat-induced soy protein gels increases first with increasing temperature, reaches a maximum, and then decreases (Furukawa, Ohta, & Yamamoto, 1980; Nagano, Hirotsuka, Mori, Kohyama, & Nishinari, 1992). The rate of self-assembling of protein molecules monotonically increases with increasing temperature due to more enhanced denaturation and diffusion, leading to the formation of thicker and hence mechanically stronger networks. However, an excessive increase in the rate of crosslinking is expected to lead to the formation of coarser and hence mechanically weaker networks. Decreases in G' and G'' with increasing temperature from 23 °C in the presence of protein-coated MMT and 10.0% glutaraldehyde (Figure 6.5B) indicate that the optimum temperature for the crosslinking reaction is less than 23 °C.

6.5. CONCLUSION

Chemical crosslinking by glutaraldehyde enhanced interactions between the matrix consisting of soy proteins and MMT particles coated with soy proteins. As a result, the incorporation of protein-coated MMT significantly promoted the development of the elastic modulus of nanocomposites containing protein-coated MMT particles dispersed in soy protein hydrogel networks. The glutaraldehyde concentration, pH, and cross-linking temperature played important roles on the network formation and mechanical strength of hydrogels. The storage

modulus gradually increased with increasing glutaraldehyde concentration. Soy protein hydrogels formed at pH 5.5 were stronger than those formed at pH 6.5 and 10.0 at an ambient temperature. Effects of temperature were suggested to exhibit parabolic trends on the mechanical strength of nanocomposites. It is thus critical to perform crossliking at the optimal temperature. These findings generally indicate that the addition of a higher level of glutaraldehyde facilitates the crosslinking reaction. The chemical cross-linking was confirmed to be beneficial for preparing bionanocomposite materials with enhanced interactions between protein-coated MMT and the matrix proteins and expected to potentially improve mechanical and barrier properties.

LIST OF REFERENCES

Arora, A., & Padua, G. W. (2010). Review: nanocomposites in food packaging. *Journal of Food Science, 75*(1), R43-R49.

Badley, R. A., Atkinson, D., Hauser, H., Oldani, D., Green, J. P., & Stubb, J. M. (1975). The structure, physical and chemical properties of the soy bean protein glycinin. *Biochim Biophys Acta, 412*, 214-428.

Caillard, R., Remondetto, G. E., & Subirade, M. (2009). Physicochemical properties and microstructure of soy protein hydrogels co-induced by Maillard type cross-linking and salts. *Food Research International, 42*(1), 98-106.

Caillard, R., Remondetto, G. E., & Subirade, M. (2010). Rheological investigation of soy protein hydrogels induced by Maillard-type reaction. *Food Hydrocolloids, 24*(1), 81-87.

Chabba, S., & Netravali, A. N. (2005). 'Green' composites Part 1: Characterization of flax fabric and glutaraldehyde modified soy protein concentrate composites. *Journal of Materials Science, 40*(23), 6263-6273.

Chen, P., Tian, H. F., Zhang, L., Chen, Y., Wang, X. Y., & Do, Y. M. (2008). Structure and properties of soy protein/alumina hydrate nanocomposites fabricated via *in situ* synthesis. *Journal of Biobased Materials and Bioenergy, 2*(3), 248-257.

Chen, P., & Zhang, L. (2006). Interaction and properties of highly exfoliated soy protein/montmorillonite nanocomposites. *Biomacromolecules, 7*(6), 1700-1706.

de Azeredo, H. M. C. (2009). Nanocomposites for food packaging applications. *Food Research International, 42*(9), 1240-1253.

de Carvalho, R. A., & Grosso, C. R. F. (2004). Characterization of gelatin based films modified with transglutaminase, glyoxal and formaldehyde. *Food Hydrocolloids, 18*(5), 717-726.

Ding, X. L., & Henrichs, S. M. (2002). Adsorption and desorption of proteins and polyamino acids by clay minerals and marine sediments. *Marine Chemistry, 77*(4), 225-237.

Essington, M. E. (2003). Soil and water chemistry: an intergrative approach *CRC Press*, p58, 65, 68.

Feng, M., Zhao, C. G., Gong, F. L., & Yang, M. S. (2004). Study on the modification of sodium montmorillonite with amino silanes. *Acta Chimica Sinica, 62*(1), 83-87.

Furukawa, T., Ohta, S., & Yamamoto, A. (1980). Texture-structure relationships in heat-induced soy protein gels. *Journal of Texture Studies, 10*(4), 333-346.

Gan, C.-Y., Latiff, A. A., Cheng, L.-H., & Easa, A. M. (2009). Gelling of microbial transglutaminase cross-linked soy protein in the presence of ribose and sucrose. *Food Research International, 42*(10), 1373-1380.

Gerrard, J. A., Brown, P. K., & Fayle, S. E. (2003). Maillard crosslinking of food proteins II: the reactions of glutaraldehyde, formaldehyde and glyceraldehyde with wheat proteins in vitro and in situ. *Food Chemistry, 80*(1), 35-43.

Gerrard, J. A., Meade, S. J., Millera, A. G., Brown, P. K., Yasir, S. B. M., Sutton, K. H., & Newberry, M. P. (2005). Protein cross-linking in food. In J. W. Baynes, V. M. Monnier, J. M. Ames & S. R. Thorpe (Eds.), *Maillard Reaction: Chemistry at the Interface of Nutrition, Aging, and Disease*, vol. 1043 (pp. 97-103).

Gunister, E., Pestreli, D., Unlu, C. H., Atici, O., & Gungor, N. (2007). Synthesis and characterization of chitosan-MMT biocomposite systems. *Carbohydrate Polymers, 67*(3), 358-365.

Jiang, Y., Tang, C.H., Wen, Q.B., Li, L., & Yang, X.Q. (2007). Effect of processing parameters on the properties of transglutaminase-treated soy protein isolate films. *Innovative Food Science & Emerging Technologies, 8*(2), 218-225.

Kumar, P. (2009). Development of bio-nanocomposite films with enhanced mechanical and barrier properties using extrusion processing. *North Carolina State University. Ph.D dissertation*.

Kumar, P., Sandeep, K. P., Alavi, S., Truong, V. D., & Gorga, R. E. (2010a). Effect of type and content of modified montmorillonite on the structure and properties of bio-nanocomposite films based on soy protein isolate and montmorillonite. *Journal of Food Science, 75*(5), N46-N56.

Kumar, P., Sandeep, K. P., Alavi, S., Truong, V. D., & Gorga, R. E. (2010b). Preparation and characterization of bio-nanocomposite films based on soy protein isolate and montmorillonite using melt extrusion. *Journal of Food Engineering, 100*(3), 480-489.

L'Hocine, L., Boye, J. I., & Arcand, Y. (2006). Composition and functional properties of soy protein isolates prepared using alternative defatting and extraction procedures. *Journal of Food Science, 71*(3), C137-C145.

Le Corre, D., Bras, J., & Dufresne, A. (2010). Starch nanoparticles: a review. *Biomacromolecules, 11*(5), 1139-1153.

Lin, J. J., Wei, J. C., Juang, T. Y., & Tsai, W. C. (2007). Preparation of protein-silicate hybrids from polyamine intercalation of layered montmorillonite. *Langmuir, 23*(4), 1995-1999.

Mallakpour, S., & Dinari, M. (2011). Preparation and characterization of new organoclays using natural amino acids and Cloisite Na(+). *Applied Clay Science, 51*(3), 353-359.

Maruyama, N., Katsube, T., Wada, Y., Oh, M. H., Barba De La Rosa, A. P., Okuda, E., Nakagawa, S., & Utsumi, S. (1998). The roles of the N-linked glycans and extension regions of soybean beta-conglycinin in folding, assembly and structural features. *Eur J Biochem, 258*, 854-862.

Nagano, T., Hirotsuka, M., Mori, H., Kohyama, K., & Nishinari, K. (1992). Dynamic viscoelastic study on the gelation of 7 S globulin from soybeans. *Journal of Agricultural and Food Chemistry, 40*(6), 941-944.

Nayak, P. L., Sasmal, A., Nayak, P., Sahoo, S., Mishra, J. K., Kang, S. C., Lee, J. W., & Chang, Y. W. (2008). Nanocomposites from polycaprolactone (PCL)/soy protein isolate (SPI) blend with organoclay. *Polymer-Plastics Technology and Engineering, 47*(6), 600-605.

Park, S. K., Bae, D. H., & Rhee, K. C. (2000). Soy protein biopolymers cross-linked with glutaraldehyde. *Journal of the American Oil Chemists Society, 77*(8), 879-883.

Payne, A., & Whittaker, R. (1971). Low strain dynamic properties of filled rubbers. *Rubber chemistry and technology, 44*, 440.

Petruccelli, S., & Anon, M. C. (1995). Soy protein isolate components and their interactions. *Journal of Agricultural and Food Chemistry, 43*(7), 1762-1767.

Quiquampoix, H., & Burns, R. G. (2007). Interactions between proteins and soil mineral surfaces: environmental and health consequences. *Elements, 3*(6), 401-406.

Renkema, J. M. S., Gruppen, H., & van Vliet, T. (2002). Influence of pH and ionic strength on heat-induced formation and rheological properties of soy protein gels in relation to denaturation and their protein compositions. *Journal of Agricultural and Food Chemistry, 50*(21), 6064-6071.

Renkema, J. M. S., Knabben, J. H. M., & van Vliet, T. (2001). Gel formation by beta-conglycinin and glycinin and their mixtures. *Food Hydrocolloids, 15*(4-6), 407-414.

Shenoy, A. V. (1999). Rheology of filled polymer systems. *Kluwer Academic Publishers*, Dordrecht, The Netherlands.

Spirkova, M., Duchek, P., Strachota, A., Poreba, R., Kotek, J., Baldrian, J., & Slouf, M. (2011). The role of organic modification of layered nanosilicates on mechanical and surface properties of organic-inorganic coatings. *Journal of Coatings Technology and Research, 8*(3), 311-328.

Tang, C. H., Choi, S. M., & Ma, C. Y. (2007). Study of thermal properties and heat-induced denaturation and aggregation of soy proteins by modulated differential scanning calorimetry. *International Journal of Biological Macromolecules, 40*(2), 96-104.

van Vliet, T. (1988). Rheological properties of filled gels. Influence of filler matrix interaction *Colloid and Polymer Science, 266*(6), 518-524.

Wolf, W. J. (1970). Soybean protiens - their functional, chemical, and physical properties. *Journal of Agricultural and Food Chemistry, 18*(6), 969-&.

Yang, Y., Zhu, Z. K., Yin, J., Wang, X. Y., & Qi, Z. E. (1999). Preparation and properties of hybrids of organo-soluble polyimide and montmorillonite with various chemical surface modification methods. *Polymer, 40*(15), 4407-4414.

Yildirim, M., & Hettiarachchy, N. S. (1998). Properties of films produced by cross-linking whey proteins and 11S globulin using transglutaminase. *Journal of Food Science, 63*(2), 248-252.

Zhao, R. X., Torley, P., & Halley, P. J. (2008). Emerging biodegradable materials: starch- and protein-based bio-nanocomposites. *Journal of Materials Science, 43*(9), 3058-3071.

APPENDIX

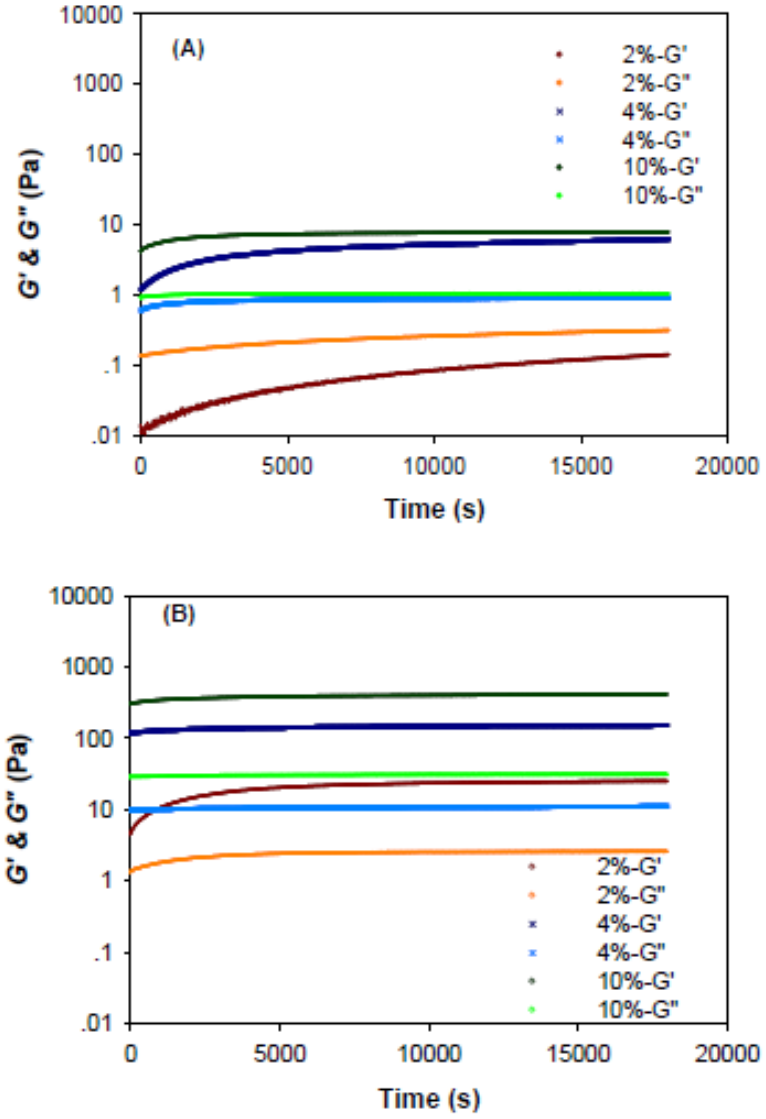

Figure 6. 1. Effects of the glutaraldehyde (GA) concentration on developments of *G′* and *G″* of 8%w/v SPI dispersions (A) without and (B) with containing 1%w/v surface-modified MMT during isothermal treatments at 23 °C and pH 10.0 for 5 hours.

Glutaraldehyde concentrations were applied at 2.0, 4.0, and 10.0% mass of SPI.

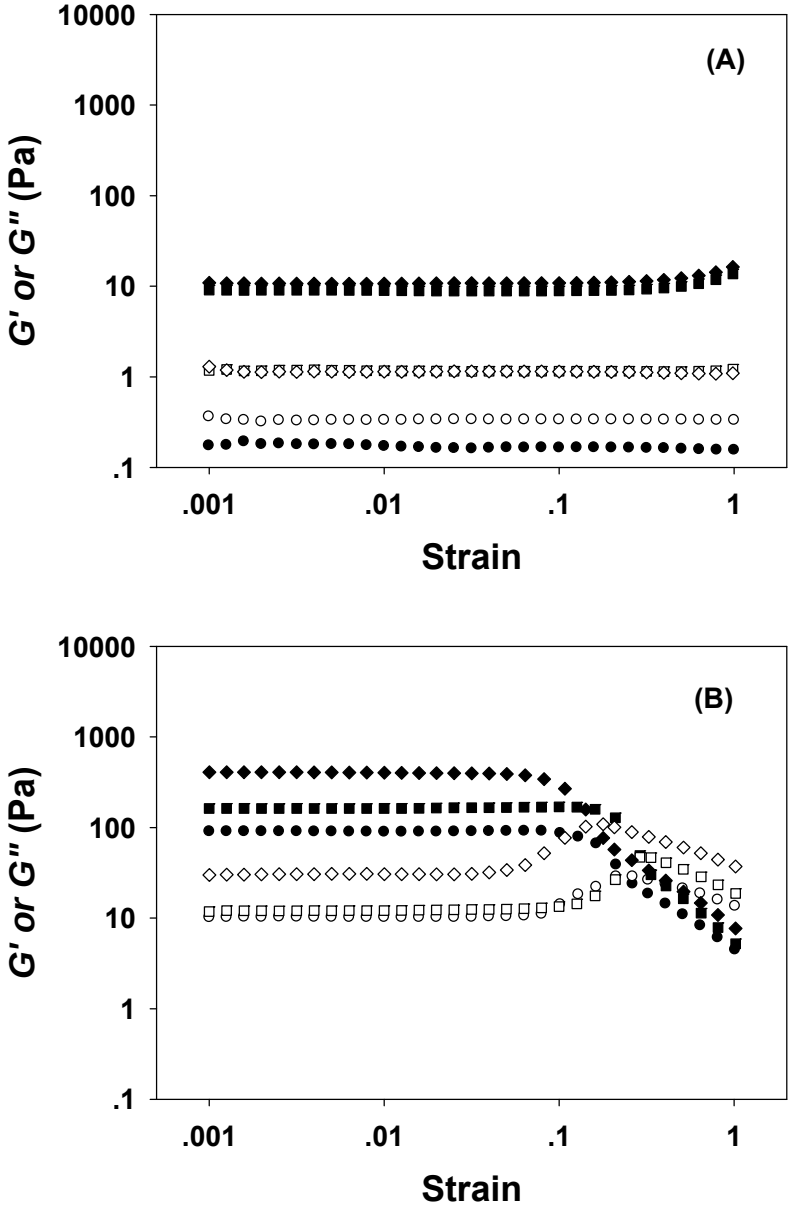

Figure 6. 2. Strain sweep profiles of 8%w/v SPI dispersions (A) without and (B) with containing 1%w/v surface-modified MMT after isothermal treatments at 23 °C and pH 10.0 for 5 hours. The glutaraldehyde concentrations were 2.0% (circles), 4.0% (square), and 10.0% (diamond) mass of SPI.

Filled and open symbols represent storage (G') and loss (G'') moduli, respectively.

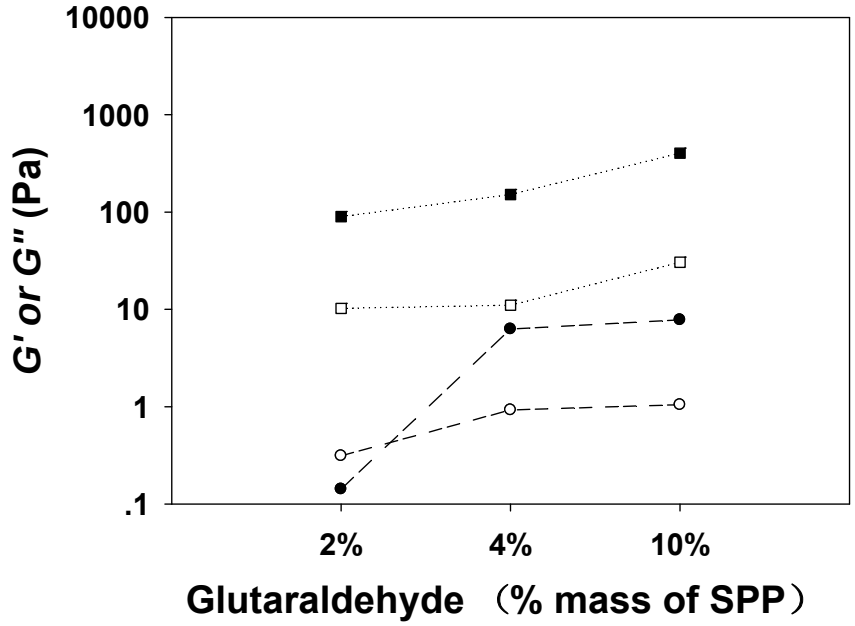

Figure 6. 3. *G′* (filled symbol) and *G″* (open symbol) of 8%w/v SPI dispersions without (circle) and with (square) 1%w/v surface-modified MMT at the end of the isothermal treatment at 23 °C and pH 10.0 for 5 hours.

Glutaraldehyde concentrations were applied at 2.0, 4.0, and 10.0% mass of SPI.

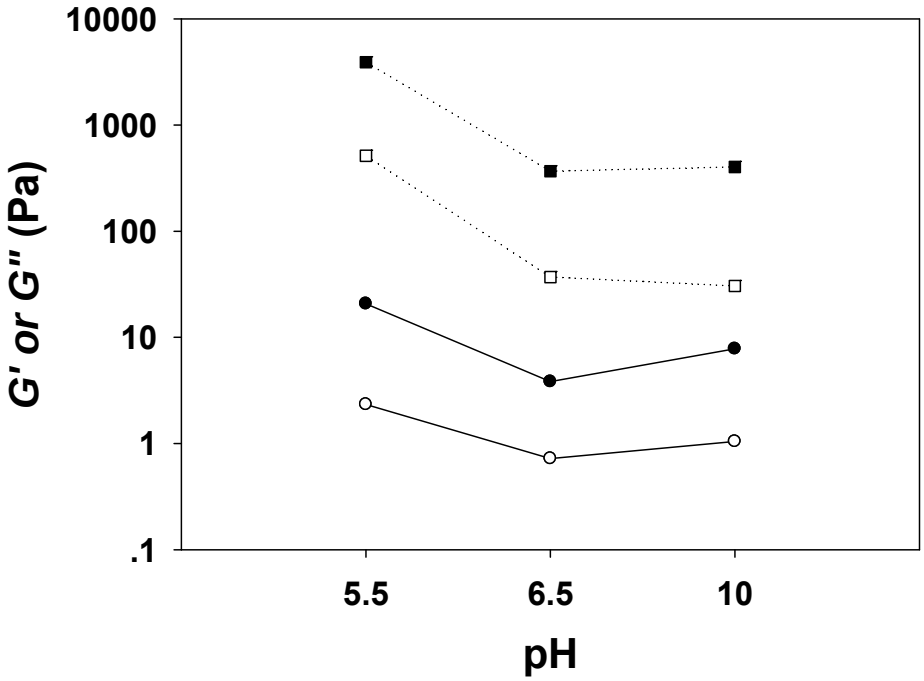

Figure 6. 4. Effects of pH on the storage modulus (G') and loss modulus (G'') of 8%w/v SPI dispersions without (circle) and with (square) 1%w/v surface-modified MMT at 10.0% glutaraldehyde after 5-h crosslinking at 23 °C and varied pH conditions.

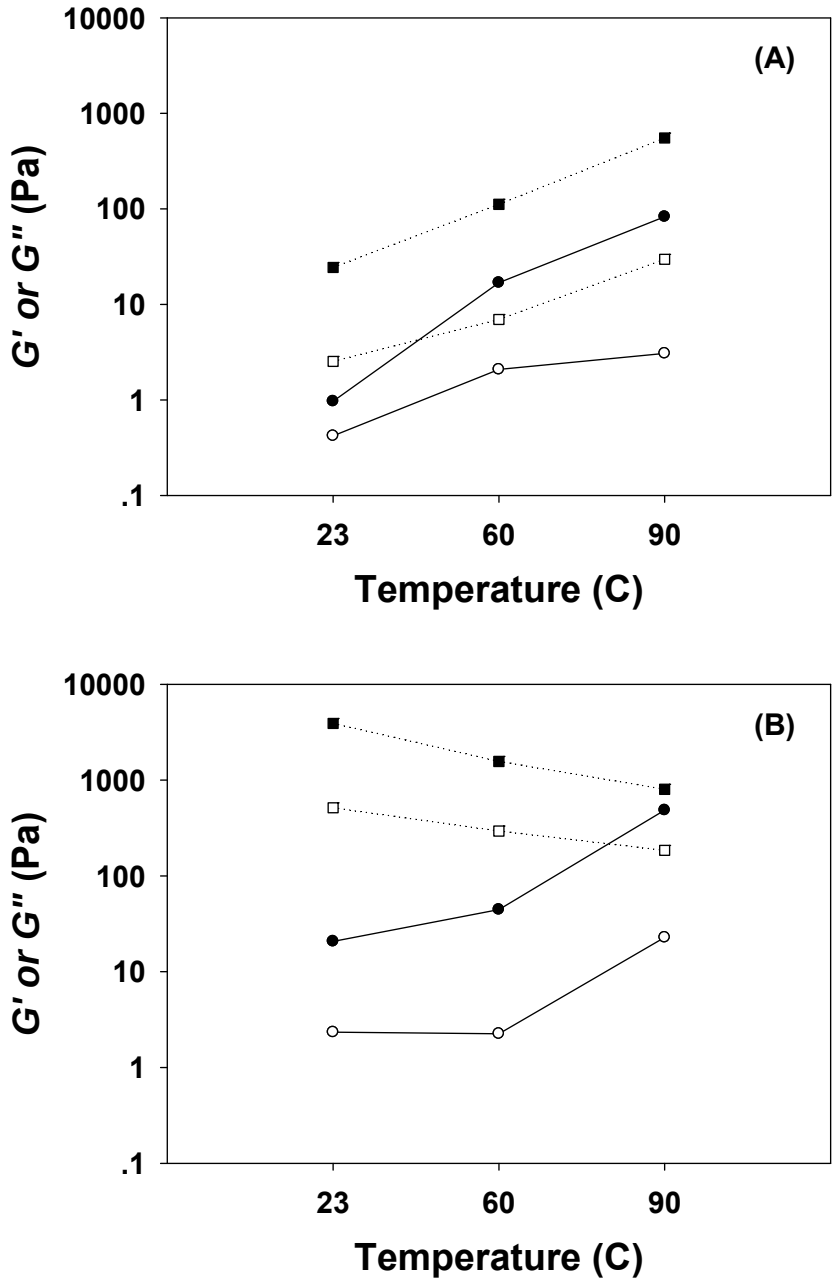

Figure 6. 5. Effects of crosslinking temperature on the storage modulus (G') and loss modulus (G'') of 8%w/v SPI dispersions without (circle) and with (square) 1%w/v surface-modified MMT at (A) 2.0% and (B) 10.0% glutaraldehyde after 5-h crosslinking at pH 5.5 and different temperatures.

CHAPTER 7 . CONCLUSIONS AND FUTURE WORK

This dissertation demonstrated that the structure of nanoclay montmorillonite (MMT) could be easily modified by a simple treatment – surface-coating with water soluble plant-sourced proteins, i.e., hominy proteins and soy proteins using a solution intercalation method. A sufficient amount of proteins and coating pH were critical to the degree of modification of MMT from highly ordered to highly intercalated and/or exfoliated structures. The highly intercalated or exfoliated MMT nanoclay has the promises to well disperse in nanocomposite in turn improve the mechanical and barrier properties of bio-nanocomposite materials. The presence of majority of coating proteins (>90%) bound on MMT at all pH conditions suggests that coating involved not only electrostatic interactions but non-coulombic forces such as hydrogen bonding between MMT and protein molecules. This practical approach on structural modification of nanoclay prior to nanocomposite production can be integrated in preparation of various nanocomposite materials.

Crosslinking was demonstrated to be an effective method to improve the interactions in the protein-based nanocomposite system. Crosslinking of proteins promoted the formation of strong covalent bondings between protein molecules in the continuous phase and between the proteins bound on MMT and those in the matrix, and thus enhanced the interactions between the incorporated MMT and the biopolymer matrix. These strengthened interactions made the protein-coated MMT to be “active” fillers in the nanocomposite system, further improve the mechanical properties of nanocomposite materials.

This dissertation work illustrated these strengthened interactions during both enzymatic and chemical crosslinking by utilizing the dynamic rheological test as a non-destructive method. Microbial transglutaminase (mTGase) and glutaraldehyde were studied for enzymatic and chemical crosslinking, respectively. Both studied crosslinking methods were confirmed to be

beneficial for preparing bionanocomposite materials with enhanced interactions between protein-coated MMT and the matrix proteins and expected to potentially improve mechanical and barrier properties. The mTGase has been used in food production, which reduces possible regulatory issues when applying to nanocomposite materials for applications such as food packaging films. In addition, crosslinking normally decreases the solubility of proteins and enhances the hydrophobic effect as an extra bonus. Thus, cross-linking approaches can be used to direct the manufacturing of biodegradable nanocomposite materials with superior functional performances.

In conclusion, the simple surface-coating method presented in this research can be used to intercalate and/or exfoliate MMT platelets. The protein-coated MMT may be utilized to manufacture various bio-nanocomposite materials with improved physical properties for applications such as bio-degradable packaging films. Crosslinking can strengthen the interactions between matrix polymers and “active” nanofillers in turn improve both mechanical and barrier properties of bio-nanocomposite materials, thus contributing to the growing bio-plastic industry.

VITA

Minfeng Jin was born on June 20, 1979 in Shanghai, China, where her mother and her sister still reside. She graduated in Huazhong Agricultural University with a bachelor's degree in Food Science and Engineering and a minor in Marketing in June of 2001. In July of 2001, Minfeng started her career as a product specialist in a healthcare food company in Shanghai. She led the new product team to develop and launch a supplementary calcium tablet fermented with beneficial bacteria to enhance the absorption ability in GI track, for which the sales was ca. $1 million in the first year after launching. After that, she joined a committee to establish a new company which produced beef/fish snack foods in Shanghai. She set up the food chemistry and food microbiology labs, and complemented the Standard Operation Procedures of processing food products and ISO management documents for the company.

Minfeng always wanted to broaden and deepen her knowledge and insight of food industry in the global economy. In August of 2006, she came to the University of Tennessee for her graduate study and completed her M.S. degree in the Food Science and Technology in two years, under the guidance of Dr. Qixin Zhong on the development of microencapsulation techniques for a naturally-occurring antimicrobial, lysozyme with a biopolymer corn zein. Since Fall 2008, Minfeng has been in her pursuit of Ph.D degree in the same lab, under the guidance of Dr. Qixin Zhong on investigating the exfoliation of montmorillonite nanoclay by surface coating and enhanced interactions by enzymatic and chemical cross-linking. After completion of her Ph.D. study, Minfeng hopes to explore opportunities in the global food industry.